

DYNAMIC RESPONSE OF NONCIRCULAR
STIFFENED CYLINDRICAL SHELLS
WITH RECTANGULAR CUTOUTS

By

MAHABALIRAJA

"

Bachelor of Engineering
University of Mysore
Mysore, India
1967

Master of Engineering
Indian Institute of Science
Bangalore, India
1969

Submitted to the Faculty of the Graduate College
of the Oklahoma State University
in partial fulfillment of the requirements
for the Degree of
DOCTOR OF PHILOSOPHY
December, 1974

Thesis
1974D
M214d
Cop. 2

MAY 11 1976

DYNAMIC RESPONSE OF NONCIRCULAR
STIFFENED CYLINDRICAL SHELLS
WITH RECTANGULAR CUTOUTS

Thesis Approved:

A. E. Boyd

Thesis Adviser

W. M. Lawless

M. M. Maroun

R. J. Lowmy

N. N. Darter

Dean of the Graduate College

938633

ACKNOWLEDGMENTS

The author wishes to express his sincere appreciation and indebtedness to the following individuals and organizations:

To Dr. Donald E. Boyd, who served as my major adviser and committee chairman, for his instruction, advice, patient and personal guidance, encouragement and inspiration;

To Drs. R. L. Lowery, W. P. Dawkins and M. M. Mamoun for serving on the author's committee and for editing this thesis;

To Dr. J. P. Chandler for his help and suggestions in numerical work;

To the School of Mechanical and Aerospace Engineering for offering graduate assistantship;

To the Ballistics Research Laboratory and the Oklahoma State University for their technical and financial support of this study under the contract number F08635-71-C-0199;

To Dr. R. L. Brugh for his encouragement and useful discussions;

To Dr. M. R. Peterson for his suggestions, discussions and assistance in computer programming;

To Mr. Eldon Hardy, Mrs. Jenny Copeland and Mrs. L. A. Dickerson for their assistance in the preparation of the final manuscript.

TABLE OF CONTENTS

Chapter	Page
I. INTRODUCTION	1
II. METHOD OF ANALYSIS	8
Geometry	9
Stiffener-Shell Compatibility Relations	13
Shell Strain-Displacement Relations	14
Stiffener Strain-Displacement Relations	15
Strain and Kinetic Energies	16
Shell Energies	19
Stringer Energies	21
Ring Energies	23
Virtual Work of External Forces	26
Displacement Functions	27
III. SOLUTION OF THE EQUATIONS OF MOTION	33
Static Loading	33
Free Vibrations	33
Time-dependent Loading	34
Computer Program	37
IV. NUMERICAL RESULTS	39
Introduction	39
Comparison with Known Solutions	40
Static Response	42
Step Response	42
Comparison with Sheng's Example	48
Special Cases of Cutouts	50
Convergence Study	53
Effect of Varying the Size of Cutout on the Modes and Frequencies	56
Effect of Varying the Location of Cutout on the Modes and Frequencies	68
Effect of Cutout on the Shell Response to a Quasi-Exponential Type of Air-blast	70

Chapter	Page
V. SUMMARY, CONCLUSIONS AND RECOMMENDATIONS	82
BIBLIOGRAPHY	86
APPENDIX A - DERIVATION OF THE STIFFENER-SHELL COMPATIBILITY RELATIONS	89
APPENDIX B - BEAM MODE FUNCTIONS	95
APPENDIX C - EQUATIONS OF MOTION	96
APPENDIX D - RING FUNCTIONS	101
APPENDIX E - LONGITUDINAL CUTOUT INTEGRALS	104
APPENDIX F - ELEMENTS OF THE FORCE MATRIX	109
APPENDIX G - STRESSES AND STRAINS	111
APPENDIX H - METHOD OF SOLUTION	118

LIST OF TABLES

Table	Page
I. Kinematic Boundary Conditions and Longitudinal Functions in the Assumed Displacement Series	29
II. Comparison of Static Response of a Freely Supported Shell to Uniform Internal Pressure	43
III. Convergence Study I: Frequencies for a Shell With a Symmetric Cutout (Span = $.1a$, arc = 30°)	54
IV. Convergence Study II: Frequencies for a Shell With a Symmetric Cutout (Span = $\frac{1}{3}a$, arc = 90°)	55
V. Effect of Cutout Size on the Frequencies of a Shell (Cutout Span = $0.1a$, Cutout Angle Varies)	57
VI. Effect of Cutout Size on the Frequencies of a Shell (Cutout Span = $0.2a$, Cutout Angle Varies)	58
VII. Effect of Cutout Size on the Frequencies of a Shell (Cutout Span = $0.3a$, Cutout Angle Varies)	59
VIII. Effect of Cutout Location on the Frequencies of a Shell (Cutout Size = $0.2a \times 90^\circ$)	69

LIST OF FIGURES

Figure	Page
1. Geometry of a Noncircular Stiffened Cylindrical Shell with Cutout	10
2. Geometry of a Typical Stringer	11
3. Geometry of a Typical Ring	12
4. Response of a Freely Supported Circular Cylindrical Shell to a Sudden Change of Uniform Internal Pressure	46
5. Axisymmetric Response of a Freely Supported Shell to a Semisinusoidal Blast	49
6. Special Cases of Cutouts	51
7. Natural Frequencies of a Cylinder With Two Cutouts of Different Sizes	62
8. SSS Modes: Circumferential Wave Forms	63
9. SSA Modes: Circumferential Wave Forms	64
10. SSS Modes: Axial Wave Forms	65
11. SSA Modes: Axial Wave Forms	66
12. Axial Wave Forms Showing the Effect of Cutout Location on the Mode Shapes	71
13. Description of Input Data for Transient Analysis	73
14. Normal Displacements and Axial Membrane Stress Resultants along the Generator at $\theta = 0^\circ$ ($t = .22$ msec.)	74

Figure	Page
15. Axial and Peripheral Bending Stress Resultants along the Generator at $\theta = 0^\circ$ ($t = .22$ msec.)	75
16. Membrane and Bending Stresses along the Generator at $\theta = 0^\circ$ ($t = .22$ msec.)	76
17. Peripheral Membrane Stress Resultants along the Generator at $\theta = 0^\circ$ ($t = .22$ msec.)	77
18. Normal Displacement Responses at $x = 7$ in., $\theta = 0^\circ$ for $t \leq .22$ msec.	79

LIST OF SYMBOLS

a	length of the shell
a_c	length of cutout
A	action integral
A_{sl}, A_{rk}	cross sectional area of the l th stringer, k th ring
D_x, D_θ	orthotropic flexural stiffness of the shell in longitudinal direction, circumferential direction
E_x, E_θ	modulus of elasticity of the shell in the longitudinal direction, circumferential direction
E_{sl}, E_{rk}	modulus of elasticity of the l th stringer, k th ring
F_x, F_θ, F_z	$x, \theta,$ and z components respectively, of the statically equivalent concentrated force vector acting on the reference surface of the shell
$G_{x\theta}$	modulus of rigidity of the shell
$(GJ)_{sl}, (GJ)_{rk}$	torsional stiffness of the l th stringer, k th ring
h	thickness of the shell
$\left. \begin{array}{l} IRA_1 \text{ to } IRA_{13} \\ IRB_1 \text{ to } IRB_{15} \end{array} \right\}$	circumferential integrals in the ring equations
$\left. \begin{array}{l} ISA_1 \text{ to } ISA_9 \\ ISB_1 \text{ to } ISB_5 \end{array} \right\}$	circumferential integrals in the shell equations

IX_1 to IX_5	longitudinal integrals in the shell and stringer equations
$I_{yy_{sl}}$, $I_{xx_{rk}}$	moment of inertia of the l th stringer, k th ring cross-sectional area about y' and x' axes, respectively
$I_{zz_{sl}}$, $I_{zz_{rk}}$	moment of inertia of the l th stringer, k th ring cross-sectional area about z' axis
$I_{yz_{sl}}$, $I_{xz_{rk}}$	product of inertia of the l th stringer, k th ring cross-sectional area about y' and z' , x' and z' axes, respectively
$K_{11_{mn, \bar{m}\bar{n}}}$, $K_{12_{mn, \bar{m}\bar{n}}}$ $K_{13_{mn, \bar{m}\bar{n}}}$, $K_{22_{mn, \bar{m}\bar{n}}}$ $K_{23_{mn, \bar{m}\bar{n}}}$, $K_{33_{mn, \bar{m}\bar{n}}}$	elements of the generalized stiffness matrix
l_c	axial location of cutout from center of shell
m	integer index associated with the longitudinal factor of a term in the assumed displacement series
\bar{m}	same as "m" but associated with a virtual displacement
m^*	number of dominant longitudinal half waves in a vibration mode of the shell
M_x	longitudinal bending moment
$M_{11_{mn, \bar{m}\bar{n}}}$, $M_{12_{mn, \bar{m}\bar{n}}}$ $M_{13_{mn, \bar{m}\bar{n}}}$, $M_{22_{mn, \bar{m}\bar{n}}}$ $M_{23_{mn, \bar{m}\bar{n}}}$, $M_{33_{mn, \bar{m}\bar{n}}}$	elements of the generalized mass matrix
n	inter-index associated with the circumferential factor of a term in the assumed displacement series
\bar{n}	same as "n" but associated with a virtual displacement

n^*	number of dominant circumferential waves in a vibration mode of the shell
N_c	total number of cutouts
N_r	total number of rings
N_s	total number of stringers
N_t	total number of terms in the assumed displacement series
p_x, p_θ, p_z	x, θ , and z components, respectively, of the statically equivalent force vector (per unit area) acting on the reference surface of the shell
$P1_{mn}, P2_{mn}, P3_{mn}$	elements of the generalized force matrix
R	radius of the shell
R_{cgk}	radius of the centroid of the kth ring
$RF_{1,k}$ to $RF_{4,k}$	longitudinal functions in ring equations
$RNG1_k$ to $RNG22_k$	constants in ring equations
S_o, S_{sl}, S_{rk}	domain of integration for the shell, l th stringer, kth ring
$SF_{1,l}$ to $SF_{8,l}$	circumferential functions in stringer equations
$STR1_l$ to $STR14_l$	constants in stringer equations
SX_1 to SX_3	} constants in shell equations
ST_1 to ST_4	
SXT_1 to SXT_4	
SPC	
T	kinetic energy
u, v, w	longitudinal, circumferential and radial displacements, respectively, of the shell median surface

$q_{mn}^{us}, q_{mn}^{vs}, q_{mn}^{ws}$	time-dependent generalized coordinates for the symmetric mode displacements, u , v , and w , respectively
$q_{mn}^{ua}, q_{mn}^{va}, q_{mn}^{wa}$	time-dependent generalized coordinates for the antisymmetric mode displacements u , v , and w , respectively
U	strain energy
$\delta U_o, \delta U_{sl}, \delta U_{rk}$	first variation of the strain energy of the shell, l th stringer, k th ring
W	external work of statically equivalent forces acting on the reference surface of the shell
X_m^u, X_m^v, X_m^w	m th longitudinal function in the assumed displacement series
x, θ, z	longitudinal, circumferential and radial coordinates of the shell
x', y', z'	longitudinal, circumferential and radial coordinates of the stiffeners
$(x_{li}, \theta_{li}), (x_{2i}, \theta_{li})$ $(x_{2i}, \theta_{2i}), (x_{li}, \theta_{2i})$	Coordinates of the lower left corner, the lower right corner, the upper left corner, the upper right corner, respectively, of the i th cutout (see Figure 1)
$\bar{x}_{rk}, \bar{y}_{sl}$	x distance of the centroid of the k th ring, y distance of the centroid of the l th stringer from the z axis passing through its point of attachment to the shell surface
z_{sl}, z_{rk}	z distance of the centroid of the l th stringer, k th ring from the middle surface of the shell
δ	variational operator
δ_{il}	$\left\{ \begin{array}{l} = 1 \text{ if } i = 0 \text{ for all } l \\ = 1 \text{ if } i \neq 0 \text{ and the } l\text{th stringer intersects the } i\text{th cutout} \\ = 0 \text{ if } i \neq 0 \text{ and the } l\text{th stringer does not intersect the } i\text{th cutout} \end{array} \right.$

δ_{ik}	$\left\{ \begin{array}{l} = 1 \text{ if } i = 0 \text{ for all } k \\ = 1 \text{ if } i \neq 0 \text{ and the } k\text{th ring intersects the } \\ \text{ } i\text{th cutout} \\ = 0 \text{ if } i \neq 0 \text{ and the } k\text{th ring does not inter-} \\ \text{ } \text{sect the } i\text{th cutout} \end{array} \right.$
θ_c	angle subtending the cutout
$\Theta_n^{us}, \Theta_n^{vs}, \Theta_n^{ws}$	n th circumferential function in the assumed displacement series for θ -symmetric modes
$\Theta_n^{ua}, \Theta_n^{va}, \Theta_n^{wa}$	n th circumferential function in the assumed displacement series for θ -antisymmetric modes
$\nu_{x\theta}, \nu_{\theta x}$	Poisson's ratios for the orthotropic shell
$\rho_o, \rho_{sl}, \rho_{rk}$	mass density of the shell, l th stringer, k th ring
σ_θ^o	circumferential mid-plane stress
ω	circular frequency (radians/sec)

Square Matrices

$[C]_i$	matrix of stiffener-shell compatibility relations for the i th element
$[D]_i$	matrix of elastic constants for the i th element
$[I]$	unit matrix
$[K]$	generalized stiffness matrix
$[M]$	generalized mass matrix

Rectangular Matrices

$[B]_i$	matrix of strain-displacement relations for the i th element
---------	--

[N] matrix of assumed functions relating the displacement vector to the vector of time-dependent generalized coordinates

Column Matrices

$\{f\}_i$ displacement vector for the i th element

$\{F\}$ external surface force vector

$\{P\}$ generalized force matrix

$\{q\}$ vector of time-dependent generalized coordinates

$\{e\}_o, \{e\}_{s\ell}, \{e\}_{rk}$ vector of strain components for the shell, ℓ th stringer, k th ring

$\{\sigma_R\}_o, \{\sigma_R\}_{s\ell}, \{\sigma_R\}_{rk}$ vector of stress resultants for the shell, ℓ th stringer, k th ring

Subscripts

c cutout

cg centroid

cf concentrated force

d distributed

i dummy subscript

k k th ring

ℓ ℓ th stringer

o shell

r ring

s stringer

Superscripts

u, v, w	associated with the shell u-displacement, v-displacement and w-displacement, respectively
s, a	associated with the θ -symmetric mode, θ -antisymmetric mode, respectively
T	transpose of a matrix

Notes

A dot (\cdot) above a quantity indicates the first derivative with respect to time.

A prime superscript ($'$) on a function denotes differentiation with respect to the independent variable (spatial).

CHAPTER I

INTRODUCTION

Many aerospace and hydrospace structures, which are basically shells of revolution, are often complicated by the presence of cutouts. Cutouts may be introduced for purposes of access and visibility (for example, cabin doors and windows in an airplane). An entirely different physical situation is the case of flying aircraft fuselage sections penetrated by projectiles from a nearby explosion, subsequently hit by the air-blast emanating from the center of explosion. The projectiles penetrating the fuselage, which is basically a shell stiffened with stringers and rings, would render certain panels and stiffening elements structurally ineffective. One may rationally idealize the structure so as to give rise to cutouts bounded by lines of curvature of the reference surface of the shell. The response of this structure to the transient pressure wave is a typical case indicating the importance of dynamic analysis of stiffened cylindrical shells with cutouts.

The free vibration problem of stiffened or unstiffened cylindrical shells has been well-studied and reported in the literature. However, the available literature on transient responses of cylindrical shells is

limited. Moreover, these investigations have been confined, for the most part, to complete shells. No published results appear to be available in the literature for determining the dynamic response of a stiffened shell with cutouts, subjected to blast loads, although this is a problem of considerable importance in the design of aircraft and missile structures.

Brogan, Forsberg and Smith (1) appear to be the first to have studied the effect of a cutout on the natural frequencies and mode shapes of an otherwise uniform shell with integral end rings. The analytical part consisted of a two-dimensional finite difference representation of the potential and kinetic energies of the shell, resulting in an algebraic eigenvalue problem by the application of the principle of minimum total energy. Later Malinin (2) applied the Ritz method to the free vibration analysis of shells of revolution with hinged ends containing one or more holes with unconstrained edges.

Forced vibration studies of shell structures have been investigated by the classical method of spectral representation (3, 4, 5). Sheng (6) applied the William's method to find the response of a thin cylindrical shell to transient surface loading. The former approach was employed by Bushnell to unstiffened and ring-stiffened cylindrical shells (7, 8). An approximate method for unstiffened ovals was developed by Klosner (9).

The method of spectral representation can be successfully applied to a shell provided the free-vibration solution is available. Consequently, it is the availability of free vibration solution which limits the applicability of this method. This limitation becomes much more pronounced for stiffened shells and even more so when cutouts are present.

A slight variation of the above method was formulated by Basdekas and applied to determine the dynamic response of plates with cutouts (10). He applied the energy method expanding the deflection in terms of the normal modes of the reference plate (i. e., plate without the cutout) and solved the resulting system of simultaneous differential equations by neglecting partially or wholly the coupling terms due to the cutout.

This thesis presents an approximate method based on an energy approach, for determining the dynamic response of ring and stringer stiffened shells with cutouts and with a variety of boundary conditions. The classical Rayleigh-Ritz method is used to obtain the equations of motion in terms of generalized coordinates which are functions of time. It is well known that the assumed series for the displacements are required to satisfy the kinematic boundary conditions (but not necessarily the kinetic ones). Thus, it is very easy to simulate the free edge conditions at cutouts in the shell.

The resulting equations of motion constitute a system of coupled, linear, second order, ordinary, nonhomogeneous, differential equa-

tions with constant coefficients. These are reduced to a system of first order equations, which are solved numerically in the time domain by means of a computationally efficient Fourth Order Runge-Kutta method with automatic step-size control (11).

Boyd and Rao (12) solved the free vibration problem of stiffened noncircular cylindrical shells treating the stiffeners as discrete elements. The suitability of a smearing technique to solve the same problem in order to reduce the complexity of analysis by reducing the order of the mass and stiffness matrices, has been discussed in (13). Brugh (14) studied the free vibration problem of stiffened cylindrical shells by both discrete and smearing approaches. The present effort extends his work to include the effects of cutouts and response to transient loads.

It appears appropriate to mention here some of the factors which favored adherence to the Rayleigh-Ritz method for analysing the problem under consideration, in preference to other methods (e.g., the finite element and the finite difference methods). The increasing need for analysing complex structures has set in motion a massive trend towards developing computer programs based on the finite element method. This is largely due to the general notion that the conventional Rayleigh-Ritz method is limited to relatively simple geometrical shapes of the total region. But, in reality, this method has been successfully applied, with relatively less effort, to the analysis of shells with significant complications (e.g., non-

circularity, stringer and ring stiffening). In addition, it has certain definite advantages over the finite element and the finite difference methods. For a given problem, the finite element method usually requires a larger number of degrees of freedom to describe accurately the behavior of the shell. Also, the preparation of input data is tedious and time-consuming, especially if one has to test convergence of the solution by refining the element mesh size. Further, if a new kind of finite element is to be developed to achieve better convergence one has to reformulate the mass and stiffness properties of the element. Very fine meshes in the finite difference methods result in large round-off errors in addition to large computer storage requirements and running times.

The Rayleigh-Ritz method is devoid of many of the difficulties associated with the finite element and finite difference methods. It is a simple matter to study convergence of the solution either by increasing the number of terms or by choosing various combinations of terms in the assumed displacement series. Besides, the structural geometric and material parameters can be easily varied, thus facilitating extensive parametric studies to gather physical insight into the problem. Even refinements in the theory used can be incorporated as a side effort without the need to restart the whole programming procedure. The admissible functions are not required to satisfy the kinetic boundary conditions, which simplifies the handling of cutouts with unrestrained edges. The cumulative effect of

all these features is to give the user a physical insight into, and a control over the computer program. Such a feeling of being at home with the program is normally absent in programs based on finite element and finite difference methods, which involve a fair amount of tedious bookkeeping.

The purpose of the above discussion is not to obscure the fact that the finite element method is capable of handling a large class of structures of various degrees of complexities, but to bring out the idea that the Rayleigh-Ritz method is capable of efficiently analysing, with relatively smaller man-hours and computer costs, at least fairly complex structures such as the one under consideration. Moreover, it can be used to obtain solutions with which to compare those obtained by other methods of analysis. To this end, the method is applied for analysing the present problem.

The objectives of this study are as follows:

1. To develop a computer program, based on the proposed method, to determine the response of noncircular ring and/or stringer stiffened cylindrical shells with rectangular cutouts to arbitrary time-dependent surface loads. For the boundary conditions at the ends of the shell, only four types, namely (a) freely supported, (b) clamped-clamped, (c) clamped-free, and (d) free-free will be considered.
2. To test the method by comparing with known solutions.
3. To study the effects, on the frequencies and mode shapes of

an unstiffened shell, of size and locations of cutouts.

4. To study the effect of cutouts on the response of an unstiffened shell to time-dependent loads typical of air-blasts.

CHAPTER II

METHOD OF ANALYSIS

Hamilton's principle may be mathematically stated as

$$\delta A = \delta \int_{t_1}^{t_2} (T - U + W) dt = 0 \quad (2.1)$$

where A is the action integral, T and U are the kinetic and strain energies, respectively, of the system, W is the work done by the external forces on the system, and t_1 and t_2 are two arbitrary points in time. The variation is associated with virtual displacements which are required to satisfy the kinematic boundary conditions of the system, but are arbitrary otherwise.

Assuming that the operations of time-wise integration and variation are commutative in Equation (2.1), it may be written as

$$\int_{t_1}^{t_2} (\delta T - \delta U + \delta W) dt = 0 \quad (2.2)$$

The structural system under study is a combination of the shell, stringers and rings, with cutouts in any of these elements.

$$\text{Thus: } \delta T = \delta T_o + \delta T_s + \delta T_r \quad (2.3)$$

and

$$\delta U = \delta U_o + \delta U_s + \delta U_r \quad (2.4)$$

where the subscripts o, s, and r refer to shell, stringer and ring, respectively.

The external loading consists of both distributed and concentrated surface loads. No edge loadings are considered in the analysis. Also the spatial and temporal variations of the loading are assumed to be separable. Thus,

$$\delta W = \delta W_d + \delta W_{cf} \quad (2.5)$$

where the subscript d refers to distributed forces and the subscript cf refers to concentrated forces.

Geometry

The geometry of a typical noncircular shell with a single cut-out bounded and intersected by stiffeners is shown in Figure 1. Only the bounding and intersecting stringers and parts of the bounding and intersecting rings are shown in thick dotted lines to avoid cluttering the figure. The middle surface of the shell is taken as the reference surface of the shell. The coordinate lines x and θ are the parametric lines of the reference surface of the shell and coincide with the orthogonal lines of principal curvature. The coordinate line z is normal to the reference surface of the shell at the point (x, θ) . Also shown in the figure is the adopted convention for the positive directions of these coordinate lines. The variable radius of curvature of the shell cross section defining the noncircularity is expressed as a function of the θ coordinate. The location and the size of cutout are specified

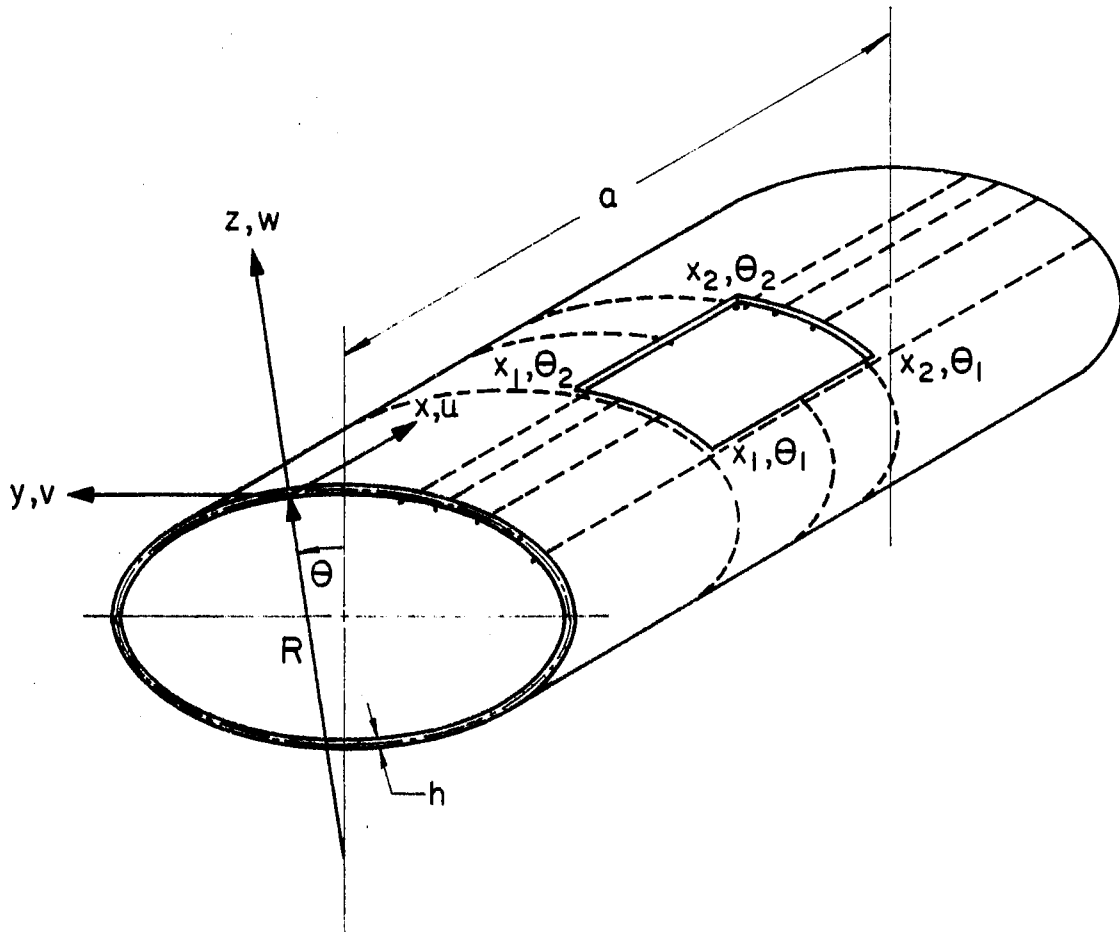


Figure 1. Geometry of a Noncircular Stiffened Cylindrical Shell with Cutout

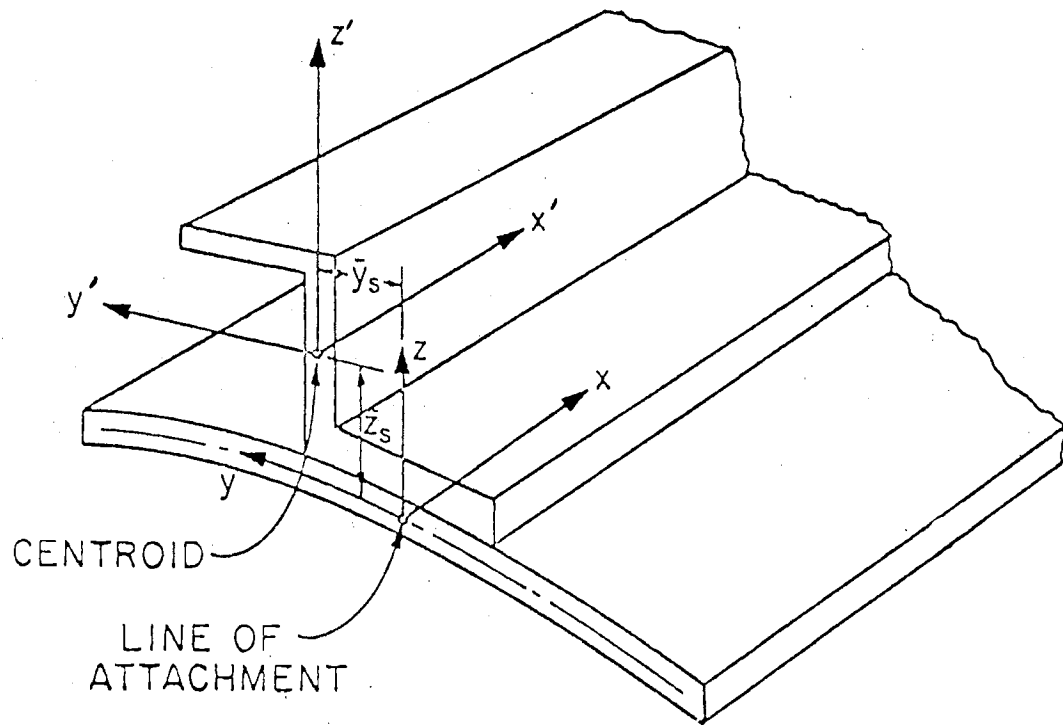


Figure 2. Geometry of a Typical Stringer

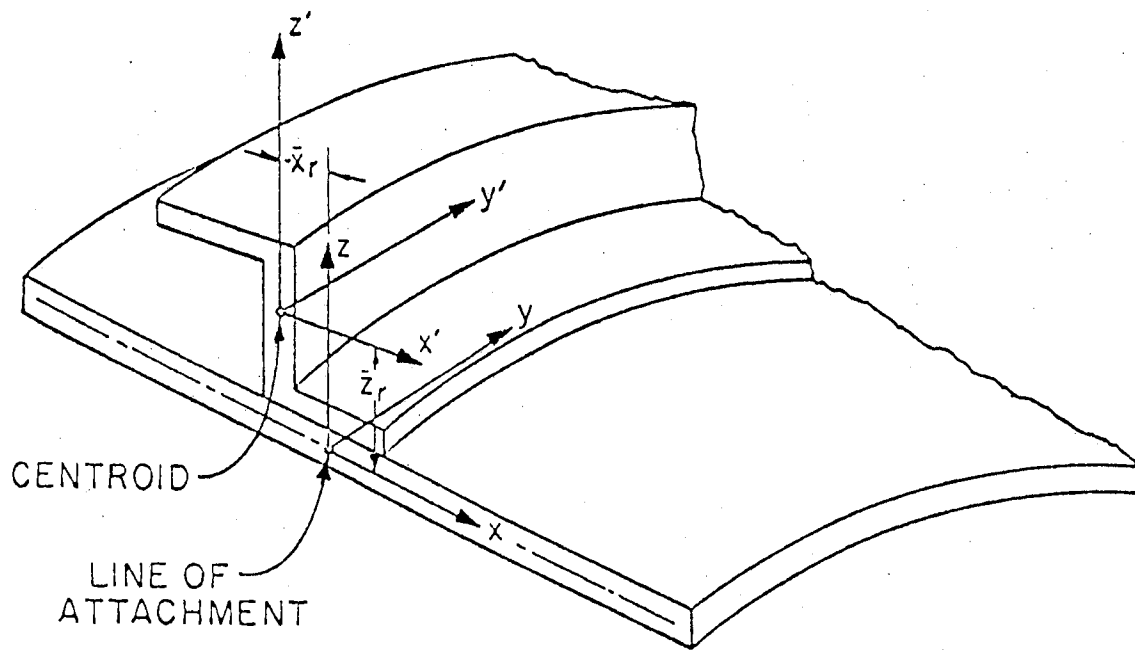


Figure 3. Geometry of a Typical Ring

by the coordinates of its four corners (x_1, θ_1) , (x_2, θ_1) , (x_2, θ_2) and (x_1, θ_2) . The geometries of a typical stringer and ring as well as their local coordinate systems with their origins located at their respective centroids are shown in Figures 2 and 3, respectively. The local coordinates x' , y' , z' of the stiffeners are measured along their local axes from the centroids of the stiffeners and are positive in the directions shown. The stiffeners may be located internal or external to the shell.

Stiffener-Shell Compatibility Relations

By the term 'stiffener-shell compatibility relations' is meant not the strain compatibility relations internal to the stiffeners, but the compatibility relations that signify the mode of attachment of the stiffeners to the shell. The stiffeners are assumed to be uniform along their length and have an arbitrary cross section. The stiffeners are assumed to be attached to the shell along a single line of attachment. It is also assumed that the cross sectional planes do not warp. The stiffener-shell compatibility relations, relating the displacements of the stiffeners to those of the middle surface of the shell are presented in Appendix A.

These compatibility relations are concisely expressed by

$$\{f\}_s = [C]_s \{f\}_o \quad (2.6a)$$

$$\{f\}_r = [C]_r \{f\}_o \quad (2.6b)$$

where

$$\{f\}_s = \begin{Bmatrix} u \\ v \\ w \end{Bmatrix}_s \quad (2.6c)$$

$$\{f\}_r = \begin{Bmatrix} u \\ v \\ w \end{Bmatrix}_r \quad (2.6d)$$

$$[C]_s = \begin{bmatrix} 1 & -(\bar{y}_s + y'_s) \frac{\partial}{\partial x} & -(\bar{z}_s + z'_s) \frac{\partial}{\partial x} \\ 0 & 1 + \frac{1}{R} (\bar{z}_s + z'_s) & -\frac{1}{R} (\bar{z}_s + z'_s) \frac{\partial}{\partial \theta} \\ 0 & -\frac{1}{R} (\bar{y}_s + y'_s) & 1 + \frac{1}{R} (\bar{y}_s + y'_s) \frac{\partial}{\partial \theta} \end{bmatrix} \quad (2.6e)$$

and

$$[C]_r = \begin{bmatrix} 1 & 0 & -(\bar{z}_r + z'_r) \frac{\partial}{\partial x} \\ -\frac{1}{R} (\bar{x}_r + x'_r) \frac{\partial}{\partial \theta} & 1 + \frac{1}{R} (\bar{z}_r + z'_r) & -\frac{1}{R} (\bar{z}_r + z'_r) \frac{\partial}{\partial \theta} \\ 0 & 0 & 1 + (\bar{x}_r + x'_r) \frac{\partial}{\partial x} \end{bmatrix} \quad (2.6f)$$

Shell Strain-Displacement Relations

The shell strain-displacement relations used in this study reflect the postulates of Love's First Approximation Theory for thin elastic shells. Accordingly, the strain-displacement relations may be expressed conveniently in matrix form as

$$\{\varepsilon\}_o = [B]_o \{f\}_o \quad (2.7a)$$

where

$$\{\epsilon\}_o = \left\{ \epsilon_x, \epsilon_\theta, \epsilon_{x\theta}, \chi_{xz}, \chi_{\theta z}, \tau \right\}_o^T, \quad (2.7b)$$

$$[B]_o = \begin{bmatrix} \frac{\partial}{\partial x} & 0 & 0 \\ 0 & \frac{1}{R} \frac{\partial}{\partial \theta} & \frac{1}{R} \\ \frac{1}{R} \frac{\partial}{\partial \theta} & \frac{\partial}{\partial x} & 0 \\ 0 & 0 & -\frac{\partial^2}{\partial x^2} \\ 0 & \frac{1}{R^2} \frac{\partial}{\partial \theta} + \frac{1}{R} \frac{\partial}{\partial \theta} \left(\frac{1}{R} \right) & -\frac{1}{R^2} \frac{\partial^2}{\partial \theta^2} - \frac{1}{R} \frac{\partial}{\partial \theta} \left(\frac{1}{R} \right) \frac{\partial}{\partial \theta} \\ 0 & \frac{1}{R} \frac{\partial}{\partial x} & -\frac{2}{R} \frac{\partial^2}{\partial x \partial \theta} \end{bmatrix} \quad (2.7c)$$

$$\{f\}_o = \begin{Bmatrix} u \\ v \\ w \end{Bmatrix} \quad (2.7d)$$

and u , v , w are the axial, circumferential and normal displacement components of a point in the middle surface of the shell.

Stiffener Strain-Displacement Relations

The strain-displacement relations for the stiffeners are based on the Bernoulli theory of bending. The centroidal axis is chosen as the reference axis for the stiffeners. Thus for the stringer

$$\{\epsilon\}_s = [B]_s \{f\}_o \quad (2.8a)$$

where

$$\{\epsilon\}_s = \left\{ \epsilon_x, \epsilon_y, \epsilon_{xy}, \chi_{xz}, \chi_{xy}, \tau \right\}_s^T \quad (2.8b)$$

$$[B]_s = \begin{bmatrix} \frac{\partial}{\partial x} & -\bar{y}_s \frac{\partial^2}{\partial x^2} & -\bar{z}_s \frac{\partial^2}{\partial x^2} \\ 0 & 0 & 0 \\ 0 & 0 & 0 \\ 0 & 0 & -\frac{\partial^2}{\partial x^2} \\ 0 & \frac{\partial^2}{\partial x^2} & 0 \\ 0 & -\frac{1}{R} \frac{\partial}{\partial x} & \frac{1}{R} \frac{\partial^2}{\partial x \partial \theta} \end{bmatrix} \quad (2.8c)$$

Likewise for the ring

$$\{\epsilon\}_r = [B]_r \{f\}_o \quad (2.9a)$$

The matrix $[B]_r$ is given by Equation (2.9b) on the following page.

Strain and Kinetic Energies

The variation of the strain energy of the shell, stringer and ring can each be expressed in terms of the middle surface strain components and stress resultants as

$$\delta U_i = \int_{S_i} \{\delta \epsilon\}_i^T \{\sigma_R\}_i dS_i \quad (2.10a)$$

$$[B]_r = \begin{bmatrix}
 0 & 0 & 0 \\
 -\frac{\bar{x}_r}{R_c} \frac{\partial}{\partial \theta} \left(\frac{1}{R} \right) \frac{\partial}{\partial \theta} - \frac{\bar{x}_r}{R_c R} \frac{\partial^2}{\partial \theta^2} & \frac{1}{R_c} \left(1 + \frac{\bar{z}_r}{R} \right) \frac{\partial}{\partial \theta} + \frac{z_r}{R_c} \frac{\partial}{\partial \theta} \left(\frac{1}{R} \right) & -\frac{z_r}{R_c R} \frac{\partial^2}{\partial \theta^2} - \frac{z_r}{R_c} \frac{\partial}{\partial \theta} \left(\frac{1}{R} \right) \frac{\partial}{\partial \theta} + \frac{1}{R_c} + \frac{x_r}{R_c} \frac{\partial}{\partial x} \\
 0 & 0 & 0 \\
 0 & -\frac{1}{R_c} \frac{\partial}{\partial \theta} \left(\frac{1}{R} \right) - \frac{1}{R R_c} \frac{\partial}{\partial \theta} & \frac{1}{R_c} \frac{\partial}{\partial \theta} \left(\frac{1}{R} \right) \frac{\partial}{\partial \theta} + \frac{1}{R R_c} \frac{\partial^2}{\partial \theta^2} \\
 -\frac{1}{R_c} \frac{\partial}{\partial \theta} \left(\frac{1}{R_c} \right) \frac{\partial}{\partial \theta} - \frac{1}{R_c^2} \frac{\partial^2}{\partial \theta^2} & 0 & \frac{w, x}{R_c} + \frac{z_r}{R_c} \frac{\partial}{\partial \theta} \left(\frac{1}{R_c} \right) \frac{\partial^2}{\partial x \partial \theta} + \frac{z_r}{R_c^2} \frac{\partial^3}{\partial x \partial \theta^2} \\
 -\frac{1}{R_c^2} \frac{\partial}{\partial \theta} & 0 & \left(-\frac{1}{R_c} + \frac{z_r}{R_c^2} \right) \frac{\partial^2}{\partial x \partial \theta}
 \end{bmatrix} \quad (2.9b)$$

where

$$\{\sigma_R\}_o = \{N_x, N_\theta, N_{x\theta}, M_\theta, M_x, M_{x\theta}\}_o^T \quad (2.10b)$$

$$\{\sigma_R\}_s = \{N_x, N_y, N_{xy}, M_y, M_z, M_x\}_s^T \quad (2.10c)$$

$$\{\sigma_R\}_r = \{N_x, N_y, N_{xy}, M_x, M_z, M_y\}_r^T \quad (2.10d)$$

$$\{\delta \epsilon\}_o = [B]_o \{\delta f\}_o \quad (2.10e)$$

$$\{\delta \epsilon\}_s = [B]_s \{\delta f\}_o \quad (2.10f)$$

$$\{\delta \epsilon\}_r = [B]_r \{\delta f\}_o \quad (2.10g)$$

$$\{\delta f\}_o = \begin{pmatrix} \delta u \\ \delta v \\ \delta w \end{pmatrix} \quad (2.10h)$$

The stress resultants can be expressed in terms of the middle surface strain components as

$$\{\sigma_R\}_i = [D]_i \{\epsilon\}_i \quad (2.10i)$$

where $[D]_i$ is the matrix of elastic constants for the i th element.

After substituting Equations (2.10b) to (2.10i) in Equation (2.10a) the variation of the strain energy is

$$\delta U_i = \int_{S_i} \{\delta f\}_i^T [B]_i^T [D]_i [B]_i \{f\}_i dS_i \quad (2.10j)$$

The variation of the kinetic energy of the shell, stringer or ring can each be expressed in terms of the middle surface displacement components as (neglecting the contribution from the rotatory inertia terms)

$$\delta T_i = \int_{S_i} m_i \{\delta f\}_i^T \{\dot{f}\}_i dS_i \quad (2.11a)$$

where m_i is the mass per unit area/length for the i^{th} element. Integrating Equation (2.11a) by parts between the limits t_1 and t_2 ,

$$\int_{t_1}^{t_2} \delta T_i dt = \int_{S_i} [m_i \{\delta f\}_i^T \{\dot{f}\}_i]_{t=t_1}^{t=t_2} dS_i - \int_{t_1}^{t_2} \int_{S_i} m_i \{\delta f\}_i^T \{\ddot{f}\}_i dS_i dt \quad (2.11b)$$

Since the virtual displacements $\{\delta f\}_i$ are arbitrary they may be prescribed to vanish at the end points of the interval $t_1 \leq t \leq t_2$.

This gives

$$\int_{t_1}^{t_2} \delta T_i dt = - \int_{t_1}^{t_2} \int_{S_i} m_i \{\delta f\}_i^T \{\ddot{f}\}_i dS_i dt \quad (2.11c)$$

$$\text{i. e., } \delta T_i = - \int_{S_i} m_i \{\delta f\}_i^T \{\ddot{f}\}_i dS_i \quad (2.11d)$$

Substituting Equations (2.6a) and (2.6b) in Equation (2.11d)

$$\delta T_i = - \int_{S_i} m_i \{\delta f\}_o^T [C]_i^T [C]_i \{\ddot{f}\}_o dS_i \quad (2.11e)$$

where $[C]_i = [I]$ for the case $i = 0$.

Shell Energies

The first variation of the shell strain energy, obtained by specializing Equation (2.10j) for the shell, is expressed as

$$\delta U_o = \int_{S_o} \{\delta f\}_o^T [B]_o^T [D]_o [B]_o \{f\}_o R d\theta dx \quad (2.12a)$$

Here

$$\int_{S_0} = \int_0^a \int_0^{2\pi} - \sum_{i=1}^{N_c} \int_{x_{li}}^{x_{2i}} \int_{\theta_{li}}^{\theta_{2i}} \quad (2.12b)$$

For the case of orthotropic material, the matrix $[D]_0$ is

$$[D]_0 = \begin{bmatrix} \frac{E_x h}{1-\nu_{x\theta}\nu_{\theta x}} & \frac{\nu_{\theta x} E_x h}{1-\nu_{x\theta}\nu_{\theta x}} & 0 & 0 & 0 & 0 \\ \frac{\nu_{x\theta} E_x h}{1-\nu_{x\theta}\nu_{\theta x}} & \frac{E_\theta h}{1-\nu_{x\theta}\nu_{\theta x}} & 0 & 0 & 0 & 0 \\ 0 & 0 & G_{x\theta} h & 0 & 0 & 0 \\ 0 & 0 & 0 & \frac{E_x h^3}{12(1-\nu_{x\theta}\nu_{\theta x})} & \frac{\nu_{\theta x} E_\theta h^3}{12(1-\nu_{x\theta}\nu_{\theta x})} & 0 \\ 0 & 0 & 0 & \frac{\nu_{x\theta} E_x h^3}{12(1-\nu_{x\theta}\nu_{\theta x})} & \frac{E_\theta h^3}{12(1-\nu_{x\theta}\nu_{\theta x})} & 0 \\ 0 & 0 & 0 & 0 & 0 & \frac{G_{x\theta} h^3}{12} \end{bmatrix} \quad (2.12c)$$

The first variation of the kinetic energy of shell is given by specializing Equation (2.11e) for the shell

$$\delta T_0 = - \int_{S_0} \rho_0 h \{ \delta f \}_0^T \{ \ddot{f} \}_0 R d\theta dx \quad (2.13)$$

Expanded forms of Equations (2.12a) and (2.13) are given by Equations (2.11) and (2.13) respectively of Reference (14) after the following modifications:

1. The double integral operator $\int_0^a \int_0^{2\pi}$ must be replaced by $\int_0^a \int_0^{2\pi} - \sum_{i=1}^{N_c} \int_{x_{li}}^{x_{2i}} \int_{\theta_{li}}^{\theta_{2i}}$ in both the equations.
2. Equation (2.13) must be preceded by a minus sign (-).
3. The parameter ' ω^2 ' must be omitted in Equation (2.13).
4. The displacements u , v , and w in Equation (2.13) must be replaced by their double derivatives with respect to time \ddot{u} , \ddot{v} , and \ddot{w} , respectively. The variational terms associated with the displacements remain unchanged.

Stringer Energies

The first variation of the strain energy for the l th stringer (located at θ_l) is expressed as

$$\delta U_{sl} = \int_{S_{sl}} [\{\delta f\}_o^T [B]_{sl}^T [D]_{sl} [B]_{sl} \{f\}_o] dx \quad \theta = \theta_l \quad (2.14a)$$

where

$$\int_{S_{sl}} = \int_0^a - \sum_{i=1}^{N_c} \delta_{il} \int_{x_{li}}^{x_{2i}} \quad (2.14b)$$

and

$$[D]_{sl} = \begin{bmatrix} E_{sl} A_{sl} & 0 & 0 & 0 & 0 & 0 \\ 0 & 0 & 0 & 0 & 0 & 0 \\ 0 & 0 & 0 & 0 & 0 & 0 \\ 0 & 0 & 0 & E_{sl} I_{yy_{sl}} & -E_{sl} I_{yz_{sl}} & 0 \\ 0 & 0 & 0 & -E_{sl} I_{yz_{sl}} & E_{sl} I_{zz_{sl}} & 0 \\ 0 & 0 & 0 & 0 & 0 & (GJ)_{sl} \end{bmatrix} \quad (2.14c)$$

The symbol $\delta_{i\ell} = 1$ if the ℓ th stringer intersects the i th cutout; otherwise it is zero.

Since the stringers are treated as discrete elements, the total first variation of the strain energy of all the stringers is given by

$$\delta U_s = \sum_{\ell=1}^N \delta U_{sl} \quad (2.14d)$$

The first variation of the kinetic energy for the ℓ th stringer, located at θ_ℓ , is expressed as

$$\delta T_{sl} = - \int_{S_{sl}} [m_{sl} \{\delta f\}_o^T [C]_{sl}^T [C]_{sl} \{\ddot{f}\}_o] dx \quad \theta = \theta_\ell \quad (2.15a)$$

The total contribution to the first variation of the kinetic energy of stringers is, for a discrete analysis

$$\delta T_s = \sum_{\ell=1}^N \delta T_{s\ell} \quad (2.15b)$$

Expanded forms of Equations (2.14a) and (2.15a) are given in Appendix B of Reference (14) after the following modifications:

1. The integral operator \int_0^a must be replaced by $\int_0^a - \sum_{i=1}^N \delta_{i\ell} \int_{x_{1i}}^{x_{2i}}$
2. The expression for $\delta T_{s\ell}$ must be preceded by a minus sign (-).
3. The parameter ' w^2 ' in the expression for $\delta T_{s\ell}$ must be omitted.
4. The displacements u, v, w and their spatial derivatives, $v_{,x}, w_{,x}, w_{,\theta}$ in the expression for $\delta T_{s\ell}$ must be replaced by their double derivatives w. r. t. time, i. e., $\ddot{u}, \ddot{v}, \ddot{w}$ and $\ddot{v}_{,x}, \ddot{w}_{,x}, \ddot{w}_{,\theta}$.

The variational terms associated with the displacements and their spatial derivatives remain unchanged.

Ring Energies

The first variation of the strain energy for the k th ring located at x_k is

$$\delta U_{rk} = \int_{S_{rk}} \left[\{ \delta f \}_o^T [B]_{rk}^T [D]_{rk} [B]_{rk} \{ f \}_o \right] R_{cgk} d\theta \quad (2.16a)$$

$x = x_k$

where

$$\int_{S_{rk}} = \int_0^{2\pi} - \sum_{i=1}^N \delta_{ik} \int_{\theta_{1i}}^{\theta_{2i}} \quad (2.16b)$$

The symbol $\delta_{ik} = 1$ if the k th ring intersects the i th cutout; otherwise, it is zero.

The matrix $[D]_{rk}$ is given by

$$[D]_{rk} = \begin{bmatrix} 0 & 0 & 0 & 0 & 0 & 0 \\ 0 & A_{rk} E_{rk} & 0 & 0 & 0 & 0 \\ 0 & 0 & 0 & 0 & 0 & 0 \\ 0 & 0 & 0 & E_{rk} I_{xx_{rk}} & -E_{rk} I_{xz_{rk}} & 0 \\ 0 & 0 & 0 & -E_{rk} I_{xz_{rk}} & E_{rk} I_{zz_{rk}} & 0 \\ 0 & 0 & 0 & 0 & 0 & (GJ)_{rk} \end{bmatrix} \quad (2.16c)$$

The total contribution of all the rings to the first variation of their strain energy is, for a discrete analysis.

$$\delta U_r = \sum_{k=1}^N \delta U_{rk} \quad (2.16d)$$

The first variation of the kinetic energy for the k th ring (located at x_k) is

$$\delta T_{rk} = - \int_{S_{rk}} [m_{rk} \{ \delta f \}_o^T [C]_{rk}^T [C]_{rk} \{ \ddot{f} \}_o] R_{cgk} d\theta \quad x = x_k \quad (2.17a)$$

The total contribution of all the rings to the first variation of their kinetic energy is, for a discrete analysis,

$$\delta T_r = \sum_{k=1}^{N_r} \delta T_{rk} \quad (2.17b)$$

Expanded forms of Equations (2.16a) and (2.17a) are given in Appendix C of Reference (14) after the following modifications:

1. The integral operator $\int_0^{2\pi}$ must be replaced by $\int_{\theta_i}^{\theta_{2i}}$ - $\sum_{i=1}^{N_c} \delta_{ik}$
2. The expression for δT_{rk} must be preceded by a minus sign (-).
3. The parameter ω^2 must be omitted from the expression for δT_{rk} .
4. The displacements u, v, w and their spatial derivatives $w_{,x}, w_{,\theta}, u_{,\theta}$ in the expression for δT_{rk} must be replaced by their double derivatives with respect to time, i.e., $\ddot{u}, \ddot{v}, \ddot{w}$ and $\ddot{w}_{,x}, \ddot{w}_{,\theta}, \ddot{u}_{,\theta}$. The variational terms associated with the displacements and their spatial derivatives remain unchanged.
5. The term R_c must be interpreted as the radius of curvature at the centroid of the kth ring.

Virtual Work of External Forces

The variation of the work done by the distributed surface forces is given by

$$\delta W_d = \int_{S_o} \{\delta f\}_o^T \{F\}_d R dx d\theta \quad (2.18a)$$

where

$$\{F\}_d = \begin{bmatrix} p_x(x, \theta) f_x(t) \\ p_\theta(x, \theta) f_\theta(t) \\ p_z(x, \theta) f_z(t) \end{bmatrix} \quad (2.18b)$$

In Equation (2.18b) the functions p_x , p_θ , p_z represent the spatial variation of the loading, where as the functions f_x , f_θ , f_z represent the temporal variation.

Similarly the variation of the work done by the concentrated surface forces is given by

$$\delta W_{cf} = \sum_{i=1}^{N_{cf}} \{\delta f_i\}_o^T \{F_i\}_{cf} \quad (2.18c)$$

where

$$\{\delta f_i\}_o = \begin{bmatrix} \delta u(x_i, \theta_i) \\ \delta v(x_i, \theta_i) \\ \delta w(x_i, \theta_i) \end{bmatrix} \quad (2.18d)$$

and

$$\{F_i\}_{cf} = \begin{cases} F_x(x_i, \theta_i) f_x(t) \\ F_\theta(x_i, \theta_i) f_\theta(t) \\ F_z(x_i, \theta_i) f_z(t) \end{cases} \quad (2.18e)$$

Displacement Functions

Using Hamilton's principle as a basis, an approximate solution of the problem is sought by the application of the Rayleigh-Ritz method. The displacements u , v , and w defining the deflected surface of the shell are expressed in the form

$$u(x, \theta, t) = \sum_m \sum_n \left[q_{mn}^{us}(t) \Theta_n^{us}(\theta) + q_{mn}^{ua}(t) \Theta_n^{ua}(\theta) \right] X_m^u(x) \quad (2.19a)$$

$$v(x, \theta, t) = \sum_m \sum_n \left[q_{mn}^{vs}(t) \Theta_n^{vs}(\theta) + q_{mn}^{va}(t) \Theta_n^{va}(\theta) \right] X_m^v(x) \quad (2.19b)$$

$$w(x, \theta, t) = \sum_m \sum_n \left[q_{mn}^{ws}(t) \Theta_n^{ws}(\theta) + q_{mn}^{wa}(t) \Theta_n^{wa}(\theta) \right] X_m^w(x) \quad (2.19c)$$

Periodic functions are used for the circumferential direction

since the shell is closed in that direction. The functions q_{mn}^{us} , q_{mn}^{vs} ,

q_{mn}^{ws} are the time-dependent generalized coordinates associated with

the θ -symmetric modes for the displacements u , v , and w ,

respectively. Similarly, the functions q_{mn}^{ua} , q_{mn}^{va} , q_{mn}^{wa} are those

associated with the θ -antisymmetric modes.

The axial mode functions for the present analysis are chosen as

$$X_m^u(x) = \frac{d}{dx} \Phi_m(x) \quad (2.19d)$$

$$X_m^v(x) = \Phi_m(x) \quad (2.19e)$$

$$X_m^w(x) = \Phi_m(x) \quad (2.19f)$$

where the functions $\Phi_m(x)$ are the characteristic functions representing the normal modes of vibration of a uniform beam. The boundary conditions provided for in this analysis and the longitudinal functions that are used for each are shown in Table I.

The circumferential mode functions for the present analysis are chosen as

$$\Theta_n^{us}(\theta) = \cos n\theta ; \quad \Theta_n^{ua}(\theta) = \sin n\theta \quad (2.19g)$$

$$\Theta_n^{vs}(\theta) = \sin n\theta ; \quad \Theta_n^{va}(\theta) = -\cos n\theta \quad (2.19h)$$

$$\Theta_n^{ws}(\theta) = \cos n\theta ; \quad \Theta_n^{wa}(\theta) = \sin n\theta \quad (2.19i)$$

In terms of the assumed displacement functions the shell displacement vector may be expressed as

$$\{f\}_o = \begin{Bmatrix} u \\ v \\ w \end{Bmatrix} = [N] \{q\} \quad (2.20a)$$

TABLE I

KINEMATIC BOUNDARY CONDITIONS AND LONGITUDINAL FUNCTIONS
IN THE ASSUMED DISPLACEMENT SERIES

Boundary Condition		Longitudinal Functions, $\Phi_m(x)$
Freely supported	$x=0: \left\{ \begin{array}{l} v=w=0 \\ x=a: \end{array} \right.$	$\Phi_m(x) = \sqrt{2} \sin \frac{m\pi x}{a}$
Clamped-clamped	$x=0: \left\{ \begin{array}{l} u=v=w=\frac{\partial w}{\partial x}=0 \\ x=a: \end{array} \right.$	$\Phi_m(x) = m^{\text{th}}$ natural vibration mode function of a clamped-clamped beam. ^{a)}
Clamped-free	$x=0: u=v=w=\frac{\partial w}{\partial x}=0$ $x=a: \text{None}$	$\Phi_m(x) = m^{\text{th}}$ natural vibration mode function of a clamped-free beam. ^{a)}
Free-Free	$x=0: \left\{ \begin{array}{l} \text{None} \\ x=a: \end{array} \right.$	$\left\{ \begin{array}{l} \Phi_0(x) = 1 \\ \Phi_1(x) = \frac{x}{a} - \frac{1}{2} \\ \Phi_m(x) = (m-1)^{\text{th}} \text{ natural vibration mode function of a free-free beam, } ^a) (m \geq 2). \end{array} \right.$

a) The beam mode functions are given in Appendix B.

where

$$[N] = \begin{bmatrix} \{N^{us}\}^T & \{N^{ua}\}^T & 0 & 0 & 0 & 0 \\ 0 & 0 & \{N^{vs}\}^T & \{N^{va}\}^T & 0 & 0 \\ 0 & 0 & 0 & 0 & \{N^{ws}\}^T & \{N^{wa}\}^T \end{bmatrix} \quad (2.20b)$$

is a $(3 \times N_t)$ rectangular matrix of displacement functions, N_t being

the total number of terms in the assumed displacement series,

and

$$\{q\} = \begin{Bmatrix} \{q^{us}\} \\ \{q^{ua}\} \\ \{q^{vs}\} \\ \{q^{va}\} \\ \{q^{ws}\} \\ \{q^{wa}\} \end{Bmatrix} \quad (2.20c)$$

is an $(N_t \times 1)$ column matrix of time-dependent generalized coordinates.

Using Equation (2.20a) all the variations of the strain and kinetic energies as well as the virtual work of external forces can be expressed in terms of the time-dependent generalized coordinates. Further, substitution in Equation (2.2) leads to a system of coupled second order ordinary nonhomogeneous differential equations with constant coefficients. This may be written in matrix form as

$$[M]\{\ddot{q}\} + [K]\{q\} = \{P\} \quad (2.21)$$

where $[M]$ and $[K]$ are the generalized mass and stiffness matrices and $\{P\}$ is the matrix of time-dependent generalized forces. Excluded details of steps leading to Equation (2.21) are given in Appendix C.

Equations (2.20a) to (2.20c) indicate that in the equations of motion defined by Equation (2.21) the 'q's associated with the θ -symmetric modes and the θ -antisymmetric modes occur alternately.

However, for the sake of convenience Equation (2.21) can be rearranged to result in the following form:

$$\begin{bmatrix} M^{ss} & M^{sa} \\ M^{sa^T} & M^{aa} \end{bmatrix} \begin{Bmatrix} \{\ddot{q}\}^s \\ \{\ddot{q}\}^a \end{Bmatrix} + \begin{bmatrix} K^{ss} & K^{sa} \\ K^{sa^T} & K^{aa} \end{bmatrix} \begin{Bmatrix} \{q\}^s \\ \{q\}^a \end{Bmatrix} = \begin{Bmatrix} \{P\}^s \\ \{P\}^a \end{Bmatrix} \quad (2.22)$$

In Equation (2.22) the off-diagonal submatrices of both the **stiffness** and mass matrices vanish if the cross-section of the stiffened shell is symmetric with respect to the $\theta = 0$ axis. Thus, the above equation is uncoupled into two matrix equations-- one for the symmetric, and the other for the antisymmetric modes. The equation for the symmetric modes may be written as

$$\begin{bmatrix} M_{11} & M_{12} & M_{13} \\ M_{12}^T & M_{22} & M_{23} \\ M_{13}^T & M_{23}^T & M_{33} \end{bmatrix} \begin{Bmatrix} \{\ddot{q}\}^u \\ \{\ddot{q}\}^v \\ \{\ddot{q}\}^w \end{Bmatrix} + \begin{bmatrix} K_{11} & K_{12} & K_{13} \\ K_{12}^T & K_{22} & K_{23} \\ K_{13}^T & K_{23}^T & K_{33} \end{bmatrix} \begin{Bmatrix} \{q\}^u \\ \{q\}^v \\ \{q\}^w \end{Bmatrix} = \begin{Bmatrix} \{P_1\}^u \\ \{P_2\}^v \\ \{P_3\}^w \end{Bmatrix} \quad (2.23)$$

Similar equations can be written for the antisymmetric modes.

The elements of the mass and stiffness matrices in Equation (2.23) are obtainable from the basic forms available in Appendix D of Reference (14) by the following procedure:

1. Calculate the elements for the complete shell from the expressions of Appendix D (14) as described therein with the exception that for the longitudinal functions in the ring integrals the expressions given in Appendix D of the present work are to be used.

2. Calculate the corresponding elements for each cutout (in the region $0 \leq \theta \leq \pi$ because of symmetry) from the expressions of Appendix D (14)

- (a) by changing the limits of integration of the circumferential integrals given in Appendix E (14) from '0 to π ' to ' θ_{1i} to θ_{2i} ,'

- (b) by using Appendix E of the present work for the longitudinal integrals over the cutouts.

3. Sum up the values of each element over the number of cutouts and subtract from the value of the corresponding element, calculated in Step 1.

The elements of the force matrix in Equation (2.23) are presented in Appendix F.

CHAPTER III

SOLUTION OF THE EQUATIONS OF MOTION

Static Loading

The static response of the stiffened shell with cutouts may be obtained as a special case of Equation (2.21) by putting the accelerations equal to zero, i. e. ,

$$[K] \{q\} = \{P\} \quad (3.1a)$$

where P is a time-independent column matrix of generalized forces.

The response in terms of the generalized coordinates is obtained as

$$\{q\} = [K]^{-1} \{P\} \quad (3.1b)$$

Free Vibrations

The natural frequencies and mode shapes are obtained as another special case of Equation (2.21) by putting the force matrix

$$\{P\} = \{0\} \quad (3.2a)$$

and

$$\{\ddot{q}\} = -\omega^2 \{q\} \quad (3.2b)$$

for harmonic motion. Thus we have

$$([K] - \omega^2 [M]) \{q\} = \{0\} \quad (3.2c)$$

which results in an eigenvalue problem.

Time-Dependent Loading

The system of N_t second-order equations (2.21) may be reduced to a system of $2N_t$ first-order equations as follows. Premultiplying Equation (2.21) by $[M]^{-1}$ we get

$$\{\ddot{q}\} + [M]^{-1} [K] \{q\} = [M]^{-1} \{P\} \quad (3.3a)$$

Introducing the new variables defined by

$$y_1 = q_1$$

$$y_2 = q_2$$

$$- \quad -$$

$$- \quad -$$

$$- \quad -$$

$$- \quad -$$

$$y_{N_t} = q_{N_t} \quad (3.3b)$$

and

$$y_{N_t+1} = \dot{q}_1$$

$$y_{N_t+2} = \dot{q}_2$$

$$- \quad -$$

$$- \quad -$$

$$- \quad -$$

$$- \quad -$$

$$y_{2N_t} = \dot{q}_{N_t}$$

we reduce Equation (3.3a) to

$$\dot{y}_1 = y_{N_t+1}$$

$$\dot{y}_2 = y_{N_t+2}$$

$$-$$

$$-$$

$$-$$

$$-$$

$$\dot{y}_{N_t} = y_{2N_t}$$

and

$$\dot{y}_{N_t+1} = - \sum_{j=1}^{N_t} \left[[M]^{-1} [K] \right]_{1j} y_j + \sum_{j=1}^{N_t} [M]_{1j}^{-1} \{P\}_j \quad (3.3c)$$

$$\dot{y}_{N_t+2} = - \sum_{j=1}^{N_t} \left[[M]^{-1} [K] \right]_{2j} y_j + \sum_{j=1}^{N_t} [M]_{2j}^{-1} \{P\}_j$$

$$-$$

$$\dot{y}_{2N_t} = - \sum_{j=1}^{N_t} \left[[M]^{-1} [K] \right]_{N_t, j} y_j + \sum_{j=1}^{N_t} [M]_{N_t, j}^{-1} \{P\}_j$$

Equation (3.3c) represent a system of $2N_t$ first-order equations

and can be represented conveniently as

$$\{\dot{y}\}_I = \{y\}_{II} \quad (3.3d)$$

$$\{\dot{y}\}_{II} = -[M]^{-1} [K] \{y\}_I + [M]^{-1} \{P\} \quad (3.3e)$$

where

$$\{y\}_I = \{y_1, y_2, \dots, y_{N_t}\}^T \quad (3.3f)$$

and

$$\{y\}_{II} = \{y_{N_t+1}, y_{N_t+2}, \dots, y_{2N_t}\}^T \quad (3.3g)$$

The system of first-order equations has been solved by means of fourth-order Runge-Kutta method with automatic step-size control (11).

Once the generalized coordinates (q's) are obtained, the various physical quantities of interest, namely displacements, strains, etc., can be calculated by tracing backwards, the analysis developed in the preceding chapter.

The displacement components of a point on the middle surface of the shell are given by

$$\begin{pmatrix} u \\ v \\ w \end{pmatrix} = [N] \{q\}$$

The displacement components of a point on the stiffener are given by

$$\begin{pmatrix} u \\ v \\ w \end{pmatrix}_i = [C]_i [N] \{q\} \quad \begin{array}{l} i = sl \text{ for } l\text{th stringer} \\ i = rk \text{ for } k\text{th ring} \end{array}$$

The components of strain for the i th element are given by

$$\{\epsilon\}_i = [B]_i [N] \{q\} \quad i = 0, sl, rk$$

The components of the stress-resultant vector for the i th element are given by

$$\{\sigma_R\}_i = [D]_i [B]_i [N] \{q\}$$

The strain energy stored in the i th element is given by

$$U_i = \frac{1}{2} \{q\}^T [K]_i \{q\} \quad i = 0, sl, rk$$

The kinetic energy of the i th element is given by

$$T_i = \frac{1}{2} \{\dot{q}\}^T [M]_i \{\dot{q}\}$$

Some of the above quantities are expanded and presented in Appendix G.

Computer Program

A computer program was developed to determine the dynamic response of a ring and /or stringer stiffened noncircular cylindrical shell with rectangular cutouts, subjected to time-dependent loads.

The structure should be symmetric about a $\theta = 0$ axis of the shell. Longitudinal asymmetry is permitted. No edge loadings are permitted in the analysis. Only surface loads distributed symmetrically or antisymmetrically with respect to $\theta = 0$ axis are allowed. The loads should be specified by analytical functions such that their spatial and temporal variations are separable.

The program is written in FORTRAN-IV language and is adapted to the Oklahoma State University IBM Model 360/65 computer. The program has options to perform static and free vibration analysis as special cases of the transient response analysis. All the four boundary conditions of Table I are allowed. An arbitrary choice of terms is permitted in each of the displacement series. Efficient use is made of computer storage by storing only the upper triangular part of the symmetric matrices.

Computational procedures used for the three different cases are described in Appendix H.

CHAPTER IV

NUMERICAL RESULTS

Introduction

The feasibility of the method of approach described in this dissertation was first studied by making comparisons of the results of this study with known solutions which correspond to special or limiting cases of the problem under consideration. This was followed by several studies to examine the effect of cutout parameters on the natural frequencies and mode shapes, as well as on the transient displacement and stress responses of the shell. The results of these studies are presented in this chapter.

The vibration problem of a complete shell with prescribed edge conditions can be studied by varying three independent parameters--the thickness-to-radius ratio, the length-to-radius ratio, and Poisson's ratio. In the presence of a cutout three additional parameters can be independently varied--the ratio of the span of the cutout to the length of the shell, the arc of cutout, and the location of cutout. Because of the large number of variables involved, it appeared necessary to limit the scope of the present investigation. Thus, the parametric study is restricted only to the cutout parameters.

Only unstiffened shells with freely supported boundary conditions are considered. In the case of transient analysis a time-dependent loading typical of an air-blast is considered. The pressure distribution is described by a sinusoidal variation along the longitudinal direction, a cosinusoidal variation around half the periphery and a quasi-exponential decay with time.

Comparison with Known Solutions

The computer program of the present work was developed from that of Reference (14) by extending the latter to include the effects of cutouts and dynamic loads. Besides, some program refinements were done and are partly detailed below.

1. The ranges over which the indices m and n vary in the displacement series could be prescribed arbitrarily.
2. A modified representation for the longitudinal mode functions was used because of their better numerical accuracy (See Appendix B).
3. More efficient subroutines for performing matrix operations, were incorporated in the computer program.

The results from the present program, on free vibrations of ring and/or stringer stiffened circular cylindrical shells without cutouts were found to be in close agreement with those of Reference (14).

The little literature published on the dynamic response of shells with cutouts did not facilitate a comparison promising enough to

establish the correctness of the computer program as to its capacity to handle cutouts. Brogan's model (1) has boundary conditions which do not correspond to any of the four boundary conditions considered here. Malinin (2) presented three frequencies and the corresponding mode shapes for a freely supported shell with a symmetric cutout of span = 6/10th the length of shell and arc = 90° . But the value of Poisson's ratio used in computation was not given in the paper. His calculations showed that the presence of the cutout decreased the lower frequencies by 2 - 3%. The present analysis (using $\nu = .3$) showed that the lowest frequency decreased by more than 50%. A substantial reduction is reasonably expected in the lowest frequency for such a large cutout. He used the same series for the displacements as in the present analysis except that, as indicated by Equation (9) of (2) the axisymmetric term ($n = 0$) is not included. By intentionally excluding the axisymmetric term, the present analysis gave results which were not too far from his results. The closest agreement in mode shape was obtained for the mode with $m^* = 1$, $n^* = 6$. No information was given in the paper as to the axial coordinate at which the circumferential wave forms were plotted. Consequently, there appeared no distinct possibilities of bringing into clearer light the sources of discrepancy. However, there was ample scope for testing the computer program by considering special cases for the general problem. Several of these test studies are presented next.

Static Response

Table II shows a comparison of the static response of a freely supported circular cylindrical shell subjected to a uniform internal pressure, with the exact solution given by Timoshenko (15). The response quantities were calculated by using Equations (l) and (n) on p. 477 of (15). The following physical constants were used: $E = 10^7$ psi; $\rho = 0.0002588 \text{ lb-sec}^2/\text{in}^4$; $\nu = 0.3$, $h = 0.1''$; $R = 10''$; $a = 20''$; $p_z = 100\text{psi}$. The number of terms used for each of u and w was 20, with $n = 0$ and $m = 1, 3, \dots, 39$. The comparison shows excellent agreement for the normal displacement and the circumferential mid-plane stress (σ_θ^0). As regards the bending moment (M_x), the values are accurate to one digit at least in the regions where considerable bending takes place. The fact that the membrane stresses have converged far better than the bending stresses may be attributed to the fact that the former does not involve any derivatives of w whereas the latter involves the second derivatives of w . Differentiation of a convergent series tends to worsen the rate of convergence. However, the accuracy of results obtained in this case suffices practical purposes, since one is interested in peak stresses and the overall stress field rather than small local variations.

Step Response

Figure 4 shows the displacement (w) and bending moment (M_x) responses for the same shell of Table II, but the pressure applied as

TABLE II

COMPARISON OF STATIC RESPONSE OF A FREELY SUPPORTED
SHELL TO UNIFORM INTERNAL PRESSURE

x (in)	$w \times 10^{+2}$ (in)		$\sigma_{\theta}^0 \times 10^{-4}$ (psi)		M_x (lb-in/in)	
	Ref. (15)	Present Analysis	Ref. (15)	Present Analysis	Ref. (15)	Present Analysis
10.0	1.0	0.999	1.0	0.999	4.492-5	-3.970-2
11.0	1.0	1.0	1.0	1.0	-2.186-4	-4.070-2
12.0	1.0	0.9999	1.0	0.9999	-7.816-4	-4.250-2
13.0	1.0	1.004	1.0	1.004	1.548-3	-4.330-2
14.0	0.9999	0.9998	0.9999	0.9998	1.340-2	-3.540-2
15.0	0.9984	0.999	0.9984	0.999	7.016-3	-4.930-2
16.0	0.9976	0.9933	0.9976	0.9933	-1.609-1	-2.276-1
17.0	1.016	1.016	1.016	1.016	-4.194-1	-5.052-1
18.0	1.064	1.064	1.064	1.064	1.250	1.129

TABLE II (Continued)

x (in)	$w \times 10^{+2}$ (in)		$\sigma_{\theta}^o \times 10^{-4}$ (psi)		M_x (lb-in/in)	
	Ref. (15)	Present Analysis	Ref. (15)	Present Analysis	Ref. (15)	Present Analysis
19.0	0.9221	0.9217	0.9221	0.9217	8.030	7.823
19.1	0.8735	0.8733	0.8735	0.8733	8.713	8.592
19.2	0.8154	0.8156	0.8154	0.8156	9.268	9.309
19.3	0.7471	0.7477	0.7471	0.7477	9.638	9.855
19.4	0.6684	0.6691	0.6684	0.6691	9.754	10.08
19.5	0.5791	0.5795	0.5791	0.5795	9.538	9.833
19.6	0.4793	0.4793	0.4793	0.4793	8.900	8.993
19.7	0.3699	0.3693	0.3699	0.3693	7.740	7.503
19.8	0.2521	0.2511	0.2521	0.2511	5.95	5.406

TABLE II (Continued)

x (in)	$w \times 10^{+2}$ (in)		$\sigma_{\theta}^o \times 10^{-4}$ (psi)		M_x (lb-in/in)	
	Ref. (15)	Present Analysis	Ref. (15)	Present Analysis	Ref. (15)	Present Analysis
19.9	0.1279	0.1271	0.1279	0.1271	3.411	2.833
20.0	0.0	0.0	0.0	0.0	0.0	0.0

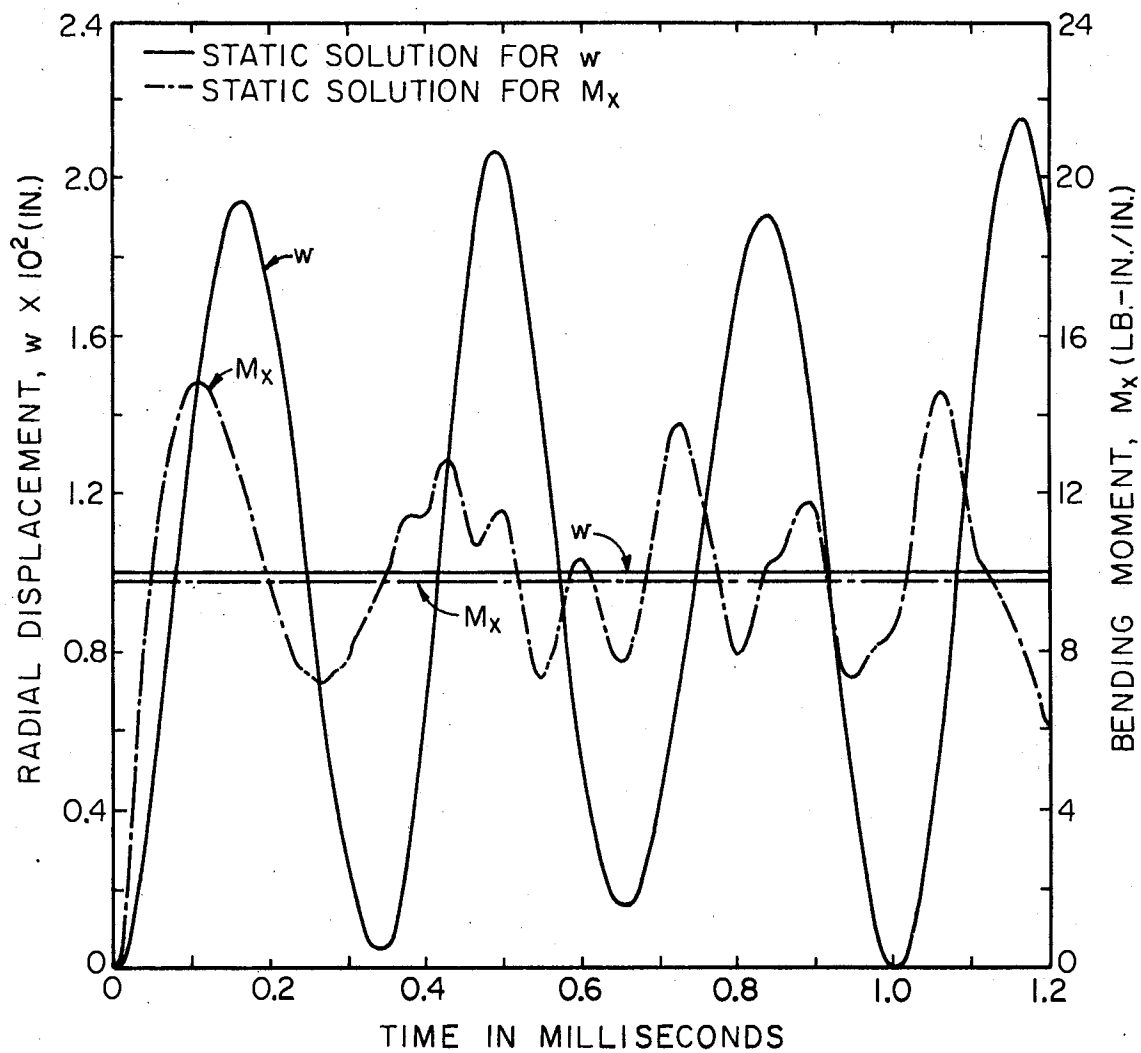


Figure 4. Response of a Freely Supported Circular Cylindrical Shell to a Sudden Change of Uniform Internal Pressure

a step function of time. The w plotted corresponds to the maximum (spatially) displacement, occurring at mid-span; the M_x plotted corresponds to the maximum (spatially) bending moment, occurring at $\cong 0.97$ span. The same number of terms as for the static case were used here. The corresponding static solutions are also shown in the figure as horizontal lines. These also form the mean positions about which the oscillations take place, as is to be expected. The displacement response of Figure 4 is quite different from that of a simple spring-mass system to a step excitation. In the latter case the mass will oscillate between zero displacement and a maximum displacement equal to twice the static displacement. The difference is seen from the fact that in the series summation of Equations (2.19a) to (2.19c), generally speaking, each term is out of phase from the others and the final result is not characterized by any single mode but rather by the diffusion of all modes. The figure also indicates the presence of higher modes in M_x . Unlike the expression for w , the expression for M_x has the time-dependent generalized coordinates multiplied by the derivatives of w . This would result in the higher modes weighed heavily for M_x . This explains the difference in the frequency spectra between the two plots.

Figure 4 also reveals that the radial displacement response plot contains a predominant oscillation whose period is approximately 0.33 milliseconds. It was found from a free vibration analysis of the same shell that the frequency of the lowest axisymmetric mode was 3044

Hz. This was a transverse mode with one axial wave. This frequency corresponds to a period of 0.328 milliseconds and thus agrees closely with the period of the predominant wave shape in the radial response plot.

Comparison with Sheng's Example

Using William's method Sheng (6) presented the response of a freely supported circular cylindrical shell to a semisinusoidal pulse of uniform pressure given by

$$p_z(\chi, \theta, t) = p_z(t) = -1000 \sin 1003t \quad 0 \leq t \leq 3.133 \text{ msec.}$$

$$p_z(\chi, \theta, t) = p_z(t) = 0 \quad t > 3.133 \text{ msec.}$$

The same problem was studied by the present method using 5 and 10 terms in each of the u- and w-displacement series and a time step = 1/200th of the period of the pulse. Halving the time step did not change the results. To ascertain that the results have converged sufficiently, a third set of results were obtained using 20 terms and a time step = 1/400th of the period of the pulse. The maximum radial displacement (20 terms solution) at the midpoint of the shell attained was $w = 0.2006$ in. at $t = 2.444$ msec. as compared to $w = 0.21$ in. at $t = 2.5$ msec. presented by Sheng. A comparison of the responses is shown in Figure 5. Sheng's curve is reproduced here without converting to the present scale, but inverted to conform to the adopted convention for w. The times at which the radial displacement first

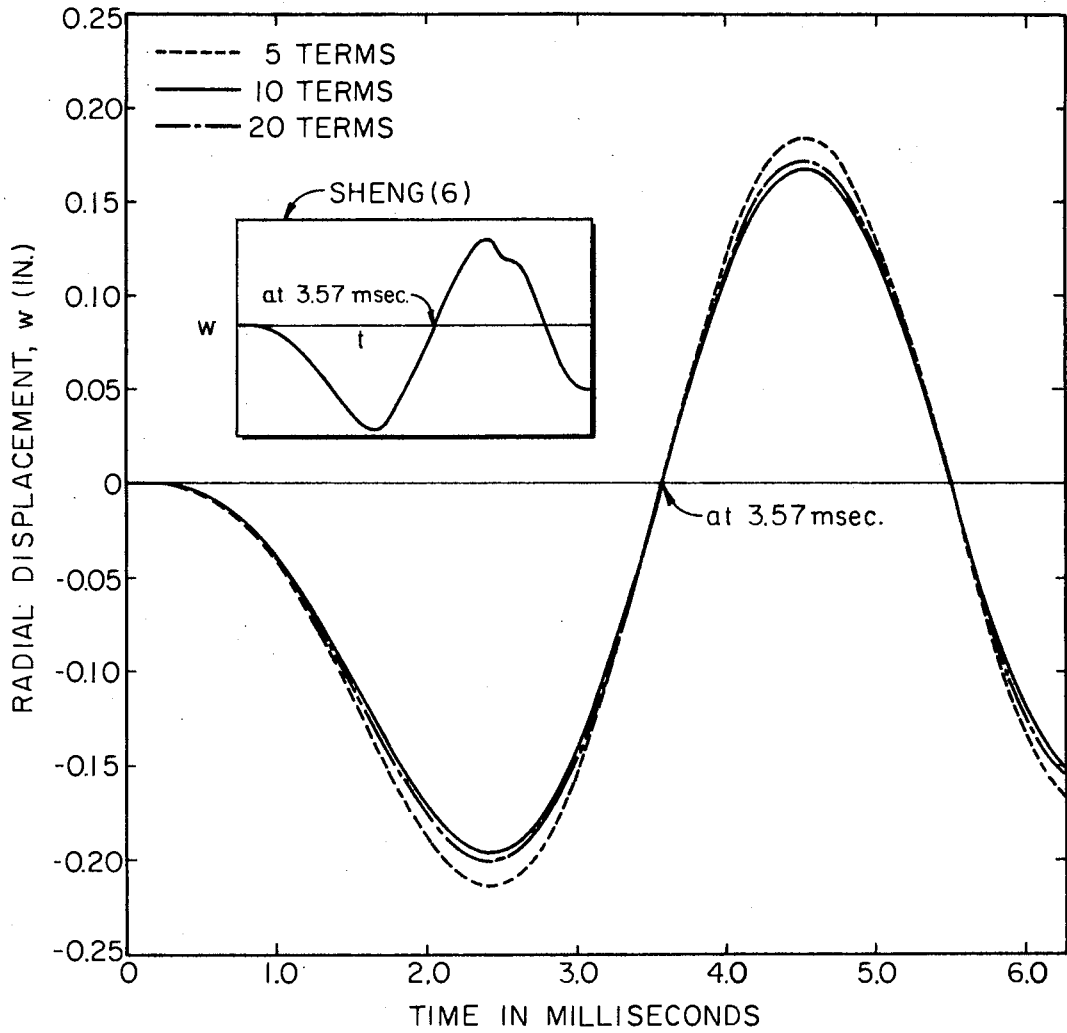


Figure 5. Axisymmetric Response of a Freely Supported Shell to a Semisinusoidal Blast

becomes zero after reaching the peak value, as calculated from Sheng's figure and the present analysis agree very well. The response patterns agree very well in general except that Sheng's figure indicates the presence of a higher mode of vibration in the response. The pulse frequency was 160 Hz., and the lowest two natural frequencies of the shell were found to be 156 Hz. and 248 Hz. It is reasonable to expect, in this case, a negligible participation of higher modes in the response and the results of the present analysis conform to this point of view.

No comparative study of the results on transient response of stiffened shells was possible due to lack of availability of published results with which results from the present program could be compared.

Special Cases of Cutouts

The capability of the program to handle cutouts was tested in the following ways.

1. A shell with one cutout may be treated as an equivalent shell with a number of smaller cutouts (see Figure 6).
2. A clamped-free shell fixed at $\chi = 0$ and free at $\chi = a$ may be treated as an equivalent shell with a length = $a + \Delta a$ terminating in a $\Delta a \times 360^\circ$ cutout at the free end (see Figure 6).
3. A clamped-free shell of length 'a' may be treated as an equivalent clamped-clamped shell of length '2a + Δa ' with a centrally located $\Delta a \times 360^\circ$ cutout (see Figure 6).

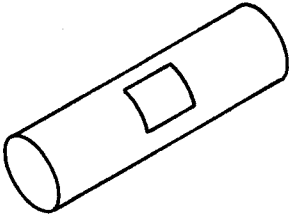
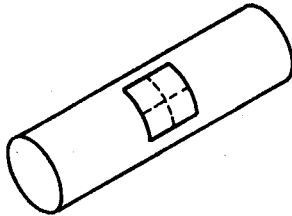
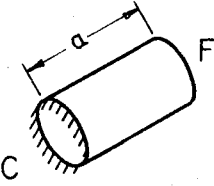
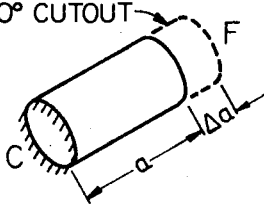
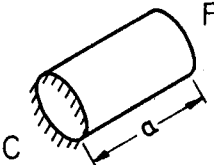
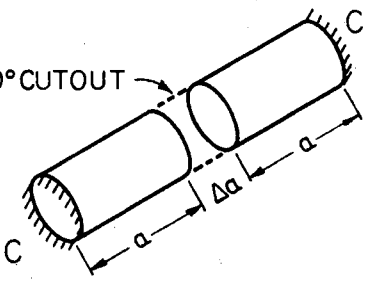
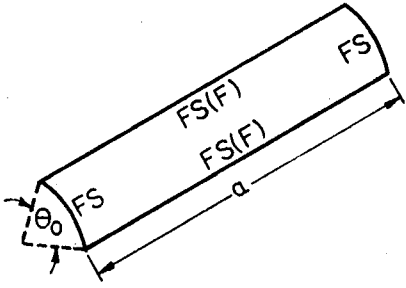
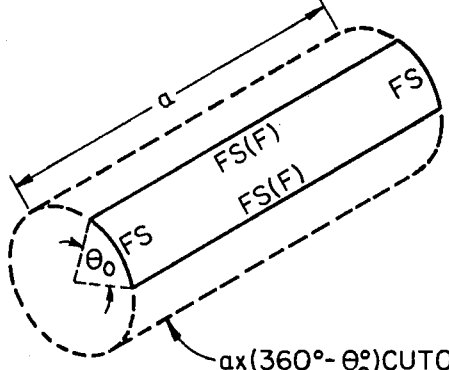
ACTUAL MODEL	EQUIVALENT MODEL
 <p data-bbox="357 568 542 596">ONE CUTOUT</p>	 <p data-bbox="885 568 1071 596">FOUR CUTOUTS</p>
	<p data-bbox="706 643 949 674">$\Delta a \times 360^\circ$ CUTOUT</p>  <p data-bbox="671 827 721 868">(2)</p>
	<p data-bbox="706 970 949 1001">$\Delta a \times 360^\circ$ CUTOUT</p>  <p data-bbox="671 1154 721 1195">(3)</p>
	 <p data-bbox="921 1573 1199 1614">$ax(360^\circ - \theta_0^\circ)$ CUTOUT</p> <p data-bbox="606 1645 778 1686">(4) and (5)</p> <p data-bbox="221 1624 571 1737"> C - CLAMPED F - FREE FS - FREELY SUPPORTED </p>

Figure 6. Special Cases of Cutouts

4. An open circular cylindrical shell of length a and included angle θ_0 with all edges freely supported may be treated as an equivalent closed shell of length a with the ends freely supported and a cutout of span a and included angle $2\pi - \theta_0$, the edges of the cutout being freely supported. In particular, for the special case where θ_0 is π divided by an interger i , the freely supported boundary conditions along the straight edges of the cutout are satisfied by choosing terms with $n = i, 3i, 5i, 7i, \dots$ for symmetric modes (see Figure 6).

5. An open circular cylindrical shell of length a and included angle θ_0 with the curved edges freely supported and straight edges free may be treated as an equivalent closed shell of length a with the ends freely supported and a cutout of span a and included angle $2\pi - \theta_0$, the edges of the cutout being free. The free edge boundary conditions may be satisfied in a limiting sense by using an appropriate linear combination of terms from the general series (see Figure 6).

For sake of clarity all the above special cases are illustrated in the same order in Figure 6.

Using typical configurations free vibration studies were performed for the equivalent models in all the five cases mentioned above. The agreement among the results was exact in Cases 1, 2, 3, and 4. In Case 5, the maximum discrepancy was found to be less than 5%. This may be attributed to the fact that the numerical results used for comparison were based on Donnell's theory with tangential inertia neglected.

Convergence Study

In the application of the Rayleigh-Ritz method, the problem of estimating the accuracy of the results is usually encountered. The accuracy of the results depends to an appreciable extent on the capability of the employed admissible functions to approximate the true shape of the deflected surface to the required degree. An increase in the number of terms tends to improve the accuracy of the results in general, but the resulting increase in the size of the matrices, round-off errors and computer costs often limits the accuracy of the results.

Table III shows a convergence study of the frequencies of vibration of a freely supported shell with a cutout of length $a/10$ and arc 30° located symmetrically about $\theta = 0^\circ$ and $\chi = a/2$. The frequencies correspond to modes which are symmetric about $\theta = 0^\circ$ and $\chi = a/2$. The number of terms were increased from $m = 1$ to 7 (odd only) in the axial direction and from $n = 0$ to 9 in the circumferential direction. The frequencies show a trend towards convergence. The results appear to have sufficiently converged. The effect of the cutout on the frequencies was quite small for this configuration.

Another convergence study was performed for a freely supported shell with a cutout having a span of $1/3$ rd the length of the shell and an included angle of 90° . The results are presented in Table IV for the lowest four frequencies corresponding to modes possessing both axial and peripheral symmetry. Several combinations of terms were

TABLE III

CONVERGENCE STUDY I: FREQUENCIES FOR A SHELL ^{a)}
 WITH A SYMMETRIC CUTOUT (SPAN = .1a, ARC = 30°)

Frequencies (hz) of Several Symmetric Modes ($m^* = 1$)								
n*	No Cutout	M=1 N=1	M=2 N=2	M=3 N=4	M=3 N=6	M=3 N=8	M=3 N=10	M=4 N=10
0	2537	2535	2535	2535	2535	2535	2536	2534
1	1565		1575	1574	1576	1576	1576	1573
2	894.1			898.2	897.6	897.4	897.4	895.0
3	529.8			530.8	530.2	529.9	529.7	527.7
4	338.6				338.1	337.8	337.7	336.2
5	235.6				235.1	234.8	234.7	233.7
6	182.1					181.7	181.6	181.0
7	162.2					162.0	161.9	161.6
8	166.9						166.9	166.7
9	188.6						188.6	188.6

a) The geometry of the shell is the same as Model 1 of (16) except for the cutout.

M = number of terms in the longitudinal direction (odd only).

N = number of terms in the circumferential direction.

TABLE IV
 CONVERGENCE STUDY II: FREQUENCIES FOR A SHELL^{a)}
 WITH A SYMMETRIC CUTOUT (SPAN = $\frac{1}{3}a$, ARC = 90°)

Frequencies (Hz.) of the Lowest Four Symmetric Mode ($m^* = 1$)							
No Cutout	M=1 N=8	M=2 N=8	M=3 N=11	M=4 N=8	M=4 N=10	M=5 N=8	M=6 N=7
307.0	309.3	298.4	251.1	170.3	168.2	146.9	144.8
334.5	335.8	331.2	296.7	296.0	290.5	295.5	301.4
362.1	372.3	349.6	329.7	331.3	329.0	330.9	333.1
412.8	420.2	416.3	407.0	401.5	399.2	399.9	402.5

a) The parameters of the shell are: $R = 12$ in., $E = 10^7$ psi., $\nu = 0.3$,
 $\rho = 0.0002588$ lb-sec²/in⁴, $a = 24$ in., $h = 0.12$ in.

used in the displacement series in order to arrive at a good upper bound for the lowest frequency.

Subsequent calculations will be performed by limiting the number of degrees of freedom to a maximum of 126. Different combinations of terms will be tried to arrive at better upper bounds for configurations with large size cutouts such as the one considered above.

Effect of Varying the Size of Cutout on the Modes and Frequencies

This section presents the natural frequencies and mode shapes of vibration of a freely supported cylinder with two rectangular cutouts symmetrically located with respect to the length of the cylinder and a diameter. This gives rise to an additional plane of symmetry thereby doubling the maximum number of terms in the displacement series for the same computer storage.

Tables V, VI, and VII present the frequencies of the above shell with various size cutouts. The frequencies correspond to modes which are symmetric with respect to $\chi = a/2$ plane and $\theta = 0^\circ$ plane, the latter passing through the centre of cutouts. The cutout sizes considered include all combinations of cutout angles of 15° , 30° , 45° , 60° , 75° , 90° and cutout spans of $0.1a$, $0.2a$, $0.3a$. Different combinations of terms were considered to obtain better upper bounds for the frequencies. With regard to the lowest frequency, the best possible estimate for the upper bound was obtained in general with 7 axial terms and 6

TABLE V

EFFECT OF CUTOUT SIZE ON THE FREQUENCIES OF A SHELL^{a)}
 (CUTOUT SPAN = 0.1a, CUTOUT ANGLE VARIES)

No Cutout	.1a X 15°	.1a X 30°	.1a X 45°	.1a X 60°	.1a X 75°	.1a X 90°
307.0 (1, 5)	304.5 (1, 5)	296.0 (1, 5)	292.2 (1, 5)	292.7 (1, 5)	290.6 (1, 5)	282.3 (1, 5)
334.5 (1, 6)	333.4 (1, 6)	327.4 (1, 6)	322.0 (1, 6)	322.6 (1, 6)	321.6 (1, 6)	315.0 (1, 6)
362.1 (1, 4)	359.0 (1, 4)	347.2 (1, 4)	341.6 (1, 4)	338.1 (1, 4)	337.8 (1, 4)	337.4 (1, 4)
412.8 (1, 7)	412.1 (1, 7)	411.4 (1, 7)	410.8 (1, 7)	409.6 (1, 7)	408.8 (1, 7)	408.5 (1, 7)
521.1 (1, 8)	520.8 (1, 8)	512.1 (1, 3)	494.3 (1, 3)	482.5 (1, 3)	480.1 (1, 3)	482.7 (1, 3)
535.1 (1, 3)	531.7 (1, 3)	520.9 (1, 8)	520.9 (1, 8)	520.3 (1, 8)	519.9 (1, 8)	519.0 (1, 8)
650.9 (1, 9)	651.0 (1, 9)	650.3 (1, 9)	650.3 (1, 9)	650.8 (1, 9)	650.1 (1, 9)	649.9 (1, 9)
798.8 (1, 10)	797.9 (1, 10)	797.6 (1, 10)	798.2 (1, 10)	798.1 (1, 10)	798.0 (1, 10)	798.1 (IR)
894.9 (1, 2)	896.1 (1, 2)	875.9 (1, 2)	850.6 (1, 2)	827.8 (1, 2)	809.3 (1, 2)	801.5 (IR)
942.4 (3, 8)	943.8 (3, 8)	941.0 (3, 8)	947.8 (3, 8)	946.5 (3, 8)	944.3 (3, 8)	950.0 (3, 8)

a) The parameters of the shell are given in Table IV. The two cutouts are located diametrically opposite and centered at midspan.

TABLE VI

EFFECT OF CUTOUT SIZE ON THE FREQUENCIES OF A SHELL^{a)}
 (CUTOUT SPAN = 0.2a, CUTOUT ANGLE VARIES)

No Cutout	.2a X 15°	.2 a X 30°	.2a X 45°	.2a X 60°	.2a X 75°	.2a X 90°
307.0 (1, 5)	301.5 (1, 5)	279.8 (1, 5)	245.5 (1, 5)	209.6 (1, 4)	177.6 (1, 4)	162.0 (1, 4)
334.5 (1, 6)	330.6 (1, 6)	307.7 (IR)	255.4 (1, 4)	211.0 (1, 5)	186.1 (IR)	169.7 (1, 3)
362.1 (1, 4)	356.2 (1, 4)	340.5 (IR)	281.4 (1, 6)	328.7 (1, 6)	320.4 (1, 6)	281.4 (1, 5)
412.8 (1, 7)	410.1 (1, 7)	408.2 (1, 7)	406.0 (1, 7)	383.4 (1, 3)	330.8 (1, 5)	308.6 (1, 6)
521.1 (1, 8)	519.5 (1, 8)	492.2 (1, 3)	440.6 (1, 3)	406.6 (1, 7)	407.0 (1, 7)	404.1 (1, 7)
535.1 (1, 3)	530.4 (1, 3)	516.9 (1, 8)	515.4 (1, 8)	518.8 (1, 8)	516.6 (1, 8)	501.7 (1, 2)
650.9 (1, 9)	650.6 (1, 9)	645.2 (1, 9)	646.4 (1, 9)	648.4 (1, 9)	605.3 (1, 2)	518.5 (1, 8)
798.8 (1, 10)	793.9 (1, 10)	791.6 (1, 10)	791.2 (1, 2)	704.8 (1, 2)	648.7 (1, 9)	648.4 (1, 9)
894.9 (1, 2)	898.3 (1, 2)	866.3 (1, 2)	800.4 (1, 10)	793.1 (1, 10)	793.0 (1, 10)	794.8 (1, 10)
942.4 (3, 8)	946.5 (3, 8)	935.3 (3, 8)	940.2 (1, 11)	946.8 (1, 11)	947.9 (1, 11)	945.7 (1, 11)

a) The parameters of the shell are given in Table IV. The two cutouts are located diametrically opposite and centered at midspan.

TABLE VII

EFFECT OF CUTOUT SIZE ON THE FREQUENCIES OF A SHELL^{a)}
 (CUTOUT SPAN = 0.3a, CUTOUT ANGLE VARIES)

No Cutout	.3a X 15°	.3a X 30°	.3a X 45°	.3a X 60°	.3a X 75°	.3a X 90°
307.0 (1, 5)	300.5 (1, 5)	277.5 (1, 5)	239.6 (1, 5)	199.2 (1, 4)	159.7 (1, 4)	132.7 (1, 4)
334.5 (1, 6)	329.5 (1, 6)	304.1 (1, 6)	250.5 (1, 4)	200.8 (1, 5)	168.3 (IR)	139.1 (1, 3)
362.1 (1, 4)	356.2 (1, 4)	338.6 (1, 4)	329.7 (1, 6)	323.8 (1, 6)	319.6 (1, 6)	276.2 (1, 5)
412.8 (1, 7)	408.5 (1, 7)	401.2 (1, 7)	395.5 (1, 7)	380.2 (1, 3)	324.9 (1, 5)	307.0 (1, 6)
521.1 (1, 8)	518.4 (1, 8)	497.0 (1, 3)	440.1 (1, 3)	404.1 (1, 7)	406.0 (1, 7)	396.0 (1, 7)
535.1 (1, 3)	531.4 (1, 3)	506.5 (1, 8)	506.0 (1, 8)	518.5 (1, 8)	507.2 (1, 8)	492.8 (1, 2)
650.9 (1, 9)	651.1 (1, 9)	630.0 (1, 9)	640.3 (1, 9)	632.5 (1, 9)	604.6 (1, 2)	508.0 (1, 8)
798.8 (1, 10)	786.7 (1, 10)	771.2 (1, 10)	784.6 (1, 10)	708.8 (1, 2)	627.6 (1, 9)	647.3 (1, 9)
894.9 (1, 2)	902.3 (1, 2)	881.1 (1, 2)	809.5 (1, 2)	757.7 (1, 10)	785.4 (1, 10)	765.6 (1, 10)
942.4 (3, 8)	946.1 (1, 11)	914.2 (3, 8)	868.5 (IR)	857.6 (IR)	890.5 (IR)	838.7 (IR)

a) The parameters of the shell are given in Table IV. The two cutouts are located diametrically opposite and centered at midspan.

circumferential terms. The author hopes that possible inaccuracies in the numerical results due to poor convergence would not be fatal enough to prevent making parametric observations.

The frequencies have simply been arranged in ascending numerical order, with the appropriate mode shape noted after the value for the frequency wherever possible. For the complete shell, the motion is sinusoidal in the circumferential as well as in the axial directions, and there is no difficulty in identifying the mode shapes. For the shell with cutouts, the eigenvectors associated with many of the frequencies revealed the presence of a dominant wave form in the mode shape. However, there were many other frequencies for which the eigenvectors revealed either a strong coupling of two distinct wave forms or a combination of several different wave forms in varying degrees. In Tables V, VI, and VII, the dominant wave form in the mode shape is identified wherever possible by the notation (m^* , n^*) after the value for the frequency. Irregular mode shapes have been denoted by the notation (IR) after the values for the corresponding frequencies.

A decrease in the frequency for a given dominant wave form was observed in general. Increasing the cutout size to $0.3a \times 90^\circ$ had an effect of reducing the lowest frequency by about 53%. In reference (1), Brogan has given a value of less than 7% for the reduction in the minimum natural frequency for a $0.3a \times 120^\circ$ cutout. His shell model had boundary conditions close to clamped-clamped ones. This results in the stiffer parts being located near the boundaries and thus away from

the cutout. In the present case, the central part of the shell is the major load carrying member and is weakened by two cutouts of size $0.3a \times 90^\circ$, thus resulting in a substantial reduction in the lowest natural frequency.

Figure 7 shows how the frequencies vary as a function of the dominant circumferential wave number for different size cutouts. In the case of a complete shell or a shell with the two cutouts of either a small span or a small angle the frequencies vary as a smooth function of the circumferential wave number. But with increase in the size of the cutouts these curves do no longer behave, as may be seen in the figure. A possible explanation for this behavior lies in the fact that, with increase in the size of cutouts, the circumferential wave number becomes less and less capable of defining the mode shape and merely represents the wave form that has the largest amplitude in the analytically obtained eigenvector. Nevertheless, this form of presenting shell vibration data conveys useful information. For instance, the curves for large size cutouts appear to break up into two distinct parts, one confined to the region of circumferential wave forms substantially affected by the cutout and the other vice versa.

A study of the mode shapes was made in many cases. Figures 8, 9, 10, and 11 show some representative wave forms. The notation 'SSS' refers to mode shapes which are symmetric about all the three planes of symmetry, namely the $x = a/2$ plane, the $\theta = 0^\circ$ plane and

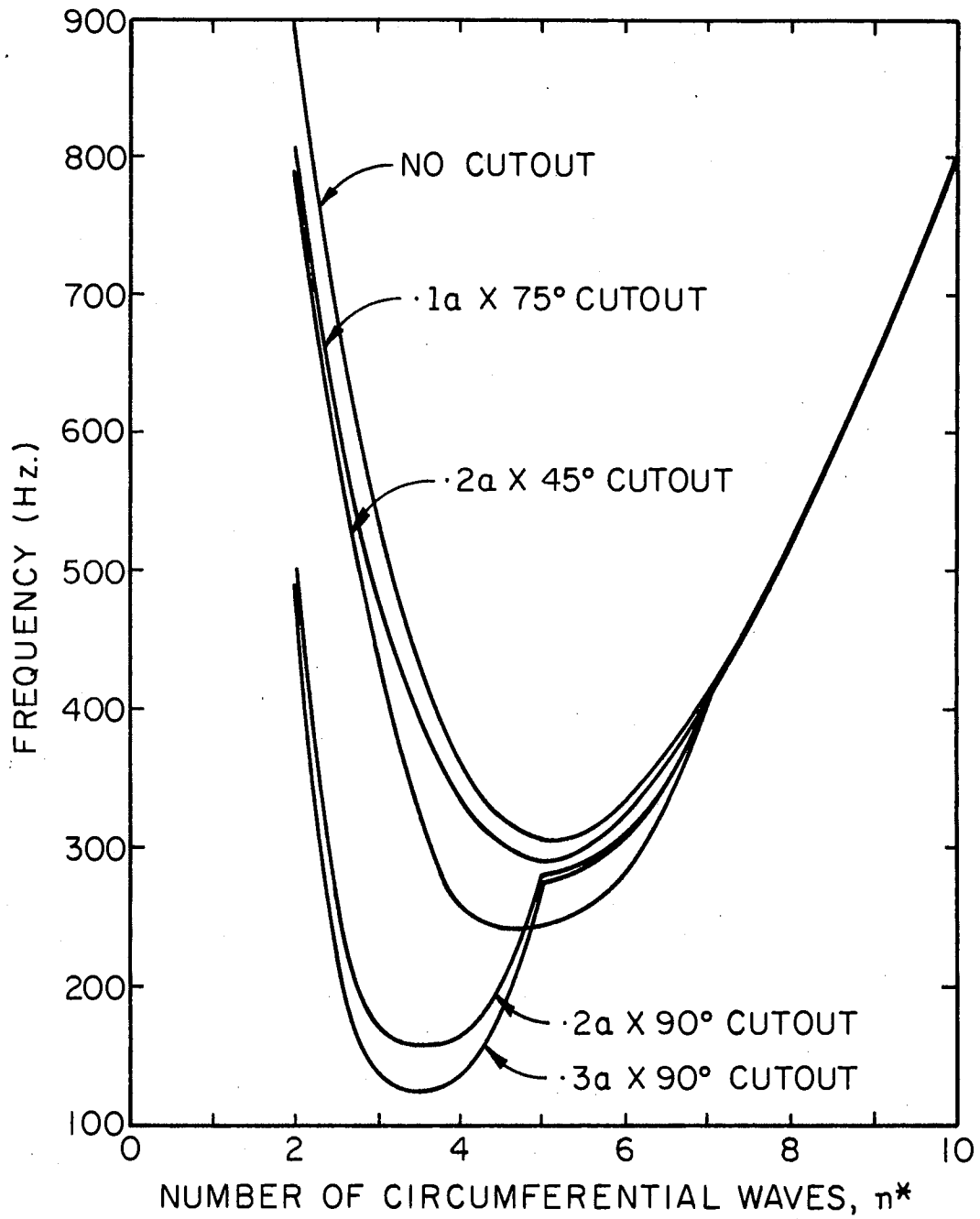
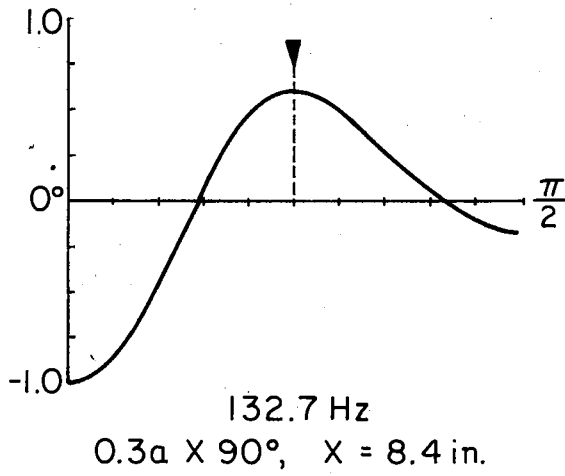
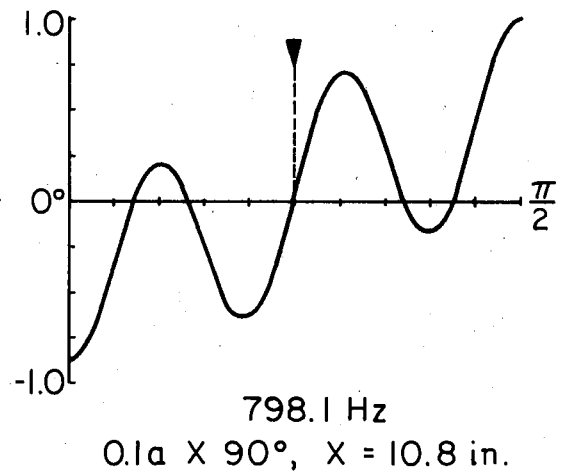


Figure 7. Natural Frequencies of a Cylinder with Two Cutouts of Different Sizes

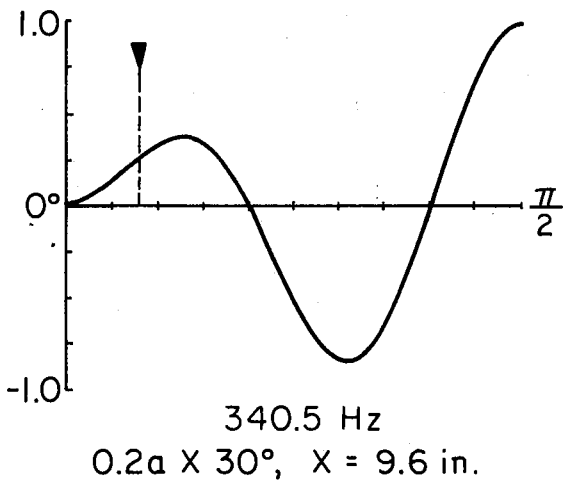


(a)

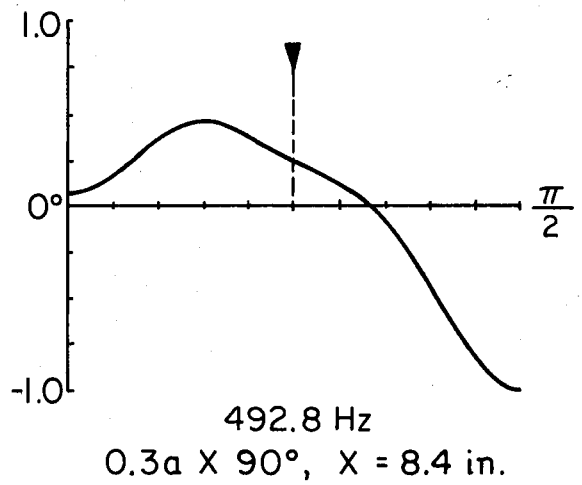


(b)

▼ ~ EDGE OF CUTOUT

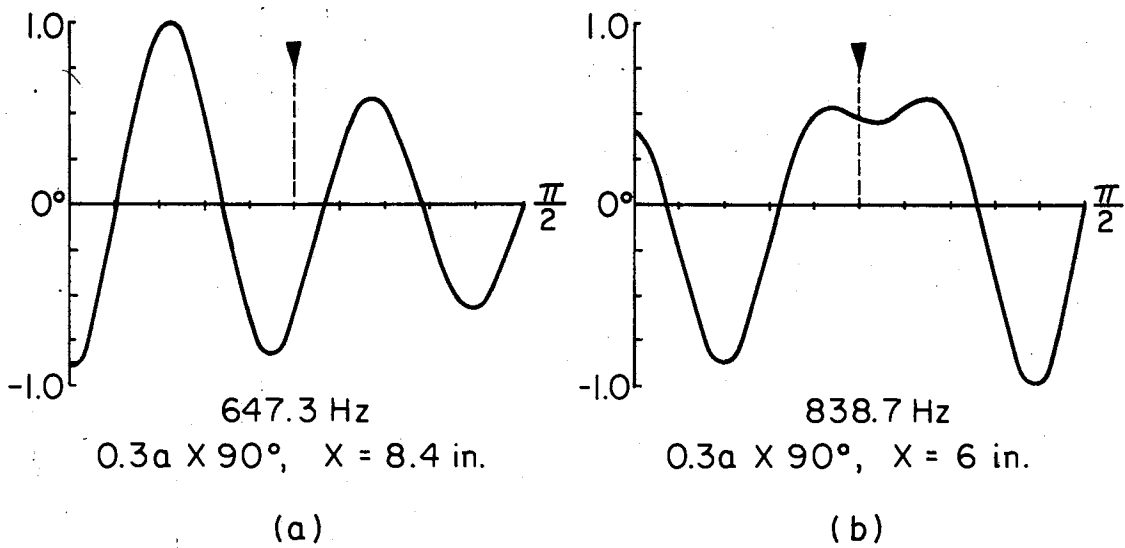


(c)



(d)

Figure 8. SSS Modes: Circumferential Wave Forms



▼ ~ EDGE OF CUTOUT

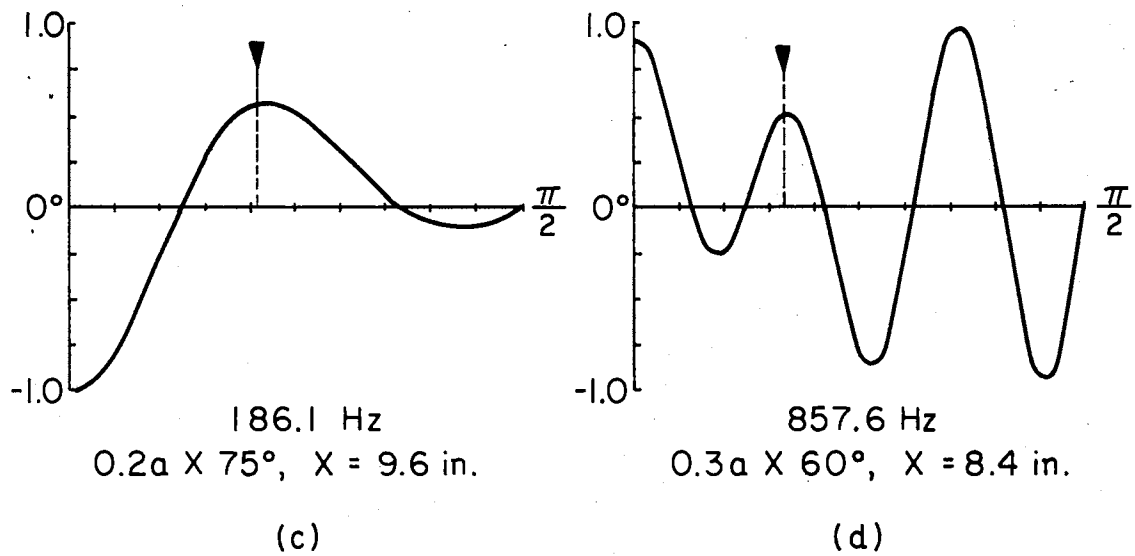


Figure 9. SSA Modes: Circumferential Wave Forms

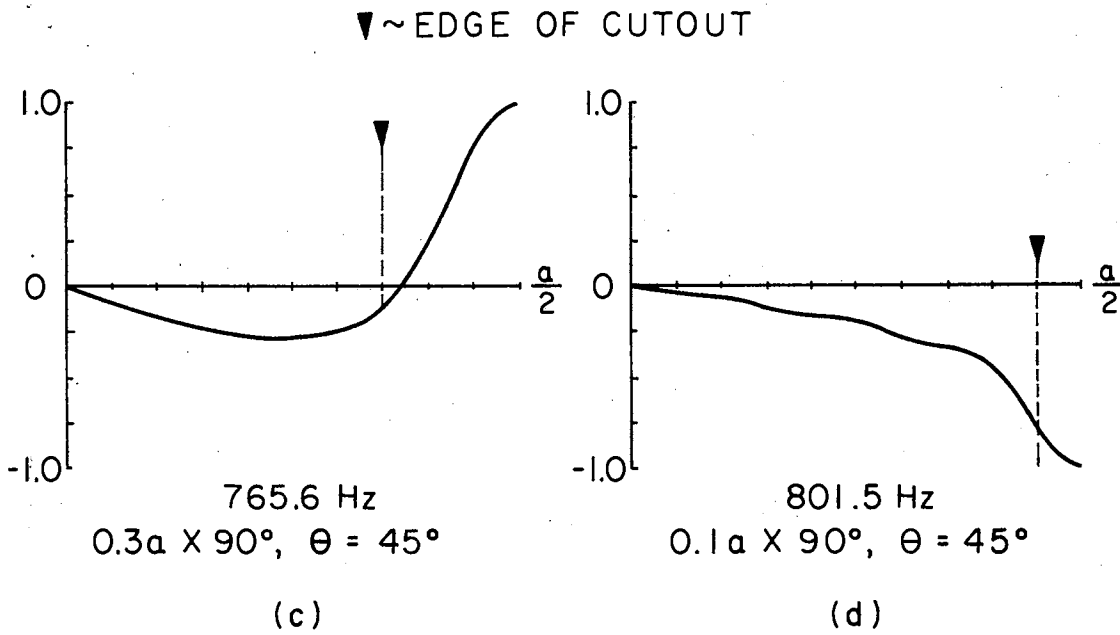
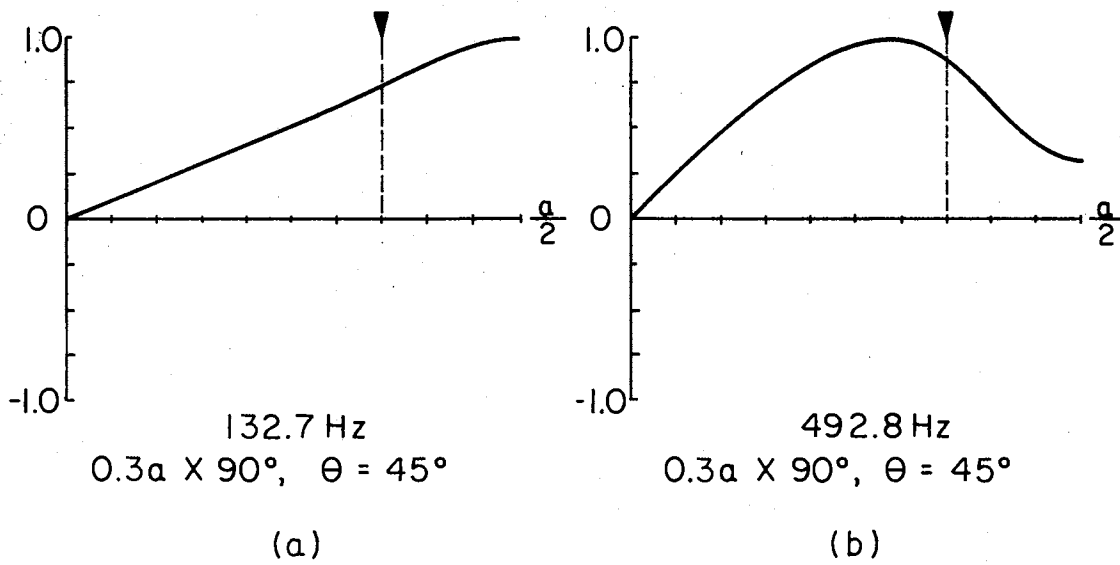


Figure 10: SSS Modes: Axial Wave Forms

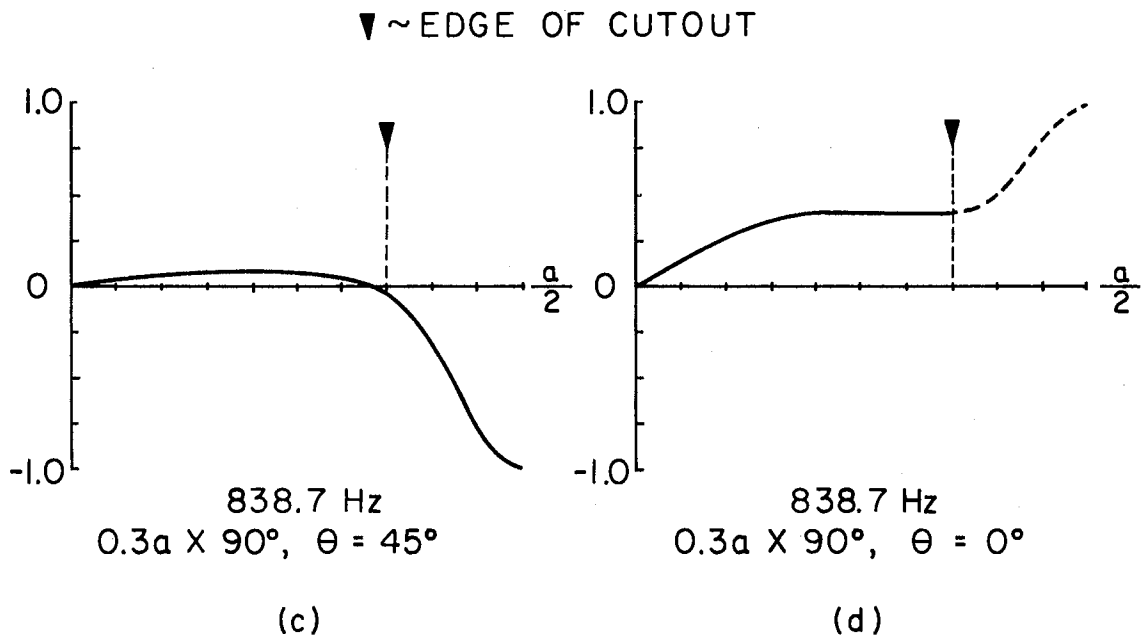
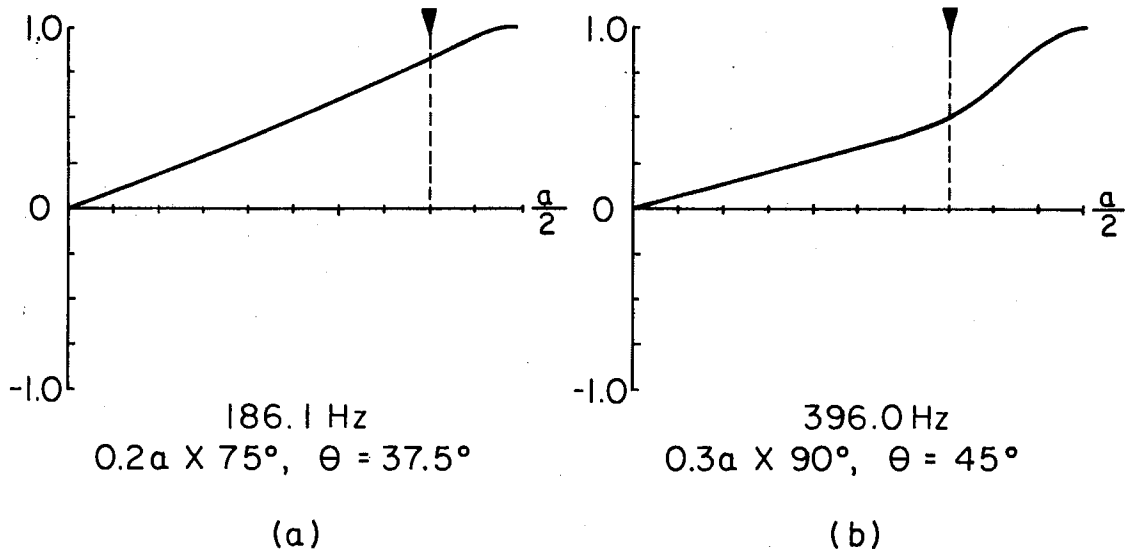


Figure 11. SSA Modes: Axial Wave Forms

the $\theta = 90^\circ$ plane. The notation 'SSA' refers to mode shapes which are antisymmetric about the $\theta = 90^\circ$ plane and symmetric about the other two planes. The circumferential wave forms are, in general, sinusoidal in appearance with varying amplitude. Some showed a sinusoidal variation on which a linear variation is superimposed, for example, see (b) in Figure 8.

Figures 10-(a), 11-(a), and 11-(b) show typical axial wave forms in which the displacement varies linearly with the axial coordinate for the most part and then bends inward or outward near the region of the cutout. In Figures 10-(c) and 10-(d) the axial variation of displacement along two generators of the shell are shown for the same frequency. Along the generator $\theta = 45^\circ$ the displacement is small until the cutout is reached and then increases rapidly along the edge of cutout. Along the generator $\theta = 0^\circ$, the displacement increases initially and then becomes constant till the edge of cutout. This is an example of how the wave forms depend on the axial or circumferential station at which they are plotted.

It is interesting to note that maximum amplitudes were reached not only near the region of the cutouts, but also in regions away from the cutouts. Figure 8-(c) shows a circumferential wave form in which the amplitude reaches a minimum near the cutout and reaches a maximum midway between the two cutouts. Such an observation was also made in Reference (1).

Effect of Varying the Location of Cutout
on the Modes and Frequencies

This section presents a study made of the influence of cutout on the modes and frequencies as the location of cutout is varied along the length of the cylinder. The same cylinder model as in the previous section will be considered, that is, a cylinder with two identical rectangular cutouts located diametrically opposite. The dimensions of the cutouts are kept constant at a span of $0.2a$ and an angle of 90° . When the cutouts are displaced from their centrally located positions, the shell loses its axial symmetry. Thus both even and odd terms have to be considered for the longitudinal terms in the displacement series. This naturally limited the accuracy of the results obtainable for a given size of the matrices. The numerical values obtained for the lowest ten frequencies for different locations of the cutouts are presented in Table VIII. The frequencies have been simply arranged in ascending numerical order along with their dominant wave forms given by the notation (m^*, n^*) . The results presented here for the case of centrally located cutouts ($a_c/a = 0$) are less accurate than those presented in Table VI, but are consistent with the rest of the results presented in Table VIII.

It is interesting to note that displacing the cutouts from the center of shell in the axial direction had a small influence on most of the frequencies including the fundamental frequency. Also, the dominant

TABLE VIII
 EFFECT OF CUTOUT LOCATION ON THE
 FREQUENCIES OF A SHELL ^{a)}
 (CUTOUT SIZE = $0.2a \times 90^\circ$)

Frequencies (Hz.) of θ -Symmetric Modes				
Location of Cutout, a_c/a				
0.0	0.1	0.2	0.3	0.4
272.2 (1, 5)	276.8 (1, 5)	282.6 (1, 5)	282.7 (1, 5)	279.4 (1, 5)
300.8 (1, 4)	309.0 (1, 4)	315.6 (1, 6)	312.0 (1, 6)	302.3 (1, 4)
323.2 (1, 6)	326.8 (1, 6)	331.9 (1, 4)	332.3 (1, 6)	330.4 (1, 6)
403.2 (1, 7)	406.3 (1, 7)	407.3 (1, 7)	406.3 (1, 7)	404.0 (1, 7)
422.0 (1, 3)	441.2 (1, 3)	461.3 (1, 3)	455.7 (1, 3)	435.4 (1, 3)
518.7 (1, 8)	518.6 (1, 8)	517.8 (1, 8)	517.0 (1, 8)	514.7 (1, 8)
587.2 (2, 7)	594.8 (2, 7)	616.3 (2, 7)	614.2 (2, 7)	577.5 (2, 7)
598.4 (2, 6)	608.5 (2, 6)	640.4 (2, 6)	633.3 (2, 6)	588.2 (2, 6)
651.4 (1, 9)	652.5 (1, 9)	654.9 (1, 9)	648.9 (1, 9)	646.5 (1, 9)
654.2 (2, 8)	656.6 (2, 8)	670.6 (2, 8)	666.6 (2, 8)	653.2 (2, 8)

a) The parameters of the shell are given in Table IV. The two cutouts are located diametrically opposite.

wave forms in the mode shapes were preserved in general. Maximum coupling was found between the wave forms with $m^* = 1$, $n^* = 4$ and $m^* = 1$, $n^* = 6$ in the second and third frequencies. The location of the cutouts has a maximum influence on the frequencies with wave numbers (1, 3), (2, 7), and (2, 6). The variation of the frequencies do not exhibit any monotonically increasing or decreasing tendency with increase in the axial location of cutouts from the center of shell. On the other-hand, most of the frequencies seem to increase initially and then decrease with increase in the axial location of the cutouts from the center of shell.

Figure 12 shows the effect of location of the cutouts on the mode shapes. The spanwise variation of the normal displacement is plotted along the $\theta = 45^\circ$ generator which is collinear with an edge of the cutout. The wave forms display how the region of large amplitudes of displacement shifts in the same direction in which the cutouts are moved. The maximum effect of cutout location is found to be on the modes which are axially antisymmetric.

Effect of Cutout on the Shell Response to a Quasi-exponential Type of Air-blast

This section presents the results of a study made on the effect of cutout on the displacement and stress responses of a shell subjected to a time-dependent load. Two shells of the same geometry, one without cutout and another with a doubly symmetric $0.2a \times 45^\circ$ cutout, are

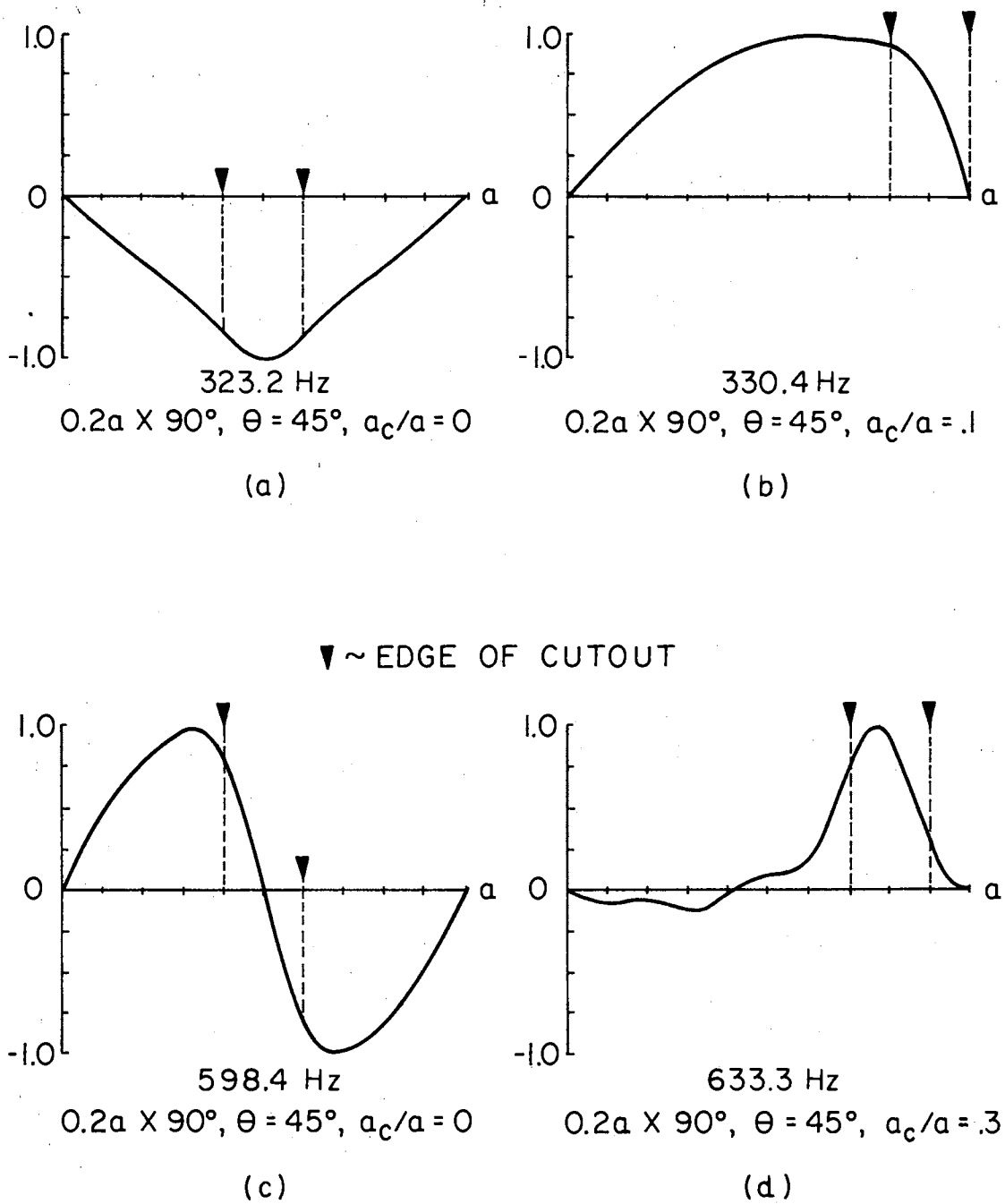


Figure 12. Axial Wave Forms Showing the Effect of Cutout Location on the Mode Shapes

subjected to a quasi-exponential type of air-blast with a sinusoidal variation along the span and a cosinusoidal variation around half the periphery. Figure 13 describes all the structural and loading data considered for the transient analysis. In the displacement series, seven successive terms (odd) were included in the spanwise direction and six successive terms in the peripheral direction. The numerical integration was performed using two different values, namely 0.001 and 0.01 for the error bounds on the truncation error associated with each of the variables. This corresponds to a maximum time step of about 2.5 μ secs. in the former case and about 5 μ secs. in the latter case. The two sets of results agreed within nearly four significant digits for the normal displacement as well as stresses. The time domain solution is performed up to 0.22 msec., which is less than 20% of the blast duration. The computational time involved is about 20 minutes for this solution time interval.

Figures 14, 15, 16 and 17 show plots of various quantities along the generator at $\theta = 0^\circ$ for both the shell without cutout and the shell with the cutout, at $t = 0.22$ msec. These figures display how the response of the shell with the cutout differs significantly from that of the complete shell. In the case of the shell without the cutout the normal displacement, the membrane and bending stresses vary as a single half sine wave along the axis, thus closely following the axial pressure profile. The cutout effects a marked deviation from this smooth behavior. For example, the normal displacement is inward initially and then be-

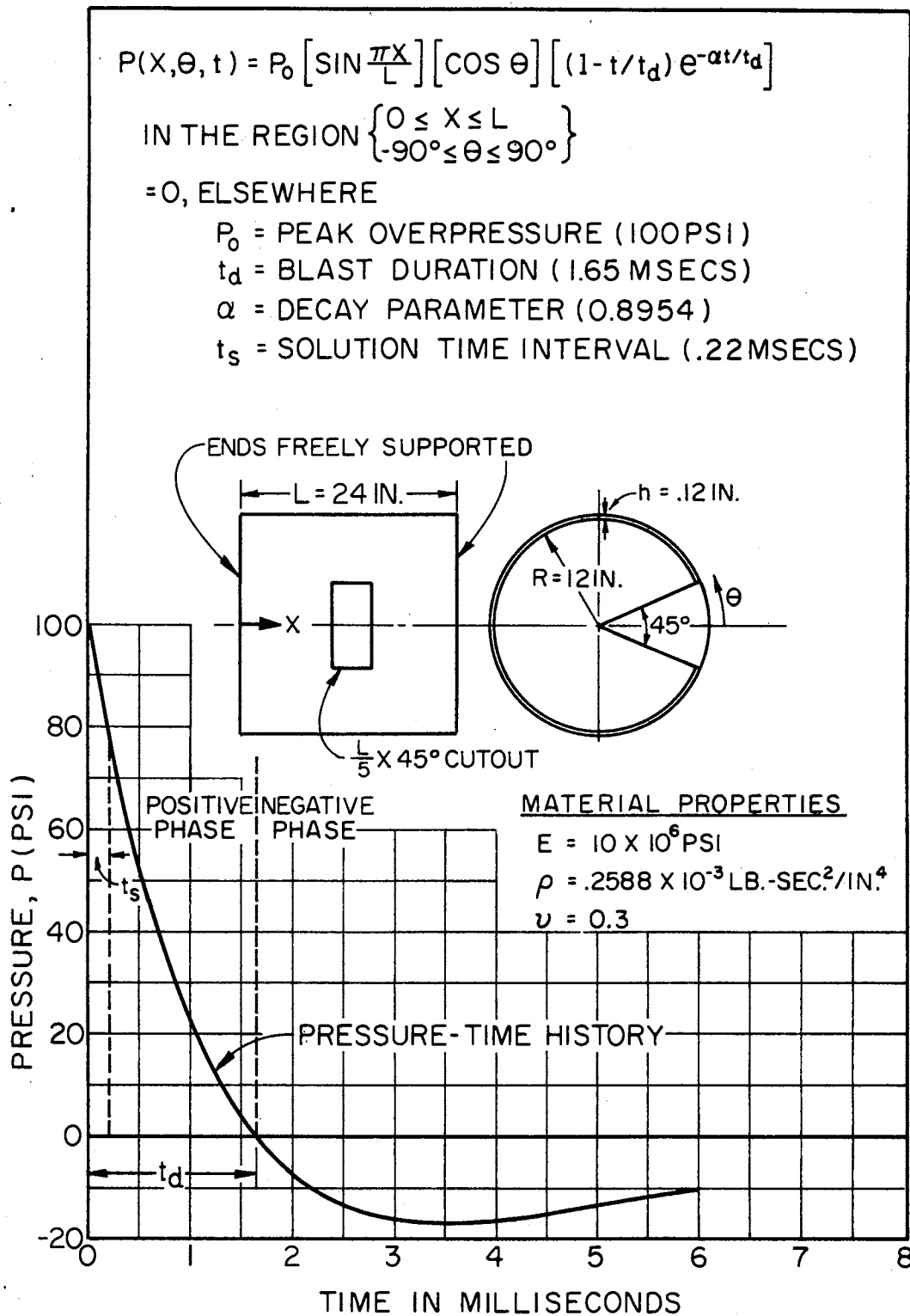


Figure 13. Description of Input Data for Transient Analysis

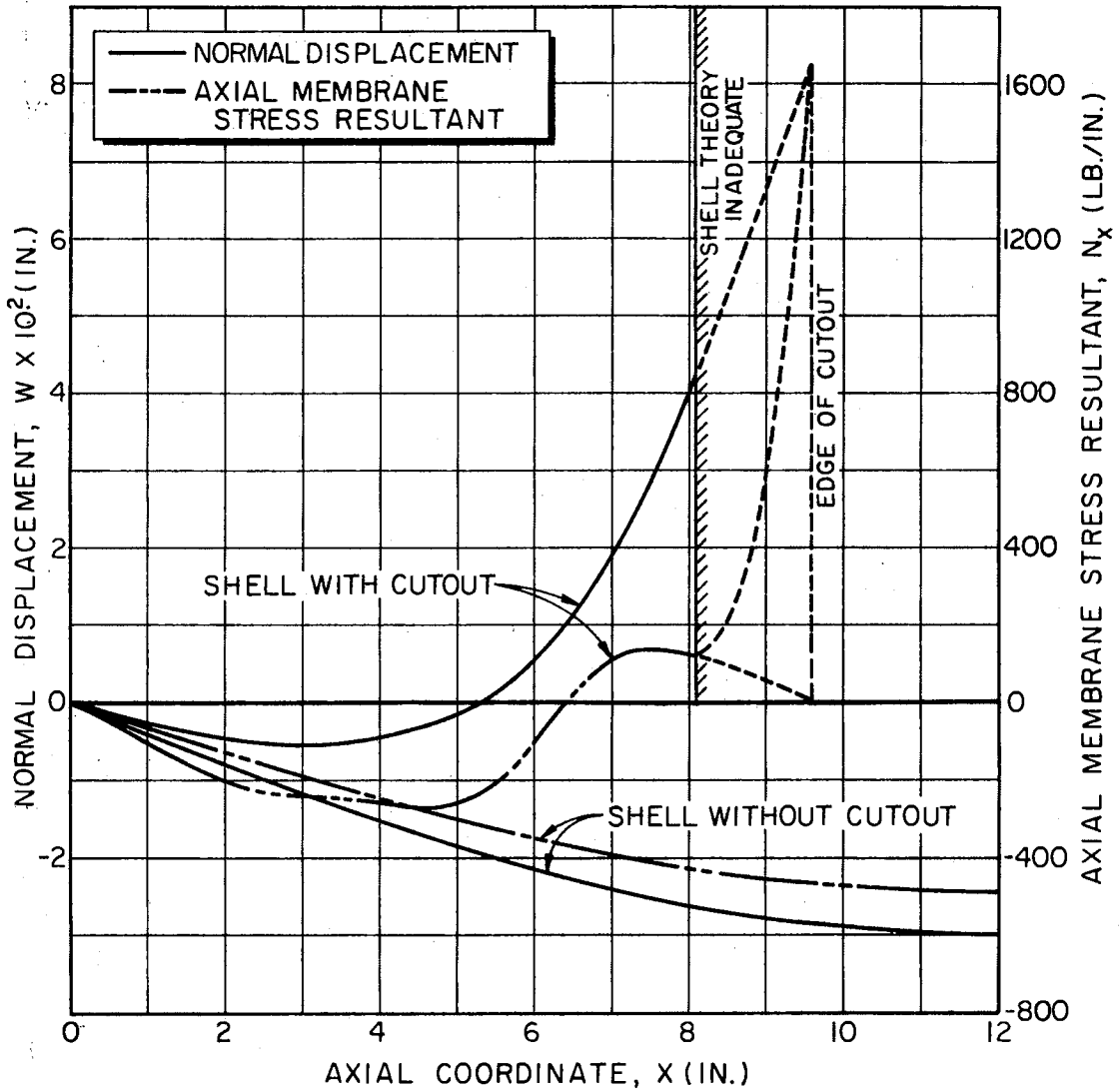


Figure 14. Normal Displacements and Axial Membrane Stress Resultants along the Generator at $\theta = 0^\circ$ ($t = .22$ msecs.)

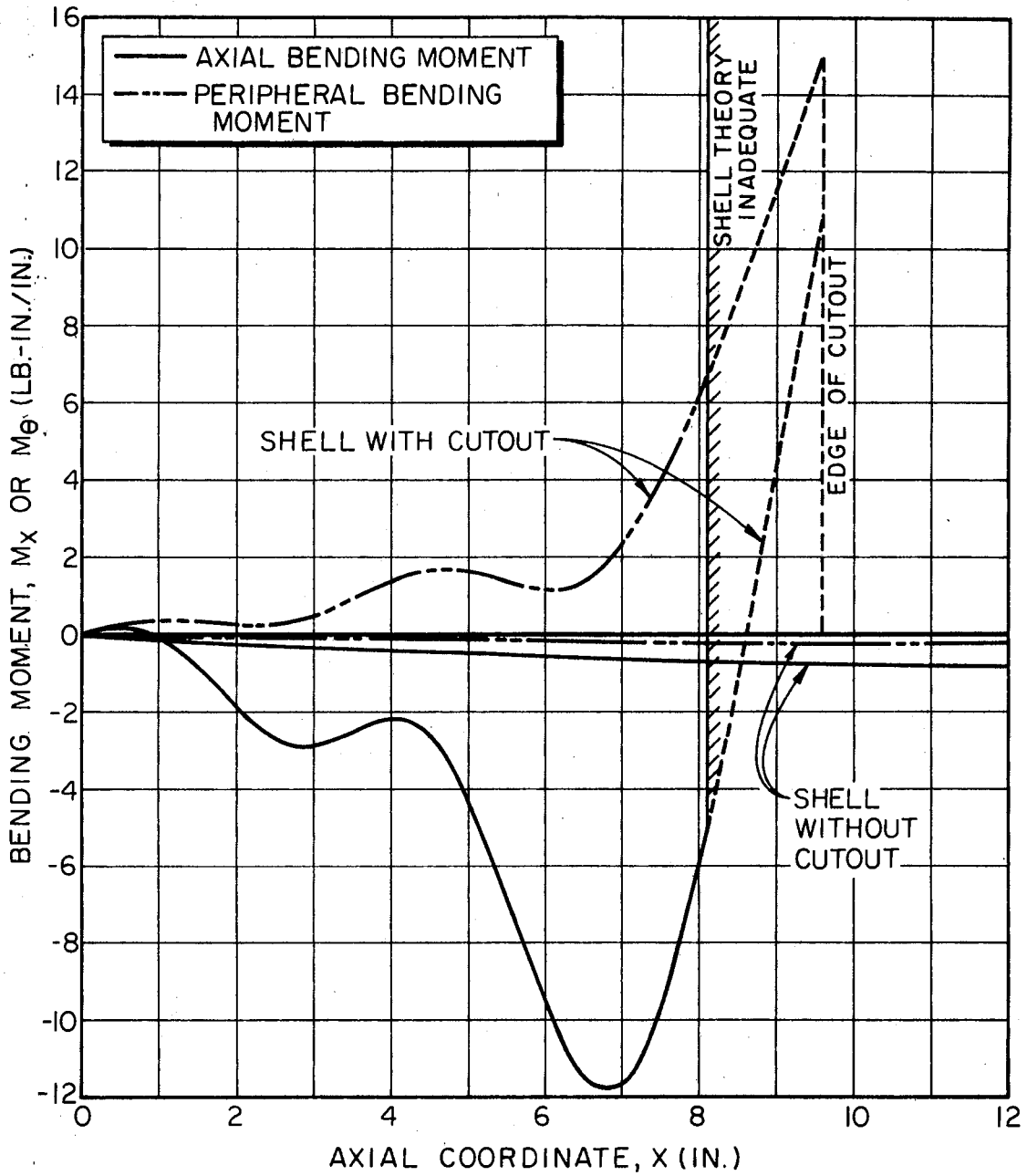


Figure 15. Axial and Peripheral Bending Stress Resultants along the Generator at $\theta = 0^\circ$ ($t = .22$ msec.)

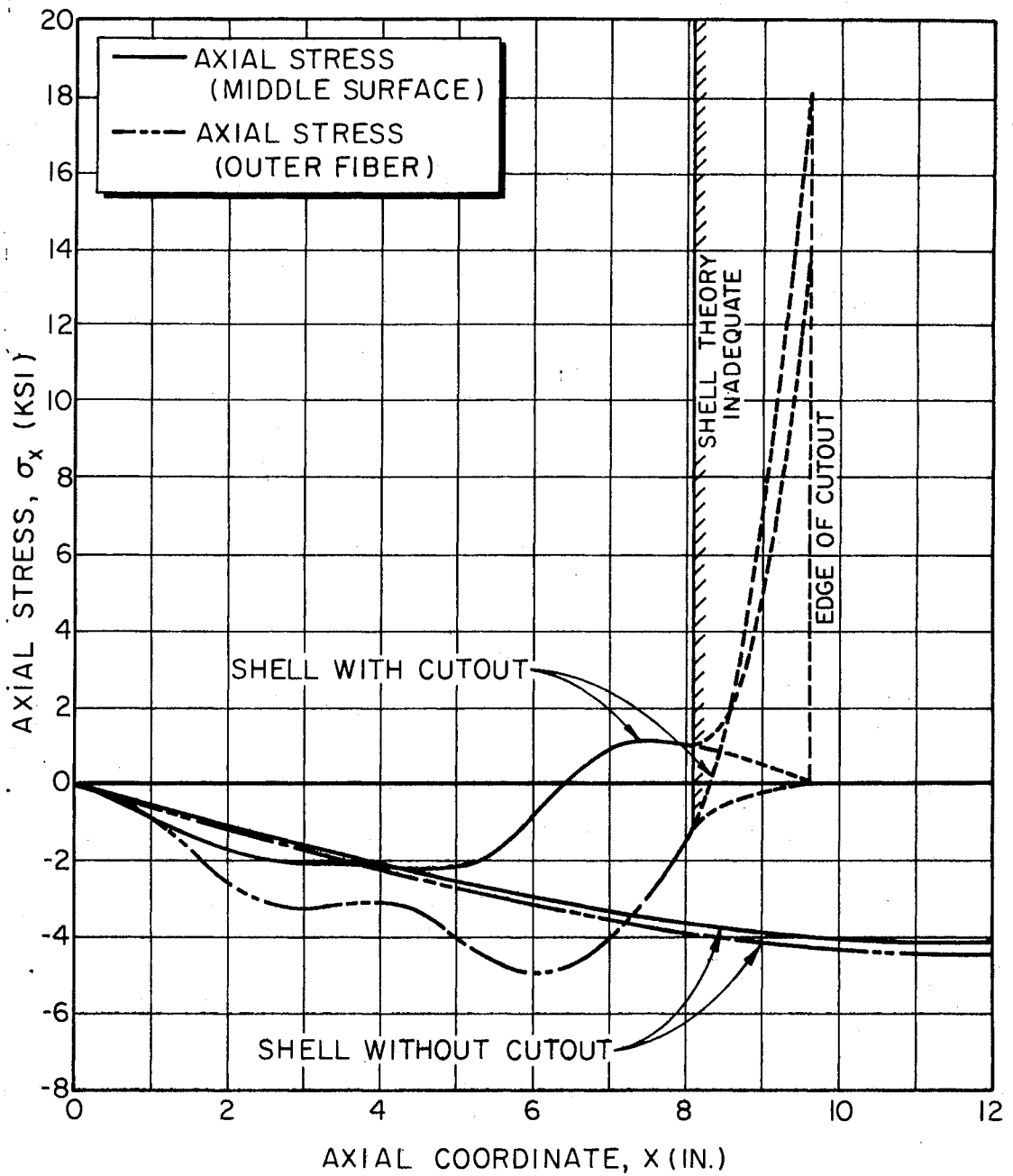


Figure 16. Membrane and Bending Stresses along the Generator at $\theta = 0^\circ$ ($t = .22$ msec.)

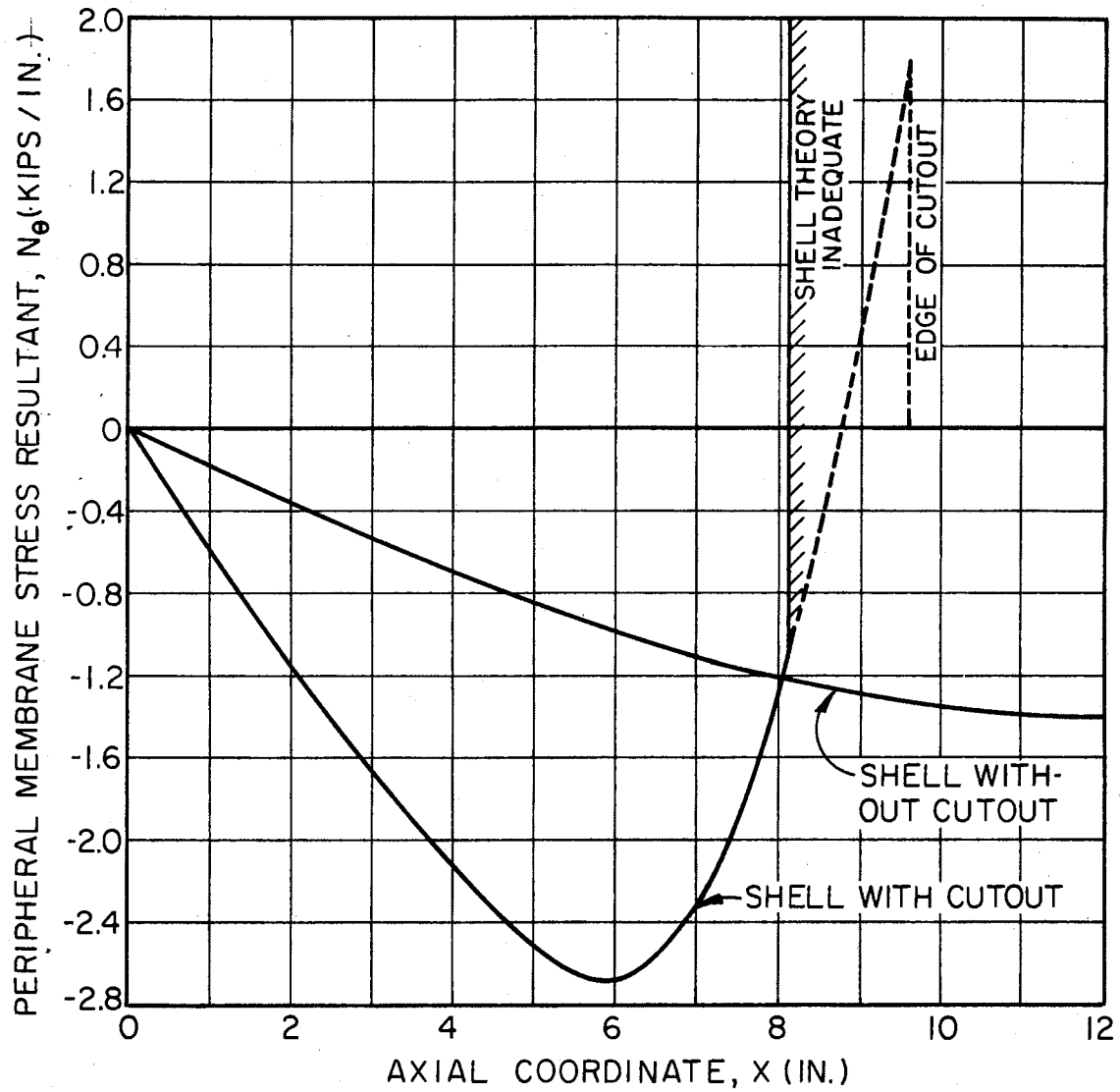


Figure 17. Peripheral Membrane Stress Resultants along the Generator at $\theta = 0^\circ$ ($t = .22$ msec)

gins to increase outward rapidly in an almost straight-line fashion towards the edge of cutout (Figure 14). Thus the displacement in the neighborhood of the cutout is out of phase with the pressure. The reason for this is better understood by referring to Figure 18 which shows a comparison between the normal displacement-time variations of the two shells at a point "A" near the edge of cutout. During a period of 0.22 msec. the normal displacement has hardly completed one-quarter of a cycle for the complete shell, where as it has completed one-half cycle for the shell with cutout. Physically this means that the cutout causes an increased participation of higher modes in the response.

Figures 14 and 15 indicate that the axial membrane stress resultant (N_x) and the axial bending stress resultant (M_x) do not satisfy the stress-free boundary conditions at the edge of cutout. On the other-hand they tend to increase rapidly in the neighborhood of the cutout. The admissible functions used in this study do not, of course, satisfy the kinetic boundary conditions at the free edges of the cutout. These are to be satisfied in a limiting sense as a by-product of minimizing the action integral with respect to the undetermined time-dependent generalized coordinates in the displacement series. The degree of success to which this is achieved is, in general, hard to predict. In the present case, the shell is discontinuous at each point along the contour of the cutout; but the displacement functions are continuous in the whole domain: $0 \leq x \leq a$, $-\pi \leq \theta \leq \pi$. This appears to be rather a

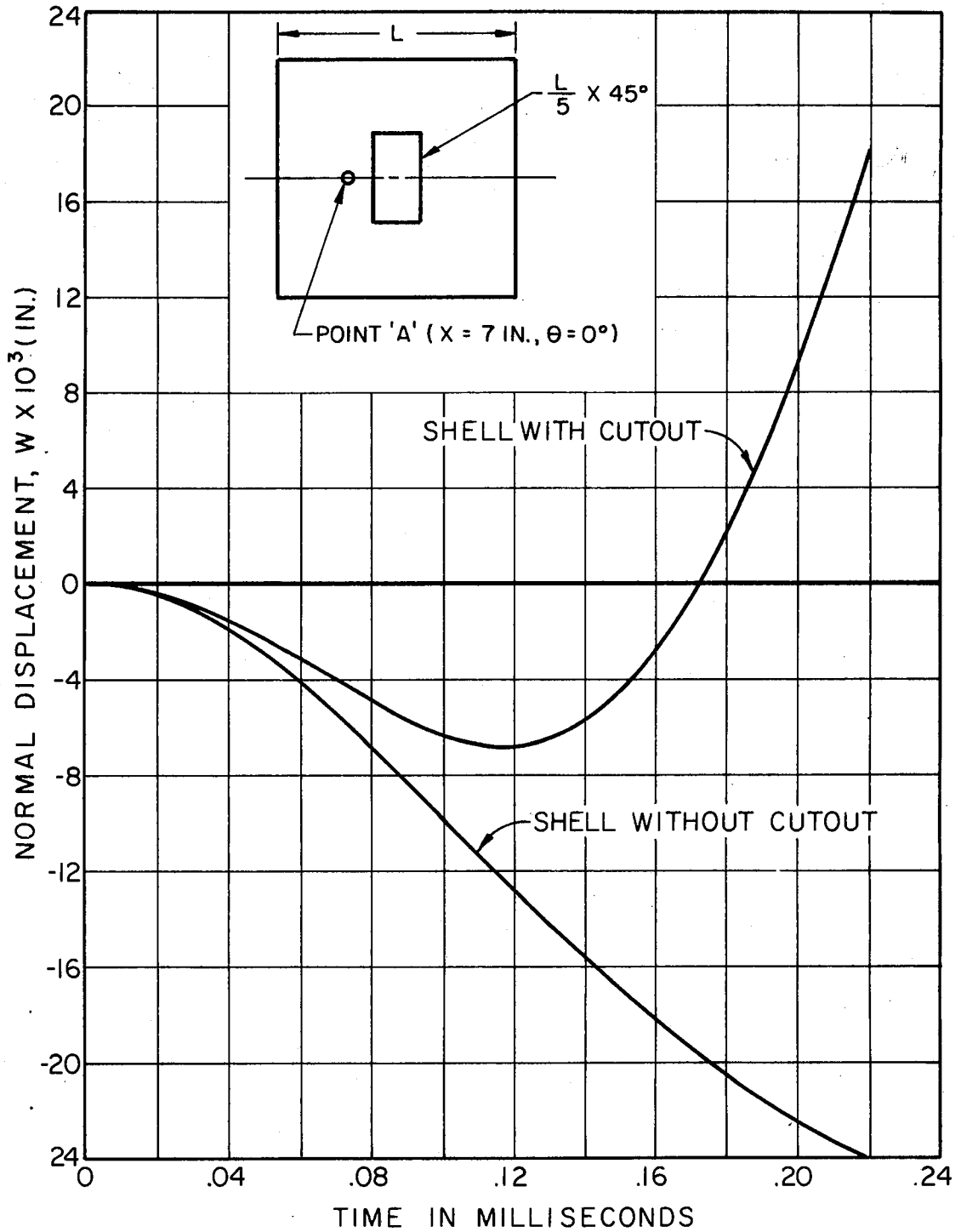


Figure 18. Normal Displacement Responses at $x = 7 \text{ in.}$, $\theta = 0^\circ$ for $t \leq .22 \text{ msec.}$

tight situation for the Rayleigh-Ritz method to handle.

The above discussion points towards the fact that the results of the present analysis are to be interpreted carefully in the region very close to the cutout. The displacement functions are continuous across and defined in the region of the cutout, and the analysis does give displacements and stresses in this region as well. These results, although not usable for the present study, reflect the fact that the analysis treats the region of the cutout as being covered by a membrane of zero thickness. However, the truncated displacement series is not strong enough to account for the sudden reduction in thickness at the edges of the cutout. It may be said that the solution at hand corresponds roughly to a case in which the thickness of the shell is brought to zero gradually in a region which extends beyond the edges of the cutout. Thus the present analysis is inadequate to determine the response in this region. Another significant factor is that the shell theory used does not take into account the effect of the transverse shear stresses on the deformation. As in the case of plates with holes, the transverse shear stresses may be large in the vicinity of the cutout.

In Figures 14, 15, 16 and 17 this region is roughly identified as "shell theory inadequate" for want of further insight and is treated accordingly in making general observations. A basis for isolating this region is found in Figure 14, where the curve for N_x appears to approach zero before increasing near the edge of cutout. Also the curve is modified as shown to bring it back to zero at the edge of cutout.

A similar thing is done in Figure 16 for the curves representing the axial membrane and bending stresses. This modification, although somewhat artificial, forces the curves to conform to a physically meaningful behavior.

Figure 16 indicates that for the complete shell a peak axial membrane stress of about -4 ksi is reached at the center of shell. For the shell with cutout it is about -2 ksi occurring at about one-fifth span, thus indicating about fifty percent reduction. This is because, in the latter case in addition to the ends of the shell the edges of the cutout are also free to move in the axial direction. The situation is reversed for the peripheral membrane stress resultant (N_{θ}) as may be seen in Figure 17. This is not surprising because the shell is closed in that direction.

The amount of bending which the two shells undergo is shown in Figure 15. The complete shell undergoes little bending relative to the shell with the cutout. In the latter case a large peak is reached in the axial bending moment. Figure 16 shows how the axial stress in the outer fiber for the shell with the cutout, is significantly affected by this bending.

CHAPTER V

SUMMARY, CONCLUSIONS AND RECOMMENDATIONS

A method of analysis has been presented to determine the static response, free vibration characteristics and transient response of noncircular stiffened cylindrical shells with rectangular cutouts. The stiffeners were treated as discretely located. This method was based on the Rayleigh - Ritz technique using Love's first approximation theory for the shell portion and the Bernoulli theory of bending for the stiffeners. Beam characteristic (axially) and trigonometric (circumferentially) functions were used in the displacement series. The resulting equations of motion were solved numerically by Fourth Order Runge-Kutta method with automatic step-size control.

The specific items of study made using this method are as follows:

1. The results on free vibrations of stiffened circular cylindrical shells without cutouts were compared and found to be in good agreement with those of the preceding work, of which the present work is an extension.

2. The results obtained from the present method of analysis on

static and dynamic response of unstiffened freely supported shells were found to be in satisfactory agreement with those obtained by other investigators using other methods.

3. Several special cases of shells with cutouts equivalent to complete shells or curved panels, were studied with success with regard to free vibration characteristics because of scarcity of published results on the dynamic response of shells with cutouts.

4. The influence of size of cutout on the natural frequencies and mode shapes of freely supported unstiffened shells was investigated.

5. A study was made to determine the effect of cutout location on the natural frequencies and mode shapes of an unstiffened freely supported shell.

6. A transient response analysis was performed on two freely supported unstiffened shells, one without cutout and the other with a cutout to study the effect of cutout on the displacement and stress responses to a quasi-exponential type of air-blast.

The major observations and conclusions from this study are listed below.

1. In general, the cutouts tend to decrease the frequencies. This effect increases with increase in the size of cutout. The largest effect is found to be on the fundamental frequency. Physically this means that introducing a cutout in a shell reduces the stiffness to a greater extent than does mass.

2. The cutout has an effect of coupling the distinct axial and circumferential wave forms of an otherwise complete shell. This effect is more predominant on the circumferential wave forms. In some cases, as a result of this, identification of the mode shape by the wave numbers becomes difficult and, even if done it is only nominal and just for the sake of convenience.

3. The maximum amplitudes in the mode shapes were reached not only at points near the edges of cutout but also at points away from them.

4. The location of cutout is found to have a less significant effect on the frequencies. Axially antisymmetric mode shapes are the ones significantly affected by the location of cutout.

5. The presence of cutout results in an increased participation of higher modes in the response of a shell subjected to an air-blast type of transient load.

6. The introduction of cutout causes the shell to undergo significant flexure under an air-blast type of transient load.

7. The Rayleigh-Ritz method as applied to a shell with cutout, with no improvement in the displacement functions to handle discontinuities is a more convenient analytical tool for estimating the overall behavior of the shell than one for obtaining the stress behavior in the region very close to the cutout.

8. A shell theory which neglects the effects of transverse shear stresses on the shell deformation is inadequate to predict the shear

distribution in the region very close to the cutout.

The following recommendations for further study are made:

1. The results using this method of analysis should be compared with those obtainable by finite element and finite difference methods to establish the relative computational efficiencies.
2. Experiments or a search for experimental data should be conducted for verifying the results of this study.
3. The possibility of increasing the capability of the Rayleigh-Ritz method to deal with cutouts should be explored by developing displacement functions which allow for singular behavior in the neighborhood of cutouts.
4. The present method of analysis should be profitably extended to include the effects of transverse shear stresses on the shell deformation.

BIBLIOGRAPHY

- (1) Brogan, F., K. Forsberg and S. Smith. "Dynamic Behavior of a Cylinder With a Cutout." AIAA Journal, Vol. 7, No. 5 (May, 1969), pp. 903-911.
- (2) Malinin, A. A. "Kolebaniia obolochek vrashcheniia s otverstiiami" (Vibrations of Shells of Revolution With Holes). Mashinostroenie, No. 7 (1971), pp. 22-27.
- (3) Kraus, H. Thin Elastic Shells. New York: John Wiley & Sons, Inc., 1967.
- (4) Meirovich, L. Analytical Methods in Vibrations. New York: The MacMillan Company, 1967.
- (5) Przemieniecki, J. S. Theory of Matrix Structural Analysis. New York: McGraw-Hill, 1968.
- (6) Sheng, J. "The Response of a Thin Cylindrical Shell to Transient Surface Loading." AIAA Journal, Vol. 3, No. 4 (April, 1965), pp. 701-709.
- (7) Bushnell, D. "Dynamic Response of Two-Layered Cylindrical Shells to Time-Dependent Loads." AIAA Journal, Vol. 3, No. 9 (Sept., 1965), pp. 1698-1703.
- (8) Bushnell, D. "Axisymmetric Dynamic Response of a Ring-Supported Cylinder to Time-Dependent Loads." Journal of Spacecraft and Rockets, Vol. 3, No. 9 (Sept., 1966), pp. 1369-1376.
- (9) Klosner, J. M. "Free and Forced Vibrations of a Long Non-circular Cylindrical Shell." PIBAL Report No. 561, Sept. 1960.
- (10) Basdekas, N. J., and M. Chi. "Dynamic Response of Plates With Cutouts." Shock and Vibration Bulletin, 41, Pt. 7 (December, 1970), pp. 29-35.

- (11) Earnest, L. D. "Kutta Integration with Step Size Control." Report No. 6D-355. Cambridge: M. I. T. Lincoln Laboratory, October, 1957.
- (12) Boyd, D. E. and C. K. P. Rao. "A Theoretical Analysis of the Free Vibrations of Ring- and/or Stringer-Stiffened Elliptical Cylinders with Arbitrary End Conditions, Volume I - Analytical Derivation and Applications." NASA CR-2151, February 1973.
- (13) Boyd, D. E. and R. L. Brugh. "On the Free Vibrations of Non-circular Cylindrical Shell Structures." Shock and Vibration Digest, Vol. 4, Issue 11 (November, 1972), pp. 1-11.
- (14) Brugh, R. L. "An Evaluation of Analytical Methods Using the Rayleigh-Ritz Approach for the Free Vibration of Stiffened Noncircular Cylindrical Shells." (Ph.D. thesis, Oklahoma State University, May 1973.)
- (15) Timoshenko, S. Theory of Plates and Shells. 2nd ed., New York: McGraw-Hill, 1959.
- (16) Sewall, J. L., W. M. Thompson, Jr. and C. G. Pusey. "An Experimental and Analytical Vibration Study of Elliptical Cylindrical Shells." NASA TN D-6089, February 1971.
- (17) Egle, D. M. and K. E. Soder, Jr. "A Theoretical Analysis of the Free Vibration of Discretely Stiffened Cylindrical Shells With Arbitrary End Conditions." NASA CR-1316, June 1969.
- (18) Chang, T. C. and R. R. Craig, Jr. "On Normal Modes of Uniform Beams." EMRL 1068. Texas: Engg. Mechs. Res. Lab, Univ. of Texas at Austin, January, 1969.
- (19) Felgar, R. P., Jr. "Formulas for Integrals Containing Characteristic Functions of a Vibrating Beam." Circular No. 14. Austin: Bureau of Engr. Res., University of Texas, 1950.
- (20) IBM Application Program System/360 Scientific Subroutine Package (360A-CM-03X) Version III Programmer's Manual. Fourth Edition. New York: IBM, 1968.
- (21) Wilkinson, J. H. The Algebraic Eigenvalue Problem. Oxford: Clarendon Press, 1965, p. 337.
- (22) Private Communication with Dr. J. P. Chandler, Associate Professor, Dept. of Computer Science, Oklahoma State Univer-

sity, Stillwater.

- (23) Peterson, M. R. "A Study of the Effects of a Longitudinal, Interior Plate on the Free Vibrations of Circular Cylindrical Shells." (Ph.D. thesis, Oklahoma State University, December 1973).

APPENDIX A

DERIVATION OF THE STIFFENER SHELL

COMPATIBILITY RELATIONS

The derivation of the stiffener-shell compatibility relations are based on the following assumptions:

1. The stiffeners are attached to the shell along a single line of attachment.
2. A stiffener cross section normal to the line of attachment before deformation remains normal to the line of attachment after deformation.
3. The components of rotation transferred from the shell middle surface to stiffeners at any point of attachment are small.

As a result of the first two assumptions, it follows that each cross-section of a stiffener is translated and rotated as a rigid body and is not subjected to warp.

According to the third assumption, the displacement vector of any point in the cross-section of the i^{th} stiffener can be written as

$$\{q\}_i = \{q\}_{ci} + \begin{bmatrix} 0 & -\varphi_z & \varphi_\theta \\ \varphi_z & 0 & -\varphi_x \\ -\varphi_\theta & \varphi_x & 0 \end{bmatrix} \times \{\Omega\}_{i/ci} \quad (\text{A.1})$$

where

$$i = \begin{cases} s & \text{for the stringer} \\ r & \text{for the ring,} \end{cases}$$

$\{q\}_i$ = the displacement vector of an arbitrary point in the cross section of the stiffener,

$\{q\}_{ci}$ = the displacement vector of the centroid of the cross section of the stiffener,

$(\varphi_x, \varphi_\theta, \varphi_z)_{i/ci}$ = the components of the rotation-vector $\{\varphi\}_{i/ci}$ at an arbitrary point in the cross section with respect to axes through the centroid of the stiffener,

$\{\Omega\}_{i/ci}$ = the position vector of an arbitrary point in the cross section relative to the centroid of the cross section of the stiffener.

These vectors may be expanded as follows:

$$\{q\}_i = \begin{pmatrix} u \\ v \\ w \end{pmatrix}_i$$

$$\{q\}_{ci} = \begin{pmatrix} u_c \\ v_c \\ w_c \end{pmatrix}_i$$

(A.2)

$$\{\phi\}_{i/ci} = \begin{Bmatrix} \phi_x \\ \phi_\theta \\ \phi_z \end{Bmatrix}_{i/ci}$$

$$\{\Omega\}_{s/cs} = \begin{Bmatrix} 0 \\ y'_s \\ z'_s \end{Bmatrix} \quad (\text{See Figure 2}) \quad (\text{A.2})$$

$$\{\Omega\}_{r/cr} = \begin{Bmatrix} x'_r \\ 0 \\ z'_r \end{Bmatrix} \quad (\text{See Figure 3})$$

The displacement vector of the centroid of the i^{th} stiffener can be written as

$$\{q\}_{ci} = \{q\}_0 + \begin{bmatrix} 0 & -\phi_z & \phi_\theta \\ \phi_z & 0 & -\phi_x \\ -\phi_\theta & \phi_x & 0 \end{bmatrix}_{ci/o} \times \{\Omega\}_{ci/o}, \quad (\text{A.3})$$

where

$\{q\}_0$ = the displacement vector of an arbitrary point on the middle surface of the shell lying on the line of attachment,

$(\phi_x, \phi_\theta, \phi_z)_{ci/o}$ = the components of the rotation-vector $\{\phi\}_{ci/o}$ at the centroid of the cross section of the i^{th} stiffener relative to the point of attachment,

$\{\Omega\}_{ci/o}$ = the position vector of the centroid of the cross section of the i^{th} stiffener relative to the point of attachment.

These vectors may be expanded as follows:

$$\{q\}_o = \begin{pmatrix} u \\ v \\ w \end{pmatrix}_o$$

$$\{\phi\}_{ci/o} = \begin{pmatrix} \phi_x \\ \phi_\theta \\ \phi_z \end{pmatrix}_{ci/o} \quad (\text{A.4})$$

$$\{\Omega\}_{cs/o} = \begin{pmatrix} 0 \\ -y_s \\ -z_s \end{pmatrix} \quad (\text{See Figure 2})$$

$$\{\Omega\}_{cr/o} = \begin{pmatrix} -x_r \\ 0 \\ -z_r \end{pmatrix} \quad (\text{See Figure 3})$$

After equation (A.3) is substituted into Equation (A.1), the following compatibility relations can be written:

$$\begin{aligned}
 \{q\}_i &= \{q\}_o + \begin{bmatrix} 0 & -\varphi_z & \varphi_\theta \\ \varphi_z & 0 & -\varphi_x \\ -\varphi_\theta & \varphi_x & 0 \end{bmatrix}_{ci/o} \times \{\Omega\}_{ci/o} \\
 &+ \begin{bmatrix} 0 & -\varphi_z & \varphi_\theta \\ \varphi_z & 0 & -\varphi_x \\ -\varphi_\theta & \varphi_x & 0 \end{bmatrix}_{i/ci} \times \{\Omega\}_{i/ci}
 \end{aligned} \tag{A.5}$$

From the second assumption, it follows that

$$\{\varphi\}_{ci/o} = \{\varphi\}_{i/ci} = \{\varphi\}_o \tag{A.6}$$

where

$\{\varphi\}_o$ = the angle of rotation vector of the middle surface of the shell at the point of attachment.

This vector may be expanded as:

$$\{\varphi\}_o = \begin{pmatrix} \varphi_x \\ \varphi_\theta \\ \varphi_z \end{pmatrix}_o \tag{A.7}$$

where

$$\varphi_x = \frac{w, \theta}{R} - \frac{v}{R}$$

$$\varphi_\theta = -w, x$$

$$\varphi_z = \begin{cases} \frac{-u, \theta}{R} & \text{for rings} \\ v, x & \text{for stringers} \end{cases}$$

After Equations (A.2), A.4) and (A.7) are substituted into Equation (A.5), the stringer-shell compatibility relations can be written in terms of displacements of the shell as follows:

$$\{q\}_s = \left\{ \begin{array}{l} u - (\bar{z}_s + z'_s)w_{,x} - (\bar{y}_s + y'_s)v_{,x} \\ v - (\bar{z}_s + z'_s) \left(\frac{w_{,\theta}}{R} - \frac{v}{R} \right) \\ w + (\bar{y}_s + y'_s) \left(\frac{w_{,\theta}}{R} - \frac{v}{R} \right) \end{array} \right\} \quad (\text{A.8})$$

Likewise, the ring-shell compatibility relations can be written as:

$$\{q\}_r = \left\{ \begin{array}{l} u - (\bar{z}_r + z'_r)w_{,x} \\ v - (\bar{x}_r + x'_r) \frac{u_{,\theta}}{R} - (\bar{z}_r + z'_r) \left(\frac{w_{,\theta}}{R} - \frac{v}{R} \right) \\ w + (\bar{x}_r + x'_r)w_{,x} \end{array} \right\} \quad (\text{A.9})$$

APPENDIX B

BEAM MODE FUNCTIONS

The characteristic modes of vibration of a uniform beam are used for the longitudinal functions in the assumed displacement series. These functions are listed below.

1. Both ends freely supported

$$\Phi_m(x) = \sqrt{2} \sin \frac{m \pi x}{a}$$

2. Both ends clamped

$$\Phi_m(x) = \frac{1}{2} \left[\delta_m e^{\beta_m x} + \gamma_m e^{-\beta_m x} \right] - \cos \beta_m x + \alpha_m \sin \beta_m x$$

3. One end clamped, other end free

$$\Phi_m(x) = \frac{1}{2} \left[\delta_m e^{\beta_m x} + \gamma_m e^{-\beta_m x} \right] - \cos \beta_m x + \alpha_m \sin \beta_m x$$

4. Both ends free

$$\varphi_0(x) = 1$$

$$\varphi_1(x) = \frac{x}{a} - \frac{1}{2}$$

$$\Phi_m(x) = \frac{1}{2} \left[\delta_m e^{\beta_m x} + \gamma_m e^{-\beta_m x} \right] + \cos \beta_m x - \alpha_m \sin \beta_m x \quad (m \geq 2)$$

The numerical values of the parameters α_m , β_m , γ_m , and δ_m are given in Reference (18).

APPENDIX C

EQUATIONS OF MOTION

The expressions for the variations of the strain and kinetic energies as well as the virtual work of external forces, developed in Chapter II were expressed in terms of the displacement vector $\{f\}$. The introduction of the assumed series for $\{f\}$ and the detailed steps leading to the equations of motion are presented here. The assumed displacement functions are given by Equations (2.19a) to (2.19c) and are expressed concisely in Equation (2.20a).

Substituting Equation (2.20a) in Equation (2.12a)

$$\delta U_o = \int_{S_o} \{\delta q\}^T [N]^T [B]_o^T [D]_o [B]_o [N] \{q\} R d\theta dx \quad (C.1a)$$

$$= \{\delta q\}^T [K]_o \{q\} \quad (C.1b)$$

$$\text{where } [K]_o = \int_{S_o} [N]^T [B]_o^T [D]_o [B]_o [N] R d\theta dx \quad (C.1c)$$

Substituting Equation (2.20a) in Equation (2.13)

$$\delta T_o = - \int_{S_o} \rho_o h \{\delta q\}^T [N]^T [N] \{\dot{q}\} R d\theta dx \quad (C.2a)$$

$$= - \{\delta q\}^T [M]_o \{\ddot{q}\} \quad (C.2b)$$

$$\text{where } [M]_o = \int_{S_o} \rho_o h [N]^T [N] R d\theta dx \quad (\text{C. 2c})$$

Substituting Equation (2.20a) in Equation (2.14a)

$$\delta U_{sl} = \int_{S_{sl}} [\{ \delta q \}^T [N]^T [B]_{sl}^T [D]_{sl} [B]_{sl} [N] \{ q \}] dx \quad \theta = \theta_l \quad (\text{C. 3a})$$

$$= \{ \delta q \}^T [K]_{sl} \{ q \} \quad (\text{C. 3b})$$

$$\text{where } [K]_{sl} = \int_{S_{sl}} ([N]^T [B]_{sl}^T [D]_{sl} [B]_{sl} [N]) dx \quad \theta = \theta_l \quad (\text{C. 3c})$$

$$\delta U_s = \sum_{l=1}^{N_s} \delta U_{sl} = \{ \delta q \}^T [K]_s \{ q \} \quad (\text{C. 3d})$$

$$\text{where } [K]_s = \sum_{l=1}^{N_s} [K]_{sl} \quad (\text{C. 3e})$$

Substituting Equation (2.20a) in Equation (2.15a)

$$\delta T_{sl} = - \int_{S_{sl}} [m_{sl} \{ \delta q \}^T [N]^T [C]_s^T [C]_s [N] \{ \dot{q} \}] dx \quad \theta = \theta_l \quad (\text{C. 4a})$$

$$= \{ \delta q \}^T [M]_{sl} \{ \dot{q} \} \quad (\text{C. 4b})$$

$$\text{where } [M]_{sl} = \int_{S_{sl}} (m_{sl} [N]^T [C]_s^T [C]_s [N]) dx \quad \theta = \theta_l \quad (\text{C. 4c})$$

$$\delta T_s = \sum_{l=1}^{N_s} \delta T_{sl} = - \{ \delta q \}^T [M]_s \{ \dot{q} \} \quad (\text{C. 4d})$$

$$\text{where } [M]_s = \sum_{l=1}^{N_s} [M]_{sl} \quad (\text{C. 4e})$$

Substituting Equation (2.20a) in Equation (2.16a)

$$\delta U_{rk} = \int_{S_{rk}} \left(\{\delta q\}^T [N]^T [B]_{rk}^T [D]_{rk} [B]_{rk} [N] \{q\} \right) R_{cgk} d\theta \quad (C.5a)$$

$$= \{\delta q\}^T [K]_{rk} \{q\} \quad (C.5b)$$

$$\text{where } [K]_{rk} = \int_{S_{rk}} \left([N]^T [B]_{rk}^T [D]_{rk} [B]_{rk} [N] \right) R_{cgk} d\theta \quad (C.5c)$$

$$\delta U_r = \sum_{k=1}^{N_r} \delta U_{rk} = \{\delta q\}^T [K]_r \{q\} \quad (C.5d)$$

$$\text{where } [K]_r = \sum_{k=1}^{N_r} [K]_{rk} \quad (C.5e)$$

Substituting Equation (2.20a) in Equation (2.17a)

$$\delta T_{rk} = \int_{S_{rk}} \left(-m_{rk} \{\delta q\}^T [N]^T [C]_{rk}^T [C]_{rk} [N] \{\dot{q}\} \right) R_{cgk} d\theta \quad (C.6a)$$

$$= \{\delta q\}^T [M]_{rk} \{\dot{q}\} \quad (C.6b)$$

$$\text{where } [M]_{rk} = \int_{S_{rk}} \left(m_{rk} [N]^T [C]_{rk}^T [C]_{rk} [N] \right) R_{cgk} d\theta \quad (C.6c)$$

$$\delta T_r = \sum_{k=1}^{N_r} \delta T_{rk} = - \{\delta q\}^T [M]_r \{\dot{q}\} \quad (C.6d)$$

$$\text{where } [M]_r = \sum_{k=1}^{N_r} [M]_{rk} \quad (C.6e)$$

Substituting Equation (2.20a) in Equation (2.18a) and Equation

(2.18c)

$$\delta W_d = \int_{S_o} \{\delta q\}^T [N]^T \{F\}_d R dx d\theta \quad (C.7a)$$

$$= \{\delta q\}^T \{P\}_d \quad (C.7b)$$

$$\text{where } \{P\}_d = \int_{S_o} [N]^T \{F\}_d R dx d\theta \quad (C.7c)$$

$$\delta W_c = \sum_{i=1}^{N_{cf}} \{\delta q\}^T [N_i]^T \{F_i\}_o \quad (C.7d)$$

$$= \{\delta q\}^T \{P\}_{cf} \quad (C.7e)$$

$$\text{where } \{P\}_{cf} = \sum_{i=1}^{N_{cf}} [N_i]^T \{F_i\}_o \quad (C.7f)$$

Substituting Equations (C.1b), (C.3d) and (C.5d) in Equation

(2.4)

$$\delta U = \{\delta q\}^T [K] \{q\} \quad (C.8a)$$

$$\text{where } [K] = [K]_o + [K]_s + [K]_r \quad (C.8b)$$

Substituting Equations (C.2b), (C.4d) and (C.6d) in Equation

(2.3)

$$\delta T = - \{\delta q\}^T [M] \{\ddot{q}\} \quad (C.9a)$$

$$\text{where } [M] = [M]_o + [M]_s + [M]_r \quad (C.9b)$$

Substituting Equations (C.7b) and (C.7e) in Equation (2.5)

$$\delta W = \{\delta q\}^T \{P\} \quad (C.10a)$$

$$\text{where } \{P\} = \{P\}_d + \{P\}_{cf} \quad (C.10b)$$

Substituting Equations (C. 8a), (C. 9a) and (C. 10a) in Equation

(2. 2)

$$\int_{t_0}^{t_1} \left(- \{\delta q\}^T [M] \{\ddot{q}\} - \{\delta q\}^T [K] \{q\} + \{\delta q\}^T \{P\} \right) dt = 0 \quad (\text{C. 11a})$$

which may be rewritten as

$$\int_{t_0}^{t_1} \{\delta q\}^T \left(-[M] \{\ddot{q}\} - [K] \{q\} + \{P\} \right) dt = 0 \quad (\text{C. 11b})$$

Since the 'q's are independent and the 'δq' are arbitrary, it

follows that

$$[M] \{\ddot{q}\} + [K] \{q\} = \{P\} \quad (\text{C. 12})$$

APPENDIX D

RING FUNCTIONS

The ring longitudinal functions (occurring in the mass and stiffness matrices) used in the present work differ from those given in Appendix E (14) in view of the modified representation of beam mode functions as taken from Chang and Kreig (18) for boundary conditions other than the freely supported one. The original representation as given by Felgar (19) were found to be in error for modes above the fifth (18). The modified ring longitudinal functions are presented here using the same notation as in Reference (14).

In all the following expressions the functions ' Φ ' for the corresponding boundary condition are presented in Appendix B.

For freely supported cylinders:

$$RF_{1,k} = \Phi'_{\bar{m}} \quad \Phi'_m$$

$$RF_{2,k} = \Phi_{\bar{m}} \quad \Phi_m$$

$$RF_{3,k} = \Phi'_{\bar{m}} \quad \Phi_m$$

$$RF_{4,k} = \Phi_{\bar{m}} \quad \Phi'_m$$

For clamped-free cylinders:

The expressions are similar to those for the freely supported case.

For clamped-clamped cylinders:

The expressions are similar to those for the freely supported

case.

For free-free cylinders:

m=0

$$\left. \begin{aligned} RF_{1,k} &= RF_{3,k} = RF_{4,k} = 0 \\ RF_{2,k} &= 1 \end{aligned} \right\} \bar{m} = 0$$

$$\left. \begin{aligned} RF_{1,k} &= RF_{4,k} = 0 \\ RF_{2,k} &= x_k/a - \frac{1}{2} \\ RF_{3,k} &= 1/a \end{aligned} \right\} \bar{m} = 1$$

$$\left. \begin{aligned} RF_{1,k} &= RF_{4,k} = 0 \\ RF_{2,k} &= \Phi_{\bar{m}} \\ RF_{3,k} &= \Phi'_{\bar{m}} \end{aligned} \right\} \bar{m} \geq 2$$

m=1

$$\left. \begin{aligned} RF_{1,k} &= RF_{3,k} = 0 \\ RF_{2,k} &= x_k/a - \frac{1}{2} \\ RF_{4,k} &= 1/a \end{aligned} \right\} \bar{m} = 0$$

$$\left. \begin{aligned} RF_{1,k} &= 1/a^2 \\ RF_{2,k} &= x_k^2/a^2 + \frac{1}{4} - x_k/a \\ RF_{3,k} &= RF_{4,k} = x_k/a^2 - \frac{1}{2}a \end{aligned} \right\} \bar{m} = 1$$

$$\begin{aligned}
 \text{RF}_{1,k} &= \frac{1}{a} \Phi'_{\bar{m}} \\
 \text{RF}_{2,k} &= \left(\frac{x}{a} - \frac{1}{2}\right) \Phi_{\bar{m}} \\
 \text{RF}_{3,k} &= \left(\frac{x}{a} - \frac{1}{2}\right) \Phi'_{\bar{m}} \\
 \text{RF}_{4,k} &= \frac{1}{a} \Phi_{\bar{m}}
 \end{aligned}
 \left. \vphantom{\begin{aligned} \text{RF}_{1,k} \\ \text{RF}_{2,k} \\ \text{RF}_{3,k} \\ \text{RF}_{4,k} \end{aligned}} \right\} \bar{m} \geq 2$$

$m \geq 2$

$$\begin{aligned}
 \text{RF}_{1,k} &= \text{RF}_{3,k} = 0 \\
 \text{RF}_{2,k} &= \Phi_{\bar{m}} \\
 \text{RF}_{4,k} &= \Phi'_m
 \end{aligned}
 \left. \vphantom{\begin{aligned} \text{RF}_{1,k} \\ \text{RF}_{2,k} \\ \text{RF}_{4,k} \end{aligned}} \right\} \bar{m} = 0$$

$$\begin{aligned}
 \text{RF}_{1,k} &= \frac{1}{a} \Phi'_m \\
 \text{RF}_{2,k} &= \left(\frac{x}{a} - \frac{1}{2}\right) \Phi_m \\
 \text{RF}_{3,k} &= \frac{1}{a} \Phi_m \\
 \text{RF}_{4,k} &= \left(\frac{x}{a} - \frac{1}{2}\right) \Phi'_m
 \end{aligned}
 \left. \vphantom{\begin{aligned} \text{RF}_{1,k} \\ \text{RF}_{2,k} \\ \text{RF}_{3,k} \\ \text{RF}_{4,k} \end{aligned}} \right\} \bar{m} = 1$$

For $m \geq 2$, $\bar{m} \geq 2$, the expressions are similar to those for the freely supported case.

$$IX_2 = \frac{1}{\beta_{\bar{m}}^4 - \beta_m^4} \left[\beta_{\bar{m}}^4 \bar{\Phi}_m \bar{\Phi}'_m - \beta_m^4 \Phi_m \Phi'_m - \bar{\Phi}''_m \bar{\Phi}'''_m + \Phi''_m \Phi'''_m \right] \begin{matrix} x_{2i} \\ x_{li} \end{matrix}$$

for $m \neq \bar{m}$

$$IX_3 = \left\{ \begin{array}{l} \frac{1}{4} \left[\bar{\Phi}_m \bar{\Phi}'_m - x(\bar{\Phi}'_m)^2 + 2x\bar{\Phi}_m \bar{\Phi}''_m + \frac{1}{\beta_m^4} \bar{\Phi}''_m \bar{\Phi}'''_m - \frac{x}{\beta_m^4} (\bar{\Phi}'''_m)^2 \right] \begin{matrix} x_{2i} \\ x_{li} \end{matrix} \\ \frac{1}{\beta_{\bar{m}}^4 - \beta_m^4} \left[\beta_m^4 (\bar{\Phi}_m \bar{\Phi}'_m - \bar{\Phi}_m \bar{\Phi}'_m) - \bar{\Phi}''_m \bar{\Phi}'''_m + \Phi''_m \Phi'''_m \right] \begin{matrix} x_{2i} \\ x_{li} \end{matrix} \end{array} \right.$$

for $m \neq \bar{m}$

$$IX_4 = \left\{ \begin{array}{l} \frac{1}{\beta_m^4 - \beta_{\bar{m}}^4} \left[\beta_{\bar{m}}^4 (\bar{\Phi}_m \bar{\Phi}'_m - \bar{\Phi}_m \bar{\Phi}'_m) - \bar{\Phi}''_m \bar{\Phi}'''_m + \Phi''_m \Phi'''_m \right] \begin{matrix} x_{2i} \\ x_{li} \end{matrix} \\ \frac{1}{4} \left[\bar{\Phi}_m \bar{\Phi}'_m - x(\bar{\Phi}'_m)^2 + 2x\bar{\Phi}_m \bar{\Phi}''_m + \frac{1}{\beta_m^4} \bar{\Phi}''_m \bar{\Phi}'''_m - \frac{x}{\beta_m^4} (\bar{\Phi}'''_m)^2 \right] \begin{matrix} x_{2i} \\ x_{li} \end{matrix} \end{array} \right.$$

for $m = \bar{m}$

$$\text{IX}_5 = \left\{ \begin{array}{l} \frac{1}{4} \left[\frac{3}{\beta_m^4} \Phi_m \Phi_m'''' + x \Phi_m'' - \frac{2x}{\beta_m^4} \Phi_m' \Phi_m'''' - \frac{1}{\beta_m^4} \Phi_m' \Phi_m'' \right. \\ \left. + \frac{x}{\beta_m^4} (\Phi_m'')^2 \right] \begin{array}{l} x_{2i} \\ x_{1i} \end{array} \quad \text{for } m = \bar{m} \\ \\ \frac{1}{\beta_{\bar{m}}^4 - \beta_m^4} \left[\Phi_m \Phi_{\bar{m}}'''' - \Phi_{\bar{m}} \Phi_m'''' - \Phi_m' \Phi_{\bar{m}}'''' + \Phi_{\bar{m}}' \Phi_m'' \right] \begin{array}{l} x_{2i} \\ x_{1i} \end{array} \quad \text{for } m \neq \bar{m} \end{array} \right.$$

For both the clamped-free and the clamped-clamped case the integrals IX₁ to IX₅ are identical to those for the freely supported case noting of course, that the corresponding 'Φ',s are to be used.

For the free-free case (for the 'i'th cutout)

m = 0

$$\left. \begin{array}{l} \text{IX}_1 = \text{IX}_2 = \text{IX}_3 = \text{IX}_4 = 0 \\ \text{IX}_5 = x_{2i} - x_{1i} \end{array} \right\} \bar{m} = 0$$

$$\left. \begin{array}{l} \text{IX}_1 = \text{IX}_2 = \text{IX}_3 = \text{IX}_4 = 0 \\ \text{IX}_5 = \frac{1}{2a} [x(x-a)] \end{array} \right\} \bar{m} = 1$$

$$IX_1 = IX_2 = IX_3 = 0$$

$$IX_4 = \left[\Phi'_m \right] \begin{matrix} x_{2i} \\ x_{1i} \end{matrix}$$

$$\overline{m} \geq 2$$

m = 1

$$IX_1 = IX_2 = IX_3 = IX_4 = 0$$

$$IX_5 = \frac{1}{2a} [x(x-a)] \begin{matrix} x_{2i} \\ x_{1i} \end{matrix}$$

$$\overline{m} = 0$$

$$IX_1 = IX_3 = IX_4 = 0$$

$$IX_2 = \frac{1}{a} [x] \begin{matrix} x_{2i} \\ x_{1i} \end{matrix}$$

$$\overline{m} = 1$$

$$IX_5 = \left[\frac{x^3}{3a^2} - \frac{x^2}{2a} + \frac{x}{4} \right] \begin{matrix} x_{2i} \\ x_{1i} \end{matrix}$$

$$IX_1 = IX_3 = 0$$

$$IX_2 = \frac{1}{a} \left[\Phi''_m \right] \begin{matrix} x_{2i} \\ x_{1i} \end{matrix}$$

$$IX_4 = \left[(x \Phi'''_m - \Phi''_m) / a - \Phi'_m / 2 \right] \begin{matrix} x_{2i} \\ x_{1i} \end{matrix}$$

$$IX_5 = \left[(x \Phi''''_m - \Phi'''_m) / a - \Phi''_m / (2 \beta \frac{4}{m}) \right] \begin{matrix} x_{2i} \\ x_{1i} \end{matrix}$$

$$\overline{m} \geq 2$$

$m \geq 2$

$$IX_1 = IX_2 = IX_4 = 0$$

$$IX_3 = [\Phi'_m] \begin{matrix} x_{2i} \\ x_{li} \end{matrix}$$

$$IX_5 = \frac{1}{\beta_m^4} [\Phi_m'''] \begin{matrix} x_{2i} \\ x_{li} \end{matrix}$$

$$\overline{m} = 0$$

$$IX_1 = IX_4 = 0$$

$$IX_2 = \frac{1}{a} [\Phi_m] \begin{matrix} x_{2i} \\ x_{li} \end{matrix}$$

$$IX_3 = [(x\Phi'_m - \Phi'_m)/a - \Phi'_m/2] \begin{matrix} x_{2i} \\ x_{li} \end{matrix}$$

$$IX_5 = \frac{1}{\beta_m^4} [(x\Phi_m''' - \Phi_m''')/a - \Phi_m'''/2] \begin{matrix} x_{2i} \\ x_{li} \end{matrix}$$

$$\overline{m} = 1$$

The integrals IX_1 to IX_5 for $m \geq 2$ and $\overline{m} \geq 2$ are identical to those for the freely supported case, noting of course that the corresponding Φ 's are to be used.

APPENDIX F

ELEMENTS OF THE FORCE MATRIX

$$\begin{aligned}
 P1_{mn} = & \left[\int_0^a \int_0^{2\pi} p_x(x, \theta) \cos n\theta \Phi'_m(x) R dx d\theta \right. \\
 & - \sum_{i=1}^{N_c} \int_{x_{li}}^{x_{2i}} \int_{\theta_{li}}^{\theta_{2i}} p_x(x, \theta) \cos n\theta \Phi'_m(x) R dx d\theta \\
 & \left. + \sum_{i=1}^{N_{cf}} F_x(x_i, \theta_i) \cos n\theta_i \Phi'_m(x_i) \right] f_x(t) \quad (F.1)
 \end{aligned}$$

$$\begin{aligned}
 P2_{mn} = & \int_0^a \int_0^{2\pi} p_\theta(x, \theta) \sin n\theta \Phi_m(x) R dx d\theta \\
 & - \sum_{i=1}^{N_c} \int_{x_{li}}^{x_{2i}} \int_{\theta_{li}}^{\theta_{2i}} p_\theta(x, \theta) \sin n\theta \Phi_m(x) R dx d\theta \\
 & + \sum_{i=1}^{N_{cf}} F_\theta(x_i, \theta_i) \sin n\theta_i \Phi_m(x_i) \quad (F.2)
 \end{aligned}$$

$$\begin{aligned}
 P_{mn}^3 &= \int_0^a \int_0^{2\pi} p_z(x, \theta) \cos n\theta \Phi_m(x) R dx d\theta \\
 &- \sum_{i=1}^{N_c} \int_0^a \int_0^{2\pi} p_z(x, \theta) \cos n\theta \Phi_m(x) R dx d\theta \\
 &+ \sum_{i=1}^{N_{cf}} F_z(x_i, \theta_i) \cos n\theta_i \Phi_m(x_i) R dx d\theta
 \end{aligned} \tag{F3}$$

The functions $\Phi_m(x)$ are given in Appendix B.

APPENDIX G

STRESSES AND STRAINS

This Appendix presents the expressions for the stresses and strains in terms of the generalized coordinates obtained by solving the equations of motion represented by Equation (2.21). The symbol θ in the expressions must be interpreted as the circumferential mode function Θ .

Shell

The normal and shearing strains, the changes in curvature and twist of the middle surface during deformation are given by

$$\epsilon_{\mathbf{x}}^{\circ} = \sum_m \sum_n q_{mn}^u \theta_n^u X_m^{u'}$$

$$\epsilon_{\theta}^{\circ} = \frac{1}{R} \left(\sum_m \sum_n \left\{ q_{mn}^v \theta_n^{v'} X_m^v + q_{mn}^w \theta_n^w X_m^w \right\} \right)$$

$$\gamma_{\mathbf{x}\theta}^{\circ} = \left(\sum_m \sum_n q_{mn}^v \theta_n^v X_m^{v'} \right) + \frac{1}{R} \left(\sum_m \sum_n q_{mn}^u \theta_n^{u'} X_m^u \right)$$

$$\chi_{\mathbf{xz}} = - \sum_m \sum_n q_{mn}^w \theta_n^w X_m^{w'}$$

$$\chi_{\theta z} = \frac{1}{R^2} \left\{ \left(\sum_m \sum_n q_{mn}^v \theta_n^{v'} X_m^v \right) - \left(\sum_m \sum_n q_{mn}^w \theta_n^{w'} X_m^w \right) \right\}$$

$$\tau = \frac{1}{R} \left\{ \left(\sum_m \sum_n q_{mn}^v \theta_n^{v'} X_m^{v'} \right) - 2 \left(\sum_m \sum_n q_{mn}^w \theta_n^{w'} X_m^{w'} \right) \right\}$$

The normal and shearing strains of a surface layer of shell at a distance z from the middle surface are given by

$$\epsilon_x = \epsilon_x^0 + z \chi_{xz}$$

$$\epsilon_\theta = \epsilon_\theta^0 + z \chi_{\theta z}$$

$$\gamma_{x\theta} = \gamma_{x\theta}^0 + z \tau$$

The stress resultants are given by

$$N_x = K \left[\left(\sum_m \sum_n q_{mn}^u \theta_n^u X_m^{u'} \right) + \frac{\nu}{r} \left\{ \left(\sum_m \sum_n q_{mn}^v \theta_n^{v'} X_m^v \right) + \left(\sum_m \sum_n q_{mn}^w \theta_n^{w'} X_m^w \right) \right\} \right]$$

$$N_\theta = K \left[\frac{1}{R} \left\{ \left(\sum_m \sum_n q_{mn}^v \theta_n^{v'} X_m^v \right) + \left(\sum_m \sum_n q_{mn}^w \theta_n^{w'} X_m^w \right) \right\} + \nu \left(\sum_m \sum_n q_{mn}^u \theta_n^u X_m^{u'} \right) \right]$$

$$N_{x\theta} = Gh \left\{ \left(\sum_m \sum_n q_{mn}^v \theta_n^v X_m^{v'} \right) + \frac{1}{R} \left(\sum_m \sum_n q_{mn}^u \theta_n^u X_m^u \right) \right\}$$

$$M_x = D \left[- \sum_m \sum_n q_{mn}^w \theta_n^w X_m^{w''} \right. \\ \left. + \frac{\nu}{R^2} \left\{ \left(\sum_m \sum_n q_{mn}^v \theta_n^{v'} X_m^v \right) \right. \right. \\ \left. \left. - \left(\sum_m \sum_n q_{mn}^w \theta_n^{w''} X_m^w \right) \right\} \right]$$

$$M_\theta = D \left[\frac{1}{R^2} \left\{ \left(\sum_m \sum_n q_{mn}^v \theta_n^{v'} X_m^v \right) - \left(\sum_m \sum_n q_{mn}^w \theta_n^{w''} X_m^w \right) \right\} \right. \\ \left. - \nu \left(\sum_m \sum_n q_{mn}^w \theta_n^w X_m^{w''} \right) \right]$$

$$M_{x\theta} = \frac{Gh^3}{12R} \left\{ \left(\sum_m \sum_n q_{mn}^v \theta_n^v X_m^{v'} \right) \right. \\ \left. - 2 \left(\sum_m \sum_n q_{mn}^w \theta_n^{w'} X_m^{w'} \right) \right\}$$

The normal and shearing stresses are given by

$$\sigma_x = \frac{N_x}{h} + 12 \frac{M_x}{h^3} z$$

$$\sigma_\theta = \frac{N_\theta}{h} + 12 \frac{M_\theta}{h^3} z$$

$$\tau_{x\theta} = \frac{N_{x\theta}}{h} + 12 \frac{M_{x\theta}}{h^3} z$$

Stringer

The centroidal strain components at a cross section of an ℓ^{th} stringer are given by

$$\epsilon_x = \left\{ \left(\sum_m \sum_n q_{mn}^u \theta_n^u X_m^{u'} \right) - \bar{z}_{sl} \left(\sum_m \sum_n q_{mn}^w \theta_n^w X_m^{w''} \right) - \bar{y}_{sl} \left(\sum_m \sum_n q_{mn}^v \theta_n^v X_m^{v''} \right) \right\}$$

$$\chi_{xz} = - \sum_m \sum_n q_{mn}^w \theta_n^w X_m^{w''}$$

$$\chi_{xy} = \sum_m \sum_n q_{mn}^v \theta_n^v X_m^{v''}$$

$$\tau = \frac{1}{R} \left\{ \left(\sum_m \sum_n q_{mn}^w \theta_n^w X_m^{w'} \right) - \left(\sum_m \sum_n q_{mn}^v \theta_n^v X_m^{v'} \right) \right\}$$

The stringer stress resultants are given by

$$N_x = E A \epsilon_x$$

$$M_y = E I_{yy} \chi_{xz} - E I_{yz} \chi_{xy}$$

$$M_z = -E I_{yz} \chi_{xz} + E I_{zz} \chi_{xy}$$

$$M_x = (GJ) \tau$$

The stringer normal stress is given by

$$\sigma_x = \frac{N_x}{A} + z' \left[\frac{I_{zz} M_y + I_{yz} M_z}{I_{yy} I_{zz} - I_{yz}^2} \right] - y' \left[\frac{I_{yz} M_y + I_{yy} M_z}{I_{yy} I_{zz} - I_{yz}^2} \right]$$

Ring

The centroidal strain components at a cross section of a k^{th} ring are given by

$$\begin{aligned} \epsilon_y = & -\frac{\bar{x}_{rk}}{R_{cgk}} \frac{1}{R} \left(\sum_m \sum_n q_{mn}^u \theta_n^{u''} X_m^u \right) \\ & + \frac{1}{R_{cgk}} \left(1 + \frac{\bar{z}_{rk}}{R} \right) \left(\sum_m \sum_n q_{mn}^v \theta_n^{v'} X_m^v \right) \\ & - \frac{\bar{z}_{rk}}{R_{cgk}} \frac{1}{R} \left(\sum_m \sum_n q_{mn}^w \theta_n^{w''} X_m^w \right) \\ & + \frac{1}{R_{cgk}} \left(\sum_m \sum_n q_{mn}^w \theta_n^w X_m^w \right) \\ & + \frac{\bar{x}_{rk}}{R_{cgk}} \frac{1}{R} \left(\sum_m \sum_n q_{mn}^w \theta_n^w X_m^{w'} \right) \end{aligned}$$

$$\begin{aligned}
x_{yz} &= -\frac{1}{R R_{cgk}} \left(\sum_m \sum_n q_{mn}^v \theta_n^{v'} X_m^v \right) \\
&+ \frac{1}{R R_{cgk}} \left(\sum_m \sum_n q_{mn}^w \theta_n^{w'} X_m^w \right) \\
x_{yx} &= -\frac{1}{R_{cgk}^2} \left(\sum_m \sum_n q_{mn}^u \theta_n^{u'} X_m^u \right) \\
&+ \frac{1}{R_{cgk}} \left(\sum_m \sum_n q_{mn}^w \theta_n^{w'} X_m^{w'} \right) \\
&+ \frac{\bar{z} rk}{R_{cgk}^2} \left(\sum_m \sum_n q_{mn}^w \theta_n^{w'} X_m^{w'} \right) \\
\tau &= -\frac{1}{R_{cgk}^2} \left(\sum_m \sum_n q_{mn}^u \theta_n^{u'} X_m^u \right) \\
&+ \left(\frac{-1}{R_{cgk}} + \frac{\bar{z} rk}{R_{cgk}^2} \right) \left(\sum_m \sum_n q_{mn}^w \theta_n^{w'} X_m^{w'} \right)
\end{aligned}$$

The ring stress resultants are given by

$$N_y = E A \epsilon_y$$

$$M_x = E I_{xx} \chi_{yz} - E I_{xz} \chi_{yx}$$

$$M_z = -E I_{xz} \chi_{yz} + E I_{zz} \chi_{yx}$$

$$M_y = (GJ) \tau$$

The ring normal stress is given by

$$\sigma_y = \frac{N_y}{A} - z \left[\frac{M_x I_{zz} + M_z I_{xz}}{I_{xx} I_{zz} - I_{xz}^2} \right] + x \left[\frac{M_z I_{xx} + M_x I_{xz}}{I_{xx} I_{zz} - I_{xz}^2} \right]$$

APPENDIX H

METHOD OF SOLUTION

Static Solution

The static analysis problem is of the form

$$[K] \{q\} = \{P\} \quad (H.1)$$

which represents a nonhomogeneous linear system of algebraic equations.

The solution vector $\{q\}$ is obtained by the following method, which requires that $[K]$ be a symmetric positive-definite matrix.

A triangular decomposition is performed on the matrix $[K]$ by the square root method of Cholesky:

$$[K] = [U]^T [U] \text{ where } [U] \text{ is an upper triangular matrix.}$$

Therefore, from Equation (H.1)

$$[U]^T [U] \{q\} = \{P\}$$

This represents two triangular systems

$$[U]^T \{r\} = \{P\} \text{ and } [U] \{q\} = \{r\}$$

The first system is solved for $\{r\}$ by forward elimination and the second system is then solved for $\{q\}$ by back substitution.

Library Subroutines (20) were used in the above steps.

Free Vibrations

The eigenvalue problem is of the form

$$[K] \{q\} = \lambda [M] \{q\} \quad (\text{H.2})$$

where λ is an eigenvalue, and $\{q\}$ an eigenvector.

The following method for solving Equation (H.2) for eigenvalues and eigenvectors of the system requires $[M]$ to be symmetric positive definite and $[K]$ to be symmetric (21).

A triangular decomposition is performed on the matrix $[M]$ by the square root method of Cholesky:

$$[M] = [L] [L]^T \text{ where } [L] \text{ is a lower triangular matrix.}$$

Therefore, from Equation (H.2):

$$[K] \{q\} = \lambda [L] [L]^T \{q\} .$$

This can be expressed as

$$[L]^{-1} [K] [L^T]^{-1} [L^T] \{q\} = \lambda [L^T] \{q\} \quad (\text{H.3})$$

$$\text{By defining } [S] = [L]^{-1} [K] [L^T]^{-1} \quad (\text{H.4})$$

$$\text{and } \{y\} = [L^T] \{q\} \quad (\text{H.5})$$

Equation (H.3) becomes

$$[S] \{y\} = \lambda \{y\} \quad (\text{H.6})$$

which is an eigenvalue problem, where $[S]$ is a symmetric matrix with eigenvalues λ which are the same as the original problem. The eigenvectors of the original system, $\{q\}$, are found from the eigenvectors of Equation (H.6), $\{y\}$, by Equation (H.5).

Because the transformation of Equation (H. 4) involves triangular matrices, the matrix $[L]^{-1}$ need not be found to determine $[S]$. Thus, no matrix inversions are required. The sequence of operations is as follows:

1. Decompose $[M]$: $[M] = [L][L^T]$

2. Perform a forward substitution through

$$[L]([L]^{-1}[K]) = [K]$$

to solve for each column of $[L]^{-1}[K]$.

3. Perform a forward substitution through

$$L([L]^{-1}[K][L^T]^{-1}) = ([L]^{-1}[K])^T$$

to solve for each column of $[L]^{-1}[K][L^T]^{-1} = [S]$.

4. Find the eigenvalues, λ and eigenvectors $\{y\}$ of $[S]$.

A Householder's method (22) was used in this analysis.

5. Determine the eigenvectors $\{q\}$ from $\{y\}$ by a back substitution through

$$[L^T]\{q\} = \{y\}$$

The subroutine that was used to carry out this procedure was reproduced from that of Reference (23) with the exception of Step 4.

Transient Response

The problem is to solve the system of ordinary second order nonhomogeneous differential equations with constant coefficients, represented by

$$[M]\{\dot{q}\} + [K]\{q\} = \{P\} \quad (\text{H. 7})$$

The adopted procedure to solve the system is given below.

Reduction to a First Order System

The matrix $[M]$ being symmetric and positive definite perform a triangular decomposition on it by the square root method of Cholesky:

$$[M] = [L][L^T] \text{ where } [L] \text{ is a lower triangular matrix.}$$

Perform a forward substitution through

$$[L]([L^T][M]^{-1}) = [I]$$

to solve for each column of $[L^T][M]^{-1} = [R]$, say.

Perform a back substitution through

$$[L^T][M]^{-1} = [R]$$

to solve for each column of $[M]^{-1}$.

Premultiply the matrix $[K]$ by $[M]^{-1}$ and also the column matrix $\{P\}$ by $[M]^{-1}$.

Now the Equation (M. 7) is transformed into

$$\{\ddot{q}\} + [M]^{-1}[K]\{q\} = [M]^{-1}\{P\}$$

Defining new variables

$$\{y\}_I = \{q\} \text{ and } \{y\}_{II} = \{\ddot{q}\}$$

the following first order system is obtained

$$\{\dot{y}\}_I = \{y\}_{II}$$

$$\dot{\{y\}}_{II} = [M]^{-1}[K]\{y\}_I + [M]^{-1}\{P\}$$

Solution of the First Order System

The solution is obtained by a Fourth Order Runge-Kutta method with automatic step size control. Based on the work of Earnest (11) a subroutine was written by Chandler (22). It was adopted to the computer program of the present work. Its superiority over the standard available subroutines (20) is attributed to the following features.

- (1) Reduction in computational time involved.
- (2) The truncation error is calculated for each dependent variable whereas it is calculated in an average sense for the whole system in (20).
- (3) The step size control is achieved by the requirement that the truncation error satisfies either a relative error bound or an absolute error bound whereas in (20) it has to satisfy an absolute error bound, the specification of which may often need a prior knowledge of the magnitude of the variables.

VITA ²

Mahabaliraja

Candidate for the Degree of

Doctor of Philosophy

Thesis: DYNAMIC RESPONSE OF NONCIRCULAR STIFFENED
CYLINDRICAL SHELLS WITH RECTANGULAR CUTOUTS

Major Field: Mechanical Engineering

Biographical:

Personal Data: Born January 10, 1945, at Pavagada, Tumkur District, Mysore State, India, the Son of Mr. and Mrs. C. Gummatarajaiah.

Education: Graduated from Municipal High School, Pavagada, Tumkur District, Mysore State, India in June, 1961; received the Degree of Bachelor of Engineering in Mechanical Engineering in 1967 from the University of Mysore; and the Master of Engineering degree in 1969 from Indian Institute of Science, Bangalore; completed the requirements for the Degree of Doctor of Philosophy in December, 1974.

Professional Experience: Lecturer, Bangalore University, August 1969 - April 1970; Senior Research Fellow/Assistant, Indian Institute of Science, May 1970 - December 1971; Graduate Teaching/Research Assistant, Oklahoma State University, 1972 - 1974.

Professional Organizations: Graduate Member of the Aeronautical Society of India.